

THE EFFECTS OF COUPLED TRANSLATIONAL -
TORSIONAL DYNAMIC RESPONSE ON BUILDINGS



By
VIOLA MENG
B. ENG. (Civil)

A Thesis

Submitted to the School of Graduate Studies
in Partial Fulfilment of the Requirements

for the Degree

Master of Engineering

McMaster University

April, 1980.

THE EFFECTS OF COUPLED TRANSLATIONAL -
TORSIONAL DYNAMIC RESPONSE ON BUILDINGS

MASTER OF ENGINEERING (1980)
(Civil Engineering)

McMASTER UNIVERSITY
Hamilton, Ontario

TITLE: The Effects of Coupled Translational -
Torsional Dynamic Response on Buildings

AUTHOR: Viola C.Y. Meng, Tungchi University

SUPERVISOR: Dr. W.K. Tso

NUMBER OF PAGES: x, 118

ABSTRACT

An investigation is made into the coupled lateral - torsional response on frame buildings to horizontally directed earthquake excitation. Attention is confined to the accuracy of the static code provision on torsional effect with special reference to the National Building Code of Canada 1977 (NBC 77).

A mathematical model to compute the dynamic response of a building is presented. The formulation of the general equation of motion to a monosymmetrical building is developed in detail. The static storey torque is compared with the dynamic torque computed by using the response spectrum technique as outlined in the Commentary K of NBC 77. It has been found that the sympathetic coupled translational torsional resonance occurs at the buildings with small eccentricities. To uniform structure, the static code torque estimate is good if the effect of sympathetic coupled resonance is not significant. To buildings with large eccentricities, sympathetic resonance is unlikely to occur and the current NBC requirement of doubling the computed torque for design is a very conservative requirement.

To buildings with eccentric offset, NBC 80 proposes a modification on the definition of structural eccentricity. A study in this aspect is made through the floor torques comparison between dynamic analysis and static codes calculations. The results show that the improvement by NBC 80 is only partial. Buildings with eccentric offsets are irregular buildings, only a dynamic approach can lead to a realistic estimate of the torque distributions.

ACKNOWLEDGEMENTS

The author wishes to express her sincere appreciation to Dr. W.K. Tso for his consistent guidance, assistance and encouragement throughout the research program. The invaluable suggestions and advices received from Dr. Tso are gratefully acknowledged.

Special thanks are also due to Dr. R.G. Drysdale and Dr. A.A. Smith for their guidance and encouragement from time to time, to Miss D. Pitkin and Mrs. D. Cosgrove for their very skillful typing of this thesis and to McMaster University and the Natural Science and Engineering Research Council for providing financial support during this research work.

TABLE OF CONTENTS

	Page
ABSTRACT	iii
ACKNOWLEDGEMENTS	iv
TABLE OF CONTENTS	v
LIST OF FIGURES	vii
LIST OF TABLES	x
CHAPTER I - INTRODUCTION	1
1.1 General	1
1.2 Review of Past Works	5
1.3 Objective and Scope	8
CHAPTER II - MATHEMATICAL MODEL	11
2.1 Introduction	11
2.2 Modelling of Plan Structure	11
2.2.1 The Configuration of the Model	11
2.2.2 The Evaluation of Spring Stiffness for Wall and Frame Structures	12
2.2.3 The Formation of Stiffness Matrix for Multi-Degree of Freedom Model	14
2.2.4 Verification of the Model	21
2.3 Spatial Structure Modelling	27
2.3.1 The Configuration of the Model	27
2.3.2 The Formulation of General Stiffness Matrix	29
2.3.3 The General Equation of Motion	41
CHAPTER III - THE EFFECTS OF COUPLED TRANSLATIONAL AND TORSIONAL MOTION IN MONOSYMMETRICAL FRAME BUILDING	50
3.1 Introduction	50
3.2 Uncoupled Fundamental Translational and Torsional Periods	51
3.3 The Comparison of Base Shear Between Stiff and Flexible Structures	52

	Page
3.4 The Consequence of Coupled Translational and Torsional Motion to Base Shear	55
3.5 The Study of Dynamic Torque Affected by Eccentricity and Coupled Motion	60
3.6 The Study of Sympathetic Resonance	71
3.7 The Discussion of the RSS Rule for Modal Contribution	83
3.8 Conclusions	89
 CHAPTER IV - TORSIONAL PROVISIONS IN BUILDING CODES	 91
4.1 Introduction	91
4.2 Torsional Provisions in Building Codes	91
4.3 Buildings with Eccentricity Offset	94
 CHAPTER V - CONCLUSIONS	 109
 REFERENCES	 112
 APPENDIX - List of Symbols	 115

LIST OF FIGURES

Figure	Title	Page
1.1	Symmetrical, Monosymmetrical and Asymmetrical Building Plans	2
1.2	Additional Shear Force due to Torsional Response	3
1.3	The Configuration of Buildings with $T_x = 0.5, 1.0, 2.0$ sec.	9
2.1	Flexural and Shear Springs	13
2.2	Shear and Flexural Deformations of Wall Structure	15
2.3	Shear and Flexural Deformations of Frame Structure	15
2.4	Relationship of Geometry and Forces of Multi-Degree of Freedom Unit	16
2.5	Testing Model 1 - R.C. Single Span Frame	22
2.6	Testing Model 2 - R.C. Wall ($t = 10''$)	22
2.7	Spatial Spring Model	28
2.8	Relationship of Elastic and Inertia Forces	30
2.9	Mono-Symmetrical Unit Plan	30
2.10	Multi-Unit Spatial Model	31
2.11	Geometric Relations of Arbitrary Point and Centers of Mass and Rigidity	42
3.1	Peak Ground Motion Bounds and Elastic Average Response Spectrum for 1.0g Max. Ground Acceleration	53
3.2	The Comparison of Dynamic and Static Base Shear due to Eccentricities and Coupled Motions	61
3.3	Comparison of Torque for Building $T_x = 1.0$ (sec), $e/D = 0.03$	62
3.4	Comparison of Torque for Building $T_x = 1.0$ (sec), $e/D = 0.10$	63
3.5	Comparison of Torque for Building $T_x = 1.0$ (sec), $e/D = 0.50$	64

Figure		Page
3.6	Comparison of Torque for Building Tx = 2.0 (sec), e/D = 0.03	65
3.7	Comparison of Torque for Building Tx = 2.0 (sec), e/D = 0.10	66
3.8	Comparison of Torque for Building Tx = 2.0 (sec), e/D = 0.5	67
3.9	Comparison of Torque for Building Tx = 0.5 (sec), e/D = 0.03	68
3.10	Comparison of Torque for Building Tx = 0.5 (sec), e/D = 0.10	69
3.11	Comparison of Torque for Building Tx = 0.5 (sec), e/D = 0.5	70
3.12	Effect of Eccentricity and Uncoupled Periods Ratios to Frequencies of Building (Tx = 1.0 sec)	76
3.13	Mode Shapes for Building Tx = 1.0 sec (e/D = 0.03, $\tau = 1.0$)	77
3.14	Mode Shapes for Building Tx = 1.0 sec (e/D = 0.1, $\tau = 1.0$)	79
3.15	Mode Shapes for Building Tx = 1.0 sec (e/D = 0.5; $\tau = 1.0$)	81
3.16	Dynamic Base Shear Comparison Between Eq. 3.4 and Eq. 3.6	86
3.17	Normalized Torque Comparison Between R.S.S. and N-R* Equation	87
3.18	Normalized Torque Comparison Between R.S.S. and N-R* Equation	87
3.19	Normalized Torque Comparison Between R.S.S. and N-R* Equation	88
	* N-R = Newmark & Rosenblueth Equation	
4.1	The Effect of Torsional Period for Building Tx = 1.0 sec, e/D = 0.03	95
4.2	The Effect of Torsional Period for Building Tx = 1.0 sec, e/D = 0.10	95

Figure		Page
4.3	Comparison of Torque for Building $T_x = 1.0 \text{ sec}$, $e/D = 0.50$	96
4.4	The Configuration of Eccentric Offset Building	98
4.5	The Transfer of Dynamic Responses From Reference Point to Floor Center of Rigidity or Mass for Eccentric Offset Building	101
4.6	Buildings with Eccentric Offset	102
4.7	Torque Envelope for Structure A	103
4.8	Torque Envelope for Structure B	104
4.9	Torque Envelope for Structure C	105
4.10	Comparison of Different Offset Structures' Torque Calculation	107

LIST OF TABLES

Table	Title	Page
2.1	The Effects of Flexural Stiffness and Shear Stiffness to a Frame Structure	23
2.2	The Effects of Flexural Stiffness and Shear Stiffness to a Wall Structure	26
3.1	Base Shear Comparison Between Static Calculation and Dynamic Analysis	54
3.2 (a)	1st Mode Dynamic Shear Forces Comparison for Buildings with $T_x = 0.5$ 1.0 sec. ($e_x = e_y = 0$) 2.0	56
(b)	2nd Mode Dynamic Shear Forces Comparison for Buildings with $T_x = 0.5$ 1.0 sec. ($e_x = e_y = 0$) 2.0	57
(c)	3rd Mode Dynamic Shear Forces Comparison for Buildings with $T_x = 0.5$ 1.0 sec. ($e_x = e_y = 0$) 2.0	58
(d)	4th Mode Dynamic Shear Forces Comparison for Buildings with $T_x = 0.5$ 1.0 sec. ($e_x = e_y = 0$) 2.0	59
3.3 (a)	Frequencies for Building $T_x = 0.5$ sec	72
(b)	Frequencies for Building $T_x = 1.0$ sec	73
(c)	Frequencies for Building $T_x = 2.0$ sec	74
3.4	Mode Shapes for Building $T_x = 1.0$ sec, $e/D = 0.03$	78
3.5	Mode Shapes for Building $T_x = 1.0$ sec, $e/D = 0.10$	80
3.6	Mode Shapes for Building $T_x = 1.0$ sec, $e/D = 0.50$	82
3.7	Base Shear and Torque for Building $T_x = 1.0$ sec, $\tau = 1.0$	84
4.1	The Formulations of Design Eccentricity of Different Countries.	93
4.2	The Frequencies of Eccentric Offset Structures	105.a

CHAPTER 1
INTRODUCTION

1.1 General

For functional and architectural requirements, buildings are generally designed as either symmetrical, monosymmetrical or asymmetrical structures as shown in Fig. 1.1. When asymmetrical buildings are subjected to earthquake ground shaking, torsional response will be produced in addition to lateral response. In design, it is necessary to account for such torsional response, which may induce additional shear force on the lateral resisting elements such as columns and walls of the building (shown in Fig. 1.2).

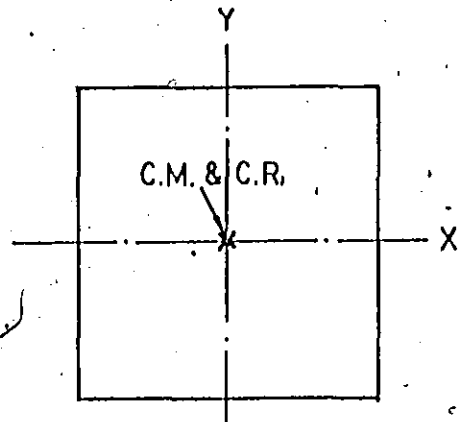
Several methods of analysis have been proposed to approximate the effect of torsion in buildings. For instance, the National Building Code of Canada 1977 (NBC77) has defined torsional moments (M_{tx}) in the horizontal plane of the building to be computed in each storey by using the following formula [1]:

$$M_{tx} = (V - \sum_{i=1}^x P_i) \cdot e_x \quad (1.1)$$

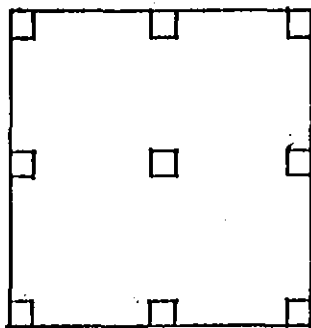
in which P_i is the lateral force applied to level i of the building, V is the base shear. e_x is the design eccentricity which shall be computed by one of the following equations, whichever provides the greater stresses:

$$e_x = 1.5e + 0.05 D_n \quad \text{or}$$

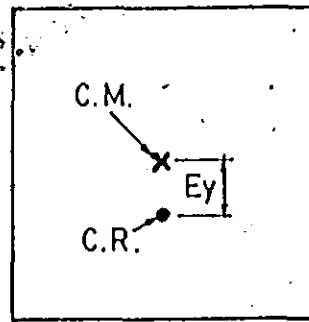
$$e_x = 0.5e - 0.05 D_n$$



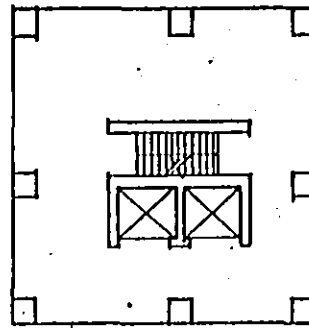
$$E_x = E_y = 0$$



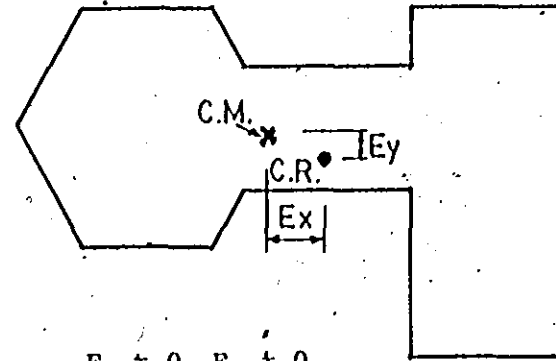
Symmetrical Plan



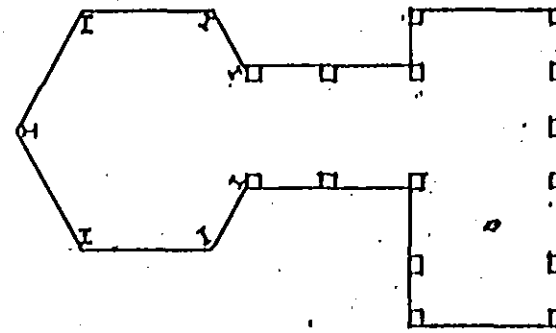
$$E_x = 0, E_y \neq 0$$



Monosymmetrical Plan



$$E_x \neq 0, E_y \neq 0$$



Asymmetrical Plan

Fig. 1.1 Symmetrical, Monosymmetrical and Asymmetrical Building Plans

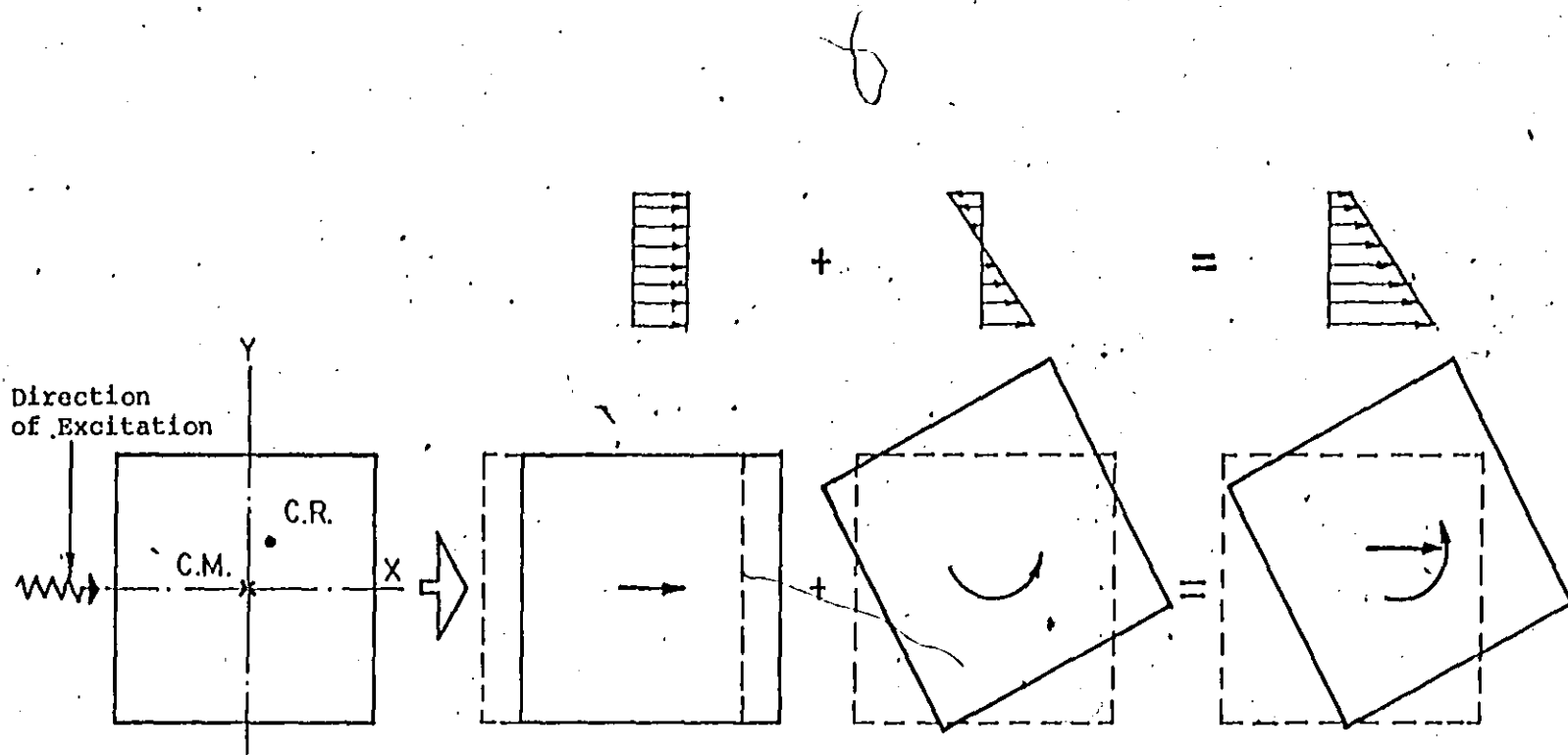


Fig. 1.2 Additional Shear Force Due to Torsional Response

When the design eccentricity e_x exceeds $0.25 D_n$, NBC77 requires that either a dynamic analysis shall be made, or the effects of torsion as computed in Eq. 1.1 shall be doubled.

As an alternative method, NBC77 also allows the dynamic response spectrum technique to be used for design calculation, provided that the dynamic value of base shear V is not less than 90% of the static base shear. [2],[3]

The equivalent static torsional provisions in most building codes in the world are generally presented in the same form as the product of shear force and design eccentricity in each floor. Under such load procedure, for a building of given dimensions and weight, a change of structural eccentricity e , i.e. the distance between the centers of mass and rigidity at one level of a building, will only affect the torsional moments at that level, but has no influence on the storey shears. However, many investigations based on dynamic analysis have pointed out that both the shear and torsional moments are functions of the building eccentricities. [4] Tso and Asmis [5] and Keintzel [6] also have shown that the modal coupling may occur in symmetrical or nearly symmetrical structures when the fundamental translational and torsional periods are nearly equal. All these observations are not reflected in the seismic code provisions.

In order to clarify the effects of coupled torsional-translational dynamic responses on buildings due to the earthquake excitations, the present study is made to assess the accuracy and applicability of the code provisions in taking the torsional response effect into account. The torsional moment distribution along the height of the building is taken as the parameter for study. The static torsional moments are compared to the torsional moments computed by the dynamic response

Particular attention is given to the following guidelines from the NBC77 and its commentaries. They are (1) the use of the design eccentricity expression $e_x = 1.5e + 0.05 D$, (2) the necessity of doubling the computed torsional moment when the design eccentricity e_x exceeds a quarter of the floor plan dimension D_n .

The current computation of static torsional moments in each floor by most of the building codes is restricted to the local horizontal plane of the building. It does not take into account the additional torsional effects due to the adjacent floors in which the centres of mass and rigidity do not lie vertically above the corresponding points in the floor under consideration.

For buildings with eccentric offsets (or setbacks), NBC80 proposes a change of the definition of structural eccentricities (e) to take care of such additional torsional effect. This aspect of the modification is studied in this thesis also.

1.2 Review of Past Works

The torsional effects in buildings due to seismic loads have been investigated in numerous studies in recent years. It has been shown that the coupling between translational and torsional vibrations for a building, in which the centers of mass and rigidity do not coincide, can lead to a considerable dynamic magnification of torsional moments. Therefore, it is useful to review the existing knowledge of the effects of coupled translational and torsional motions by citing some of the studies carried out by different authors.

The possibility of induced torsional motions to a symmetrical structure subjected to ground motion was illustrated by Tso and Asmis^[5].

Similarly, the study done by Keintzel^[6] also showed that in the case of close periods of torsional and translational vibration, a resonance like increase of the vibrational amplitudes could occur.

Due to the earthquake wave motion, N. M. Newmark^[7] developed a rational basis for determining torsional earthquake effects in symmetrical buildings. He concluded that the ratio of the accidental eccentricity to the long plan dimension varied almost directly with the fundamental frequency of vibration of the building and with the transit time of the earthquake wave motion. He also pointed out that the yielding in torsion might be much more serious than yielding in flexure or in linear displacements, and design should provide greater assurance of resistance to torsional yielding than to other types of yielding.

During the 1971 San Fernando earthquake, the importance of rotational component of ground motion on the torsional responses of many buildings were observed^[8]. Since all strong motion seismographs were designed to record the three perpendicular translational motions only, no actual record on the rotational component of earthquake had been obtained. Based on the fundamental relations in the theory of elasticity, the rotation about a vertical axis could be derived by spatial differentiation from horizontal displacements; Tso and Hsu^[9] presented torsional spectrum for design purpose.

Seismic analysis of asymmetrical structures subjected to orthogonal components of ground acceleration were studied by Tso, Biswas^[10] and Fajfar, Zele^[11]. These authors all claimed that the response from bidirectional excitation could be approximated by combining the responses of the system subjected to individual unidirectional excitation in a root-sum-square (RSS) manner. As another observation, Tso and Biswas

had examined the sensitivity of the response parameters considered to the phase relationship between the two components of ground excitation.

Kan and Chopra^[4] developed a simple procedure for the analysis of elastic response of torsional coupled building to earthquake ground motion. They observed that lateral and torsional motions would be strongly coupled when the eccentricities were large, and less obvious perhaps, but clearly displayed by force vibration tests, was the strong coupling between lateral and torsional motions of buildings with close natural frequencies and essentially coincident centers of mass and resistance. As a very important conclusion, they pointed out that coupling between lateral and torsional motions induced torque and in general reduced base shear, and the effect of torsional coupling decreased as damping increased^{[12], [13]}.

The root-sum-square procedure in dynamic response spectrum technique applies only if the periods T_1 , T_2 are well separated. The study done by Rutenberg, Hsu and Tso^[14] mentioned that the proper phase relationship between the lateral load effect and torsional effect should be accounted for on a modal basis. The conventional method which obtained the response from the worst combination of RSS lateral and RSS torsional loadings, generally tended to overestimate the response.

In order to take the torsional effects into account, particularly when the periods ratio $\tau = T_\phi/T_x$, in which T_ϕ is the uncoupled torsional period and T_x is the uncoupled translational period in x axis direction, is close to one, the new German Seismic Code DIN4149 provides a supplementary fictitious eccentricity in the design eccentricity calculation to approximate the dynamic effect of vibration coupling. Müller and Keintzel recommend that the approximate method is not excessively conservative^[15].

1.3 Objective and Scope

The purpose of the present analysis is to study the effects of coupled translational-torsional dynamic response on buildings due to earthquake excitation. Taking into account the torsional response effect, both the static and dynamic format of National Building Code of Canada (NBC77) are used and compared to examine the accuracy and applicability of the static code.

To reflect the behaviour of a building undergoing lateral loads, a mathematical model consisting of lumped masses and flexural, shear and torsional springs is created in Chapter 2. The formulation of the stiffness matrix referred to an arbitrary reference point is discussed in detail in this chapter also.

Chapter 3 is devoted to the study of the effects of base shear and torque envelopes when coupled torsional-lateral motions are considered. Three uniform monosymmetrical frame buildings, as shown in Fig. 1.3, are used as examples for this study. One building is a six-storey structure with uncoupled translational period in X axis (T_x) is equal to 0.5 sec. The second building is a twelve-storey structure with T_x equal to 1.0 sec. The twenty-four storey building with T_x equal to 2.0 sec., is chosen as the third example. For simplicity, the 1400 kips of floor weight is used in each building. The floor plans for these three buildings are shown. The plan dimensions in both X and Y axes are equal to 100 feet. Small, moderate and exceptionally large eccentricities are expressed by the ratios of eccentricity (e_y) to plan dimension (D_y), i.e. $e_y/D_y = 0.03$, $e_y/D_y = 0.10$ and $e_y/D_y = 0.50$ respectively (shown in Fig. 1.3(d)). Associated with various eccentricities, the dynamic response spectrum method, according to Commentary K of NBC77, is used to study the effects of coupled translational-torsional motion.

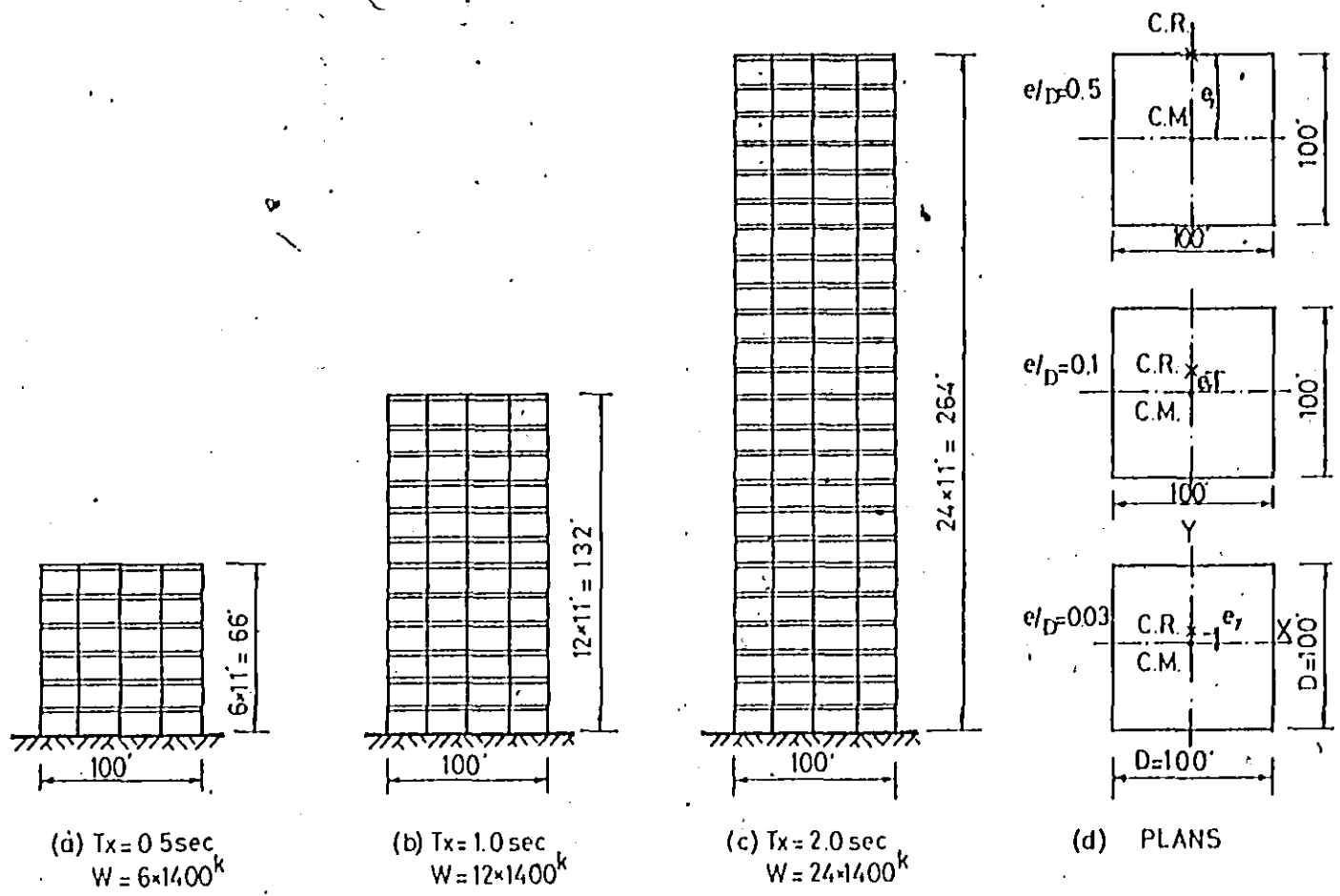


Fig. 1.3 The Configuration of Buildings with $T_x = 1.0$ Sec.
 0.5
 2.0

The ratios (τ) of uncoupled torsional periods (T_ϕ) to uncoupled lateral periods (T_x) vary in the range of 0.6 to 1.4. Dynamic responses in shear force and torque envelopes of the three buildings show the similar shape. For detailed examination, the twelve storey building is chosen to be studied in detail for the effect of sympathetic coupled torsional-lateral resonance.

The accuracy and applicability of current static code (NBC77) in the torsional provisions is studied in Chapter 4. The formulation of design eccentricity (e_x), and the requirement of doubling torque when design eccentricity exceeds 0.25 of the planned dimension are studied. Torsional provisions in four other countries' (Germany, New Zealand, Mexico and U.S.A.) building codes are also investigated.

Buildings with eccentric offset (or setbacks) will induce additional torsional effect besides the local floor torque due to the non-coincidence of centers of mass and rigidity in the plan. NBC80 provides a modification on the definition of structural eccentricity (e) to take this situation into account^[16]. Buildings with top two, four and six floors as the eccentric offset portion of the twelve storey frame building are taken as examples to examine the improvements and discrepancies of NBC80 modification.

It is hoped that the present work will provide some insight to the effects of coupled translational-torsional motions on buildings and provide some comments on the adequacy and accuracy of the current National Building Code of Canada.

CHAPTER 2 MATHEMATICAL MODEL

2.1 Introduction

When a building is subjected to lateral loads, a frame structure will deflect predominantly in a shear mode and a shear wall structure will deflect predominantly in a bending mode. In order to perform dynamic analysis and study the effect of coupled translational and torsional motion for buildings which consist of frames or walls, a dynamic mathematical model comprised of lumped masses and shear and flexural springs is created to represent the two types of structures.

A two-dimensional plane model is first studied to verify the accuracy of the model. By applying static horizontal forces to the models and their corresponding real structures, the horizontal deformations can be compared. These results demonstrate that the proposed model can represent the building behaviour when the building is subjected to horizontal force.

The dynamic analysis of an asymmetrical building will need a three-dimensional model which will consist of shear, flexural and torsional springs. The derivation of the stiffness matrix for this spatial model will be discussed in detail within this chapter also.

2.2 Modelling of Plane Structures

2.2.1 The Configuration of the Model

Under horizontal loading, the lateral deflection of a building will consist of two parts, namely, chord drift and web drift. To

delineate the flexural and shear behaviour of a structure, a unit model, which includes shear (K_s) and flexural (K) springs and mass, will be considered as shown in Fig. 2.1(a). Fig. 2.1(b) shows that when the mass of the model is rotated θ by moment M , the spring K_s will not be affected. Fig. 2.1(c) describes the mass as it is shifted Δ horizontally by a force P , the spring K will not be stretched. Therefore the stiffnesses of springs K and K_s can be taken to represent the bending and shear stiffnesses of the structure.

2.2.2 The Evaluation of Spring Stiffness for Wall and Frame Structures

The stiffness of flexural springs (K) can be derived as shown in Fig. 2.1(b). Consider unit rotation to be $\theta = 1$ due to external moment (M). The internal forces (F) developed by elongation and shortening of (K) springs are

$$F = K \cdot \left(\frac{a}{2} \cdot \theta\right)$$

To satisfy the static equilibrium condition, the external force (M) must be equal to the internal force ($F \cdot a$). Hence,

$$M = K \cdot \frac{a^2}{2} \cdot \theta$$

and the stiffness of flexural spring (K) is

$$K = \frac{2}{a^2} \cdot \frac{M}{\theta} \quad (2.1)$$

in which the term of $\left(\frac{M}{\theta}\right)$ represents the flexural stiffness (K_f) of the unit model.

The stiffness of shear spring (K_s) can be defined as the shear stiffness of the unit directly. As shown in Fig. 2.1(c), the stiffness of the shear spring (K_s) is

$$K_s = \frac{P}{\Delta} \quad (2.2)$$

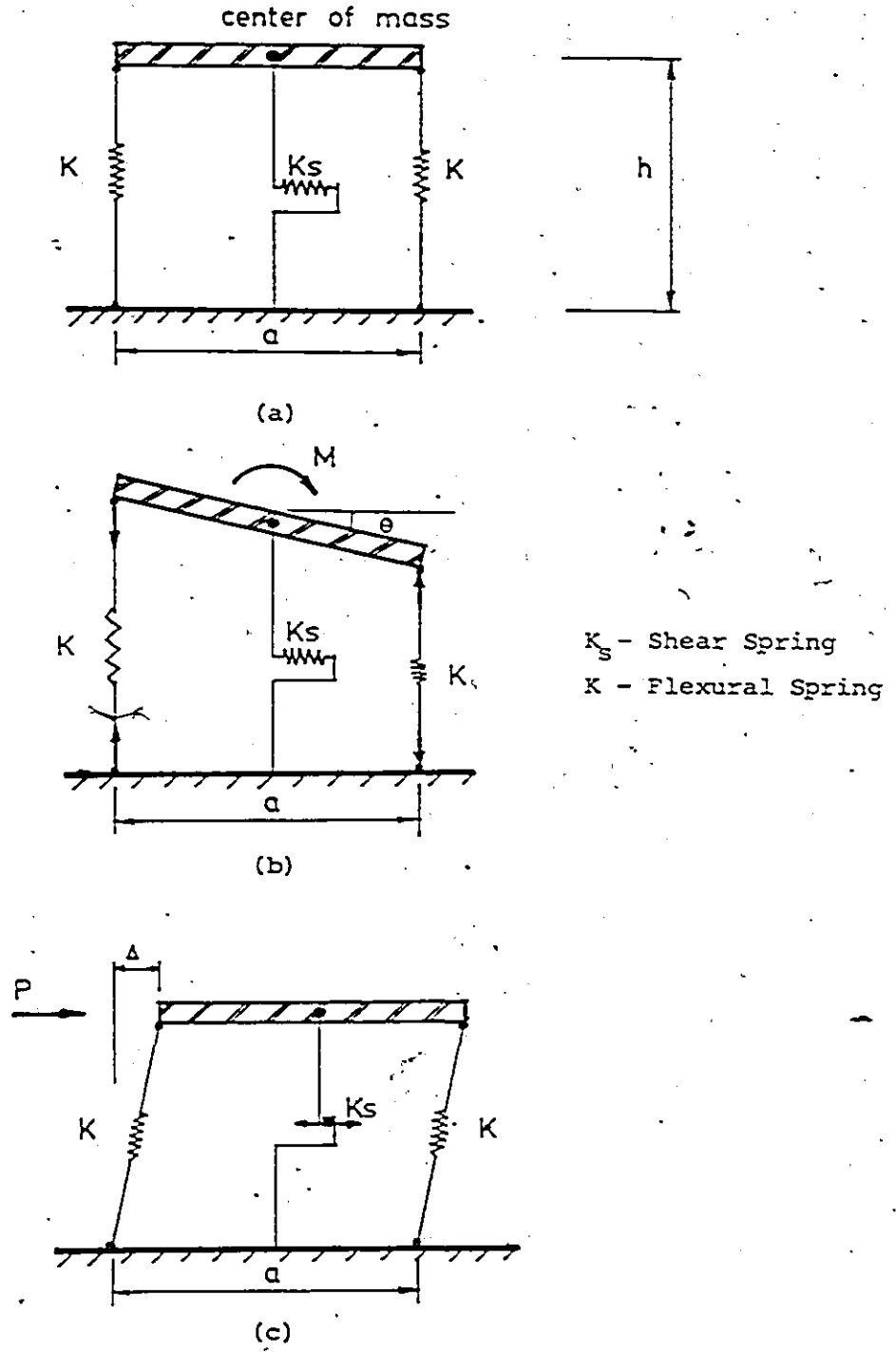


Fig.2.1 Flexural and Shear Springs

Figs. 2.2 and 2.3 show that flexural deformation dominates wall structure and shear deformation is predominate in frame structure. To represent the wall structures, the stiffnesses of shear spring and flexural spring of the model can be taken as

$$K_s, \text{ wall} = \frac{12EI}{h^3} \left(\frac{1}{4 + \frac{6Ea^2}{5Gh^2}} \right) \quad (2.3)$$

$$K, \text{ wall} = \frac{2EI}{a^2 h} \quad (2.4)$$

For frame structure, according to Heidebrecht and Smith^[17], the shear spring stiffness is

$$K_s, \text{ frame} = \sum_i \frac{12EI}{h^3} \left[\frac{1}{1 + \frac{2I_i}{I_{b_1} + \frac{I_{b_2}}{h(\frac{1}{b_1} + \frac{1}{b_2})}}} \right] \quad (2.5)$$

assuming that the contraflexural points are located at the mid-span of the beams and mid-height of the columns. The flexural spring stiffness for the frame structure is given by

$$K, \text{ frame} = \alpha \frac{AE}{h} \quad (2.6)$$

where α is a factor which depends on the structural plan layout and geometric properties of the columns. For example, for a four-bay, frame structure (shown in Fig. 2.3), $\alpha = 1.25$ assuming the area, Young's modulus and height of the columns are uniform.

2.2.3 The Formation of Stiffness Matrix for Multi-Degree of Freedom Model

For a multi-unit model, (shown in Fig. 2.4(a)), a single unit is first isolated to study the equilibrium of the static elastic forces

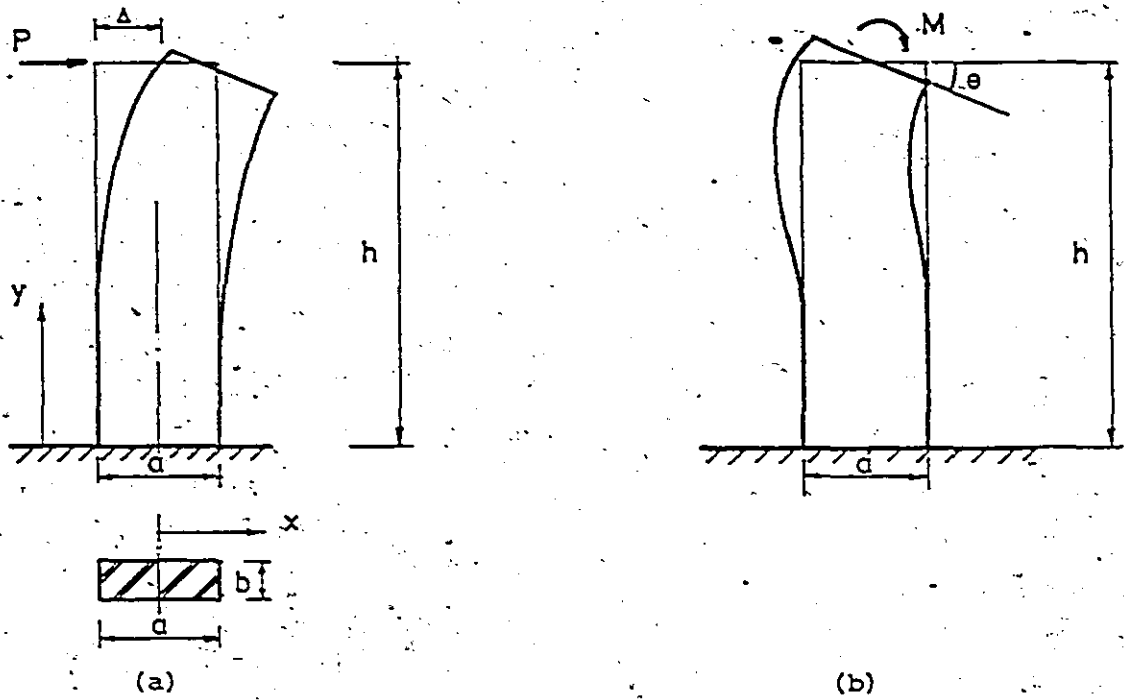


Fig.2.2 Shear and Flexural Deformations of Wall Structure

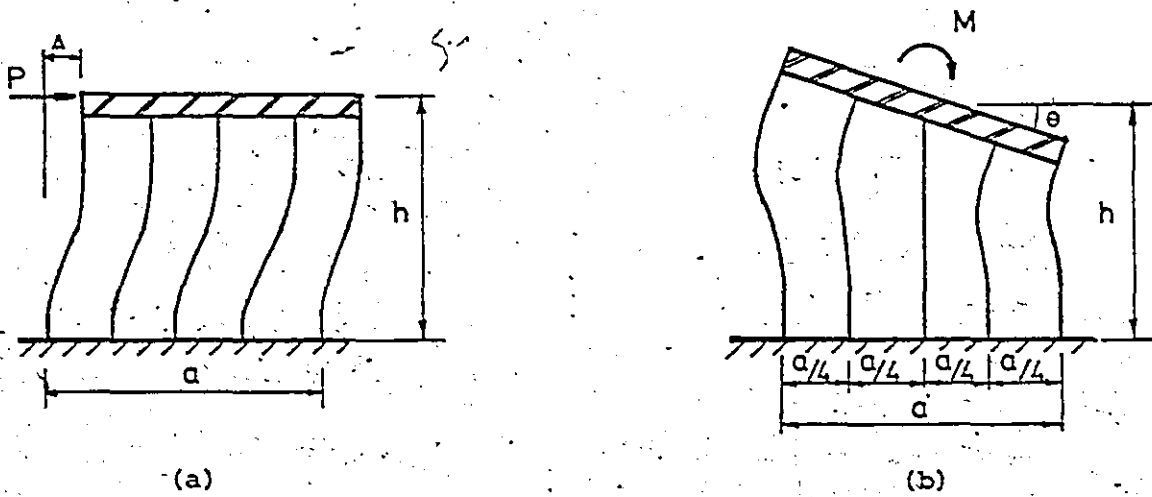


Fig.2.3 Shear and Flexural Deformations of Frame Structure

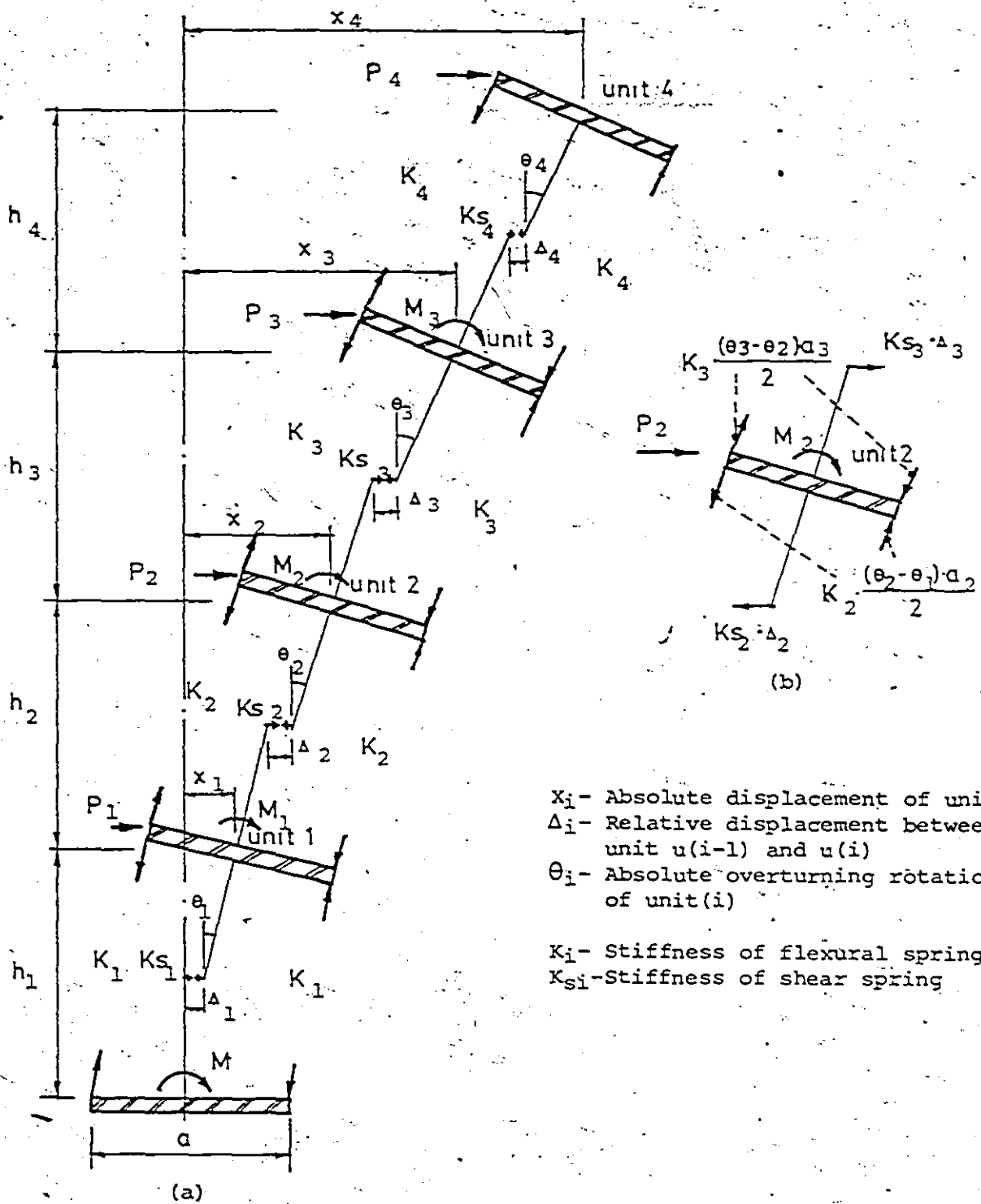


Fig.2.4 Relationship of Geometry and Forces of Multi-degree of Freedom Unit

when the model is subjected to external lateral forces (shown in Fig. 2.4(b)). Consider the second unit for example; horizontal force equilibrium gives

$$P_2 - K_{s2} \cdot \Delta_2 + K_{s3} \cdot \Delta_3 = 0$$

and moment equilibrium leads to

$$\begin{aligned} M_2 - \frac{1}{2} \cdot K_2 \cdot (\theta_2 - \theta_1) \cdot a_2^2 + \frac{1}{2} \cdot K_3 \cdot (\theta_3 - \theta_2) \cdot a_3^2 \\ + K_{s2} \cdot \Delta_2 \cdot \frac{h_2}{2} + K_{s3} \cdot \Delta_3 \cdot \frac{h_3}{2} = 0 \end{aligned} \quad (2.7)$$

in which K_{s2} , K_{s3} , K_2 and K_3 are the stiffnesses of shear and flexural springs for unit 2 and 3 respectively, Δ_2 and Δ_3 are the relative horizontal displacements and θ_2 and θ_3 are the absolute rotations with respect to the vertical axis for units 2 and 3.

For any unit (i), Eq. 2.7 can be generalized as

$$P_i = K_{s_i} \cdot \Delta_i - K_{s_{i+1}} \cdot \Delta_{i+1}$$

and

$$\begin{aligned} M_i = \frac{a_i^2}{2} \cdot (\theta_i - \theta_{i-1}) \cdot K_i - \frac{a_{i+1}^2}{2} \cdot (\theta_{i+1} - \theta_i) \cdot K_{i+1} \\ - \frac{h_i}{2} \cdot \Delta_i \cdot K_{s_i} - \frac{h_{i+1}}{2} \cdot \Delta_{i+1} \cdot K_{s_{i+1}} \end{aligned} \quad (2.8)$$

Fig. 2.4(a) shows that the absolute horizontal displacement X_i of any unit can be expressed by the relative displacement Δ_i and overturning rotations θ_i , θ_{i-1} , such that

$$X_i = X_{i-1} + \Delta_i + (\theta_{i-1} + \theta_i) \cdot \frac{h_i}{2}$$

or

$$\Delta_i = X_i - X_{i-1} - (\theta_{i-1} + \theta_i) \cdot \frac{h_i}{2} \quad (2.9)$$

Substituting Eq. 2.9 into Eq. 2.8 yields

$$\begin{aligned}
 P_i = & -(K_{S_i}) \cdot X_{i-1} + (K_{S_i} + K_{S_{i+1}}) \cdot X_i - (K_{S_{i+1}}) \cdot X_{i+1} \\
 & - \left(\frac{1}{2}K_{S_i} \cdot h_i\right) \cdot \theta_{i-1} - \left(\frac{1}{2}K_{S_i} \cdot h_i - \frac{1}{2}K_{S_{i+1}} \cdot h_{i+1}\right) \\
 & \cdot \theta_i + \left(\frac{1}{2}K_{S_{i+1}} \cdot h_{i+1}\right) \cdot \theta_{i+1}
 \end{aligned} \tag{2.10}$$

and

$$\begin{aligned}
 M_i = & \left(\frac{K_{S_i} \cdot h_i}{2}\right) \cdot X_{i-1} - \left(\frac{K_{S_i} \cdot h_i}{2} - \frac{K_{S_{i+1}} \cdot h_{i+1}}{2}\right) \cdot X_i \\
 & - \left(\frac{K_{S_{i+1}} \cdot h_{i+1}}{2}\right) \cdot X_{i+1} + \left(\frac{K_{S_i} \cdot h_i^2}{4} - \frac{K_i \cdot a_i^2}{2}\right) \cdot \theta_{i-1} \\
 & + \left(\frac{K_i \cdot a_i^2}{2} + \frac{K_{i+1} \cdot a_{i+1}^2}{2} + \frac{K_{S_i} \cdot h_i^2}{4} + \frac{K_{S_{i+1}} \cdot h_{i+1}^2}{4}\right) \cdot \theta_i \\
 & - \left(\frac{K_{i+1} \cdot a_{i+1}^2}{2} - \frac{K_{S_{i+1}} \cdot h_{i+1}^2}{4}\right) \cdot \theta_{i+1}
 \end{aligned} \tag{2.11}$$

Rearranging the Eqs. 2.10 and 2.11 into a matrix form, the stiffness matrix for the four-unit plane model is given in Eq. 2.12 and it can be symbolized as,

$$\left\{ \begin{matrix} P \\ M \end{matrix} \right\} = \begin{bmatrix} K_{xx} & K_{x\theta} \\ K_{\theta x} & K_{\theta\theta} \end{bmatrix} \left\{ \begin{matrix} X \\ \theta \end{matrix} \right\} \tag{2.13}$$

where $[K_{\theta x}]^T = [K_{x\theta}]$

$$\begin{Bmatrix} P_1 \\ P_2 \\ P_3 \\ P_4 \\ \hline M_1 \\ M_2 \\ M_3 \\ M_4 \end{Bmatrix} = \begin{bmatrix} K_{xx} & & & K_{xe} \\ & & & \\ & & & \\ \hline & & & \\ \text{sym} & & & K_{ee} \end{bmatrix} \begin{Bmatrix} x_1 \\ x_2 \\ x_3 \\ x_4 \\ \hline \theta_1 \\ \theta_2 \\ \theta_3 \\ \theta_4 \end{Bmatrix} \quad (2.12)$$

where

$$[K_{xx}] = \begin{bmatrix} K_{11} & K_{12} & 0 & 0 \\ & K_{22} & K_{23} & 0 \\ & & K_{33} & K_{34} \\ \text{sym} & & & K_{44} \end{bmatrix}$$

and

$$K_{11} = K_{s1} + K_{s2}$$

$$K_{12} = -K_{s2}$$

$$K_{22} = K_{s2} + K_{s3}$$

$$K_{23} = -K_{s3}$$

$$K_{33} = K_{s3} + K_{s4}$$

$$K_{34} = -K_{s4}$$

$$K_{44} = K_{s4}$$

$$[K_{x6}] = \begin{bmatrix} K_{11} & K_{12} & 0 & 0 \\ K_{21} & K_{22} & K_{23} & 0 \\ 0 & K_{32} & K_{33} & K_{34} \\ 0 & 0 & K_{43} & K_{44} \end{bmatrix}$$

and

$$K_{11} = -\frac{1}{2} (K_{s_1} \cdot h_1 - K_{s_2} \cdot h_2)$$

$$K_{12} = \frac{1}{2} K_{s_2} \cdot h_2$$

$$K_{21} = -\frac{1}{2} K_{s_2} \cdot h_2$$

$$K_{22} = -\frac{1}{2} (K_{s_2} \cdot h_2 - K_{s_3} \cdot h_3)$$

$$K_{23} = \frac{1}{2} K_{s_3} \cdot h_3$$

$$K_{32} = -\frac{1}{2} K_{s_3} \cdot h_3$$

$$K_{33} = -\frac{1}{2} (K_{s_3} \cdot h_3 - K_{s_4} \cdot h_4)$$

$$K_{34} = \frac{1}{2} K_{s_4} \cdot h_4$$

$$K_{43} = -\frac{1}{2} K_{s_4} \cdot h_4$$

$$K_{44} = -\frac{1}{2} \cdot K_{s_4} \cdot h_4$$

$$[K_{\theta\theta}] = \begin{bmatrix} K_{11} & K_{12} & 0 & 0 \\ & K_{22} & K_{23} & 0 \\ & & K_{33} & K_{34} \\ \text{sym} & & & K_{44} \end{bmatrix}$$

and

$$K_{11} = \frac{1}{2} (a_1^2 \cdot K_1 + a_2^2 \cdot K_2) + \frac{1}{4} (K_{s_1} \cdot h_1^2 + K_{s_2} \cdot h_2^2)$$

$$K_{12} = -\frac{1}{2} a_2^2 \cdot K_2 + \frac{1}{4} K_{s_2} \cdot h_2^2$$

$$K_{22} = \frac{1}{2} (a_2^2 \cdot K_2 + a_3^2 \cdot K_3) + \frac{1}{4} (K_{s_2} \cdot h_2^2 + K_{s_3} \cdot h_3^2)$$

$$K_{23} = -\frac{1}{2} a_3^2 \cdot K_3 + \frac{1}{4} K_{s_3} \cdot h_3^2$$

$$K_{33} = \frac{1}{2} (a_3^2 \cdot K_3 + a_4^2 \cdot K_4) + \frac{1}{4} (K_{s_3} \cdot h_3^2 + K_{s_4} \cdot h_4^2)$$

$$K_{34} = -\frac{1}{2} a_4^2 \cdot K_4 + \frac{1}{4} K_{s_4} \cdot h_4^2$$

$$K_{44} = \frac{1}{2} a_4^2 \cdot K_4 + \frac{1}{4} K_{s_4} \cdot h_4^2$$

2.2.4 Verification of the Model

To ascertain whether the model can be used to represent the behaviour of a building under horizontal loading, a five-storey single bay reinforced concrete frame structure (shown in Fig. 2.5) and a ten-storey reinforced concrete wall structure (shown in Fig. 2.6) are chosen as examples. Based on the proposed model, a 'plane frame' programme and also the moment area method are used to compare the corresponding horizontal displacements of the two structures and their equivalent models, when they are subjected to lateral loads.

Table (2.1) lists the comparison of horizontal displacements in five cases for the five-storey frame building. By using Eq. 2.6 for the flexural spring stiffness (K) and Eq. $K_s = \Sigma \frac{12EI}{h^3}$, which assumes infinite rigid beam for the frame structure, Case I displays the proposed model's horizontal absolute displacements (X_i , where i represents the number of unit of the model or the floor of the building). Case II uses the same shear spring stiffness (K_s) as Case I but greatly increases the flexural spring stiffness (K) to examine the influence of flexural spring stiffness of the model for frame structure. Case III adopts Eq. 2.5 to evaluate the shear spring stiffness and

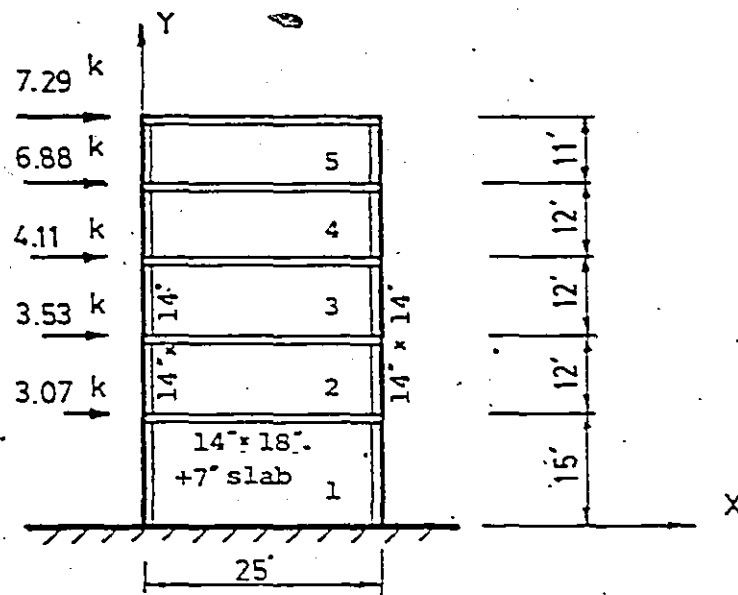


Fig.2.5 Testing Model 1 - R.C. Single Span Frame

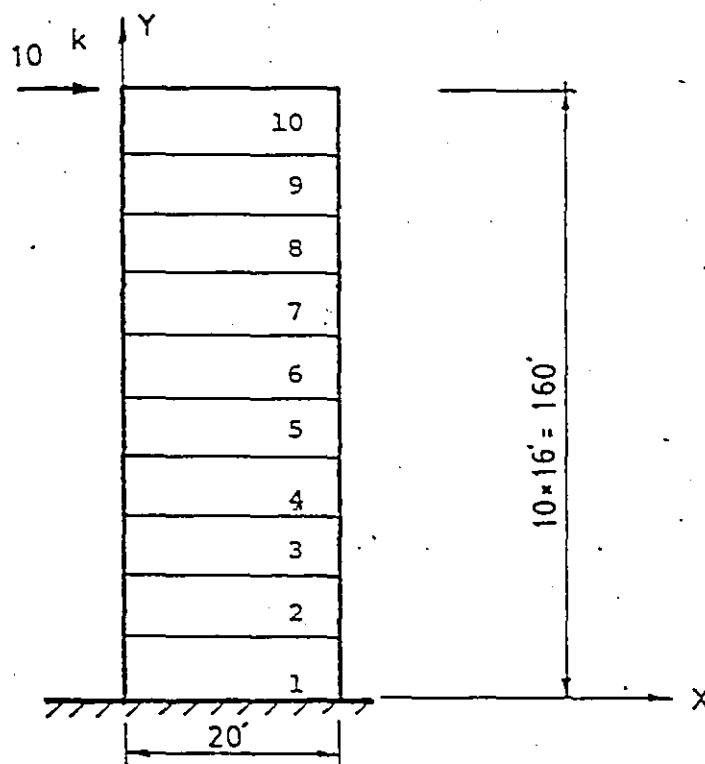


Fig.2.6 Testing Model 2 - R.C. Wall (t=10")

Unit Floor	Height of Unit	Weight of Unit	CASE I			CASE II			CASE III			CASE IV			CASE V
			$K = \frac{AE}{h}$	$K_B = \frac{12EI}{h^3}$	Dis- placement X ₁	K	K _B	X ₁	K	K _B *	X ₁	K	K _B *	X ₁	X ₁
1	15'	57.76 ^k	39200	474.22	0.053	10 ¹⁰	474.22	0.0525	10 ¹⁰	231.98	0.107	10 ¹⁰	313.83	0.0793	0.070
2	12'	57.76 ^k	49000	926.22	0.078	10 ¹⁰	926.22	0.0760	10 ¹⁰	463.17	0.154	10 ¹⁰	463.17	0.126	0.110
3	12'	57.76 ^k	49000	926.22	0.099	10 ¹⁰	926.22	0.0957	10 ¹⁰	463.17	0.194	10 ¹⁰	463.17	0.166	0.160
4	12'	57.76 ^k	49000	926.22	0.116	10 ¹⁰	926.22	0.111	10 ¹⁰	463.17	0.224	10 ¹⁰	463.17	0.196	0.190
5	11'	47.76 ^k	53455	1202.48	0.124	10 ¹⁰	1202.48	0.117	10 ¹⁰	661.44	0.235	10 ¹⁰	661.44	0.207	0.205

$$K_B = \frac{12EI}{h^3} \left[\frac{1}{1 + \frac{2I}{(\frac{I_1}{b_1} + \frac{I_2}{b_2}) h}} \right]$$

Unit - K = Kip/ft
X = ft
E = 3000 ksi

Table 2.1 The Effects of Flexural Stiffness and Shear Stiffness to a Frame Structure. (Static Analysis).

assumes that the contraflexural points are all located at the mid-span of the beams and mid-height of the columns. As a further comparison, the shear spring stiffness evaluation at the ground floor of the frame building is modified in Case IV. The contraflexural points of the columns at the ground floor are raised to $2/3 H_1$ to consider that the columns at the fixed end are not allowed to rotate. By using the 'plane frame' programme, Case V displays the 'exact' static horizontal displacements (X_i , $i = 1$ to 5) for the 'real' frame building. Some observations can be generalized as follows:

- (1) The flexural spring stiffness (K) is an insignificant factor in frame structures. It can be deduced from Cases I and II in which the displacements are very close despite the fact that the magnitude of flexural spring stiffness (K) are changed greatly in Case II.
- (2) The assumption of flexible floor beams is significant in assessing the shear stiffness for frame structures. For example, the shear stiffness (K_s) calculated using Eq. 2.5 in Case III is almost 50% that of Cases I and II.
- (3) To allow for the flexibility of the floor beams and columns, the assumption of points of contraflexure at mid-span of beams and mid-height of columns is valid to most of the frame structure. However, the end condition of the columns at the ground should be taken into account. In Case IV, the inflection points of columns move upward at about $2/3 H_1$, as suggested by W. Schueller^[18], and the lateral displacements calculated in this case are the closest to the 'exact' solution given by the 'plane frame' programme indicated in Case V.

The validity of the model to represent wall structure can be studied in Table 2.2. According to Eqs. 2.3 and 2.4, the stiffnesses of shear and flexural springs are used to calculate the horizontal displacements for the reinforced concrete wall structure in Case I. By keeping the same flexural spring stiffness as in Case I, Case II considers the magnitude of shear spring stiffness to be increased grossly. As a comparison, the 'exact' horizontal displacements of the wall structure computed by moment area method are listed in Case III.

Some observations can be drawn as follows:

- (1) The shear spring stiffness is an insensible parameter to wall structure. The comparison of lateral displacements in Case I and Case II show only 2% change in lateral displacement; while the shear spring stiffness K_s is changed by 8,440 times.
- (2) The static lateral displacements are nearly equal in Case II from the model and Case III from the 'real' structure. This is a result that in beam theory, shear deformation of the beam is neglected.

Based on these sample calculations, it is felt that the mathematical model is a fairly good model to represent the behaviour of wall and frame structures subjected to lateral loading. Moreover, ignoring shear deformation in wall structure and flexural deformation in frame structure is justified in evaluating the shear and flexural spring stiffnesses respectively. This model will be used in the dynamic analysis of building in the remaining portion of this thesis:

Unit Floor	Height	Weight	CASE I			CASE II			CASE III (Moment Area Method)
			K	K _g	X.10 ⁻²	K	K _g	X.10 ⁻²	X.10 ⁻²
1	16'	3.11 ^k	107500	118507.8	0.065	107500	10 ¹⁰	0.057	0.058
2	16'	3.11 ^k	107500	118507.8	0.237	107500	10 ¹⁰	0.220	0.222
3	16'	3.11 ^k	107500	118507.8	0.505	107500	10 ¹⁰	0.479	0.482
4	16'	3.11 ^k	107500	118507.8	0.855	107500	10 ¹⁰	0.822	0.826
5	16'	3.11 ^k	107500	118507.8	1.28	107500	10 ¹⁰	1.24	1.240
6	16'	3.11 ^k	107500	118507.8	1.76	107500	10 ¹⁰	1.71	1.715
7	16'	3.11 ^k	107500	118507.8	2.29	107500	10 ¹⁰	2.23	2.237
8	16'	3.11 ^k	107500	118507.8	2.85	107500	10 ¹⁰	2.79	2.794
9	16'	3.11 ^k	107500	118507.8	3.44	107500	10 ¹⁰	3.37	3.376
10	16'	3.11 ^k	107500	118507.8	4.04	107500	10 ¹⁰	3.96	3.969

Unit : E = 4300 ksi
K = Kip/ft
X = ft

Table 2.2 The Effect of Flexural Stiffness and Shear Stiffness to a Wall Structure. (Static Analysis)

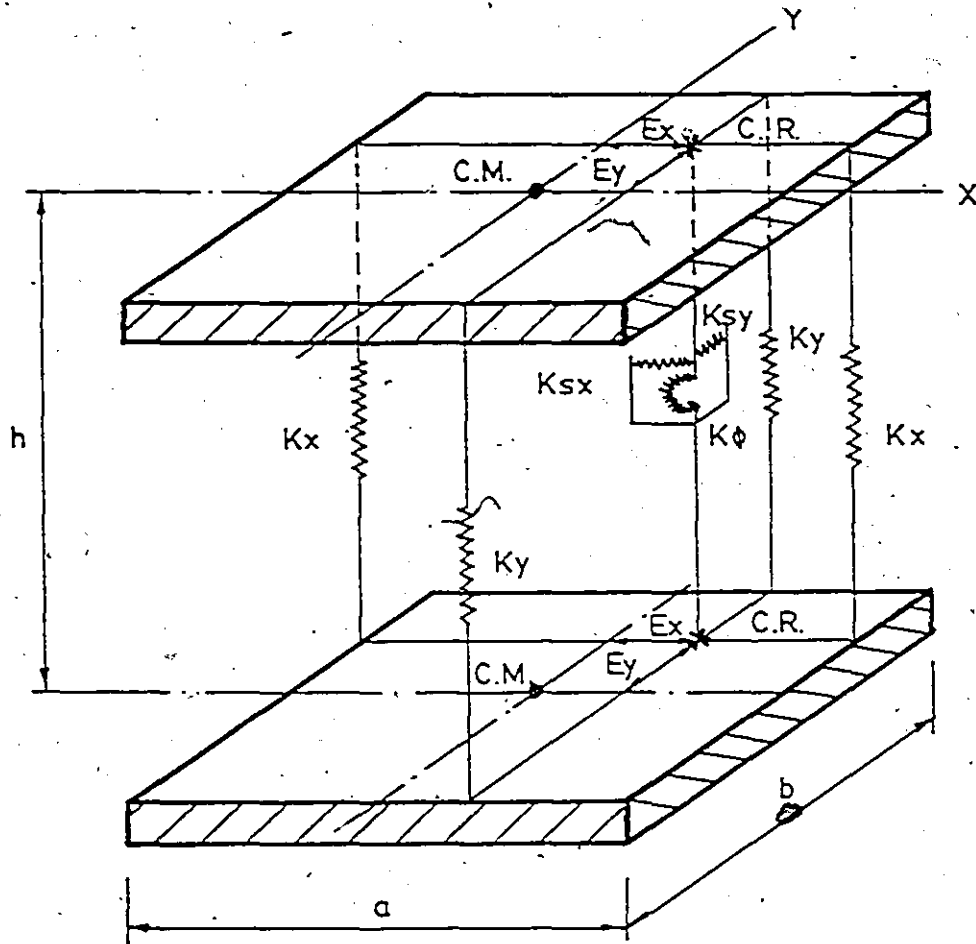
2.3 Spatial Structure Modelling

2.3.1 The Configuration of the Model

In order to study the coupled torsional-translational seismic responses on buildings, a three dimensional model based on the similar features of the plane structure model is created as shown in Fig. 2.7. Analogous to Fig. 2.1, K_{sx} , K_{sy} and K_x , K_y are the shear springs and flexural springs of the unit in X and Y directions respectively. For the unit with center of mass and center of rigidity does not coincide, an additional torsional spring K_ϕ is added between the units and e_x , e_y represent the eccentricities in the X and Y directions.

Any transverse force applied through the center of rigidity (or shear center) will not cause torsion, also, when the structure is subjected to applied torque, the twist takes place around the shear center and there is no lateral displacement. Following these mechanical principles and the definition of stiffness, the shear springs are arranged to allow the reaction forces in both X and/or Y directions to pass through the shear center, the flexural springs in either X or Y direction are located in a plane which crosses the center of rigidity. To represent the torsional stiffness of the model the torsional spring is left in a position to let the torque be directly applied around the shear center (shown in Fig. 2.7). Therefore, when the reference point is at the center of rigidity, the stiffness matrix $[K]$ of this model would be a diagonal matrix, regardless whether it represents a symmetrical, monosymmetrical or asymmetrical structure. Symbolically, the stiffness matrix of a unit model, referring to the center of rigidity is

$$[K] = \begin{bmatrix} K_x & 0 & 0 \\ 0 & K_y & 0 \\ 0 & 0 & K_\phi \end{bmatrix} \quad (2.14)$$



K_x, K_y - Flexural springs in X and Y axes
 K_{sx}, K_{sy} - Shear springs in X and Y axes
 K_ϕ - Torsional spring

Fig.2.7 Spatial Spring Model

in which K_x and K_y are the translational stiffnesses of the unit in X, Y axes directions respectively and K_ϕ is the torsional stiffness of the unit referring to its center of rigidity.

2.3.2 The Formulation of General Stiffness Matrix

In the dynamic analysis, the resultant of the inertia forces act at the center of mass, the elastic forces occur at the center of rigidity (shown in Fig. 2.8). When these two centers do not coincide, torsional response will result.

For a spatial multi-unit model, the stiffness matrix and mass matrix can be very complex, especially when the reference point is arbitrary. In order to illustrate the process of stiffness matrix formulation, a monosymmetrical multi-unit model (shown in Figs. 2.9 and 2.10) with reference point of each unit at the center of mass is studied in detail. The units of the model are uniform and the centers of mass and rigidity of each unit are originally located on two vertical axes.

The study is split into three parts which are lateral response in X direction, torsional and overturning responses of the unit. Fig. 2.10 displays that the absolute lateral displacement X_i of any unit is:

$$X_i = X_{i-1} + \Delta X_i + (\theta_{i-1} + \theta_i) \cdot \frac{h_i}{2} + (\phi_i - \phi_{i-1}) \cdot e_{y_i}$$

Therefore, the relative displacement ΔX_i of shear spring of unit i is:

$$\Delta X_i = X_i - X_{i-1} - (\theta_{i-1} + \theta_i) \cdot \frac{h_i}{2} - (\phi_i - \phi_{i-1}) \cdot e_{y_i} \quad (2.15)$$

The equilibrium equation of motion for one unit in the X direction is

$$M_i \ddot{X}_i + K_{sx_i} \cdot \Delta X_i - K_{sx_{i+1}} \cdot \Delta X_{i+1} = -M_i \ddot{g}_x(t)_i \quad (2.16)$$

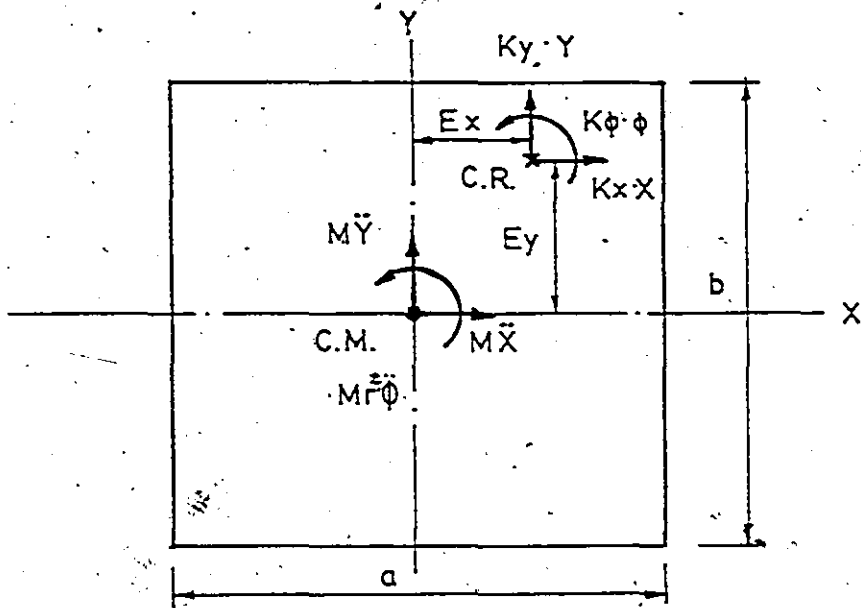


Fig.2.8 Relationship of Elastic and Inertia Forces

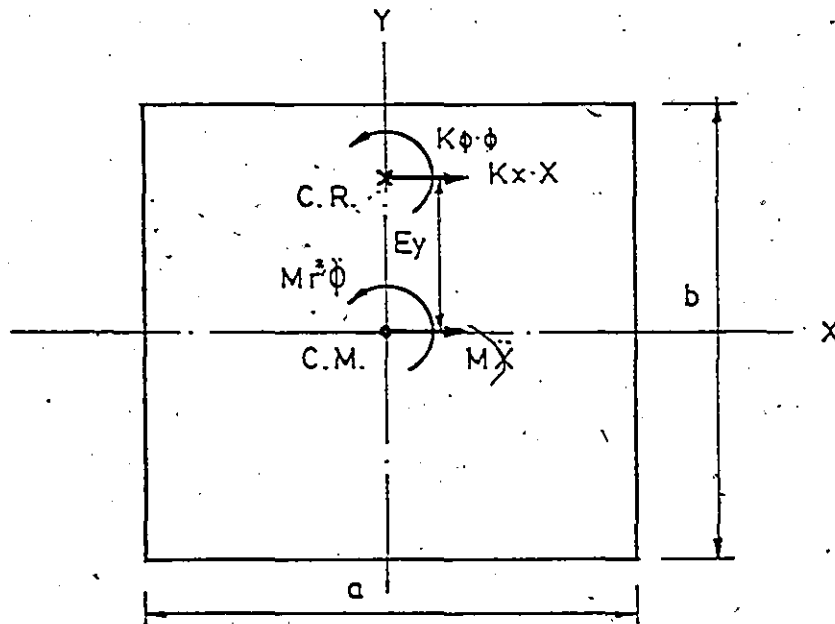


Fig.2.9 Mono-symmetrical Unit Plan

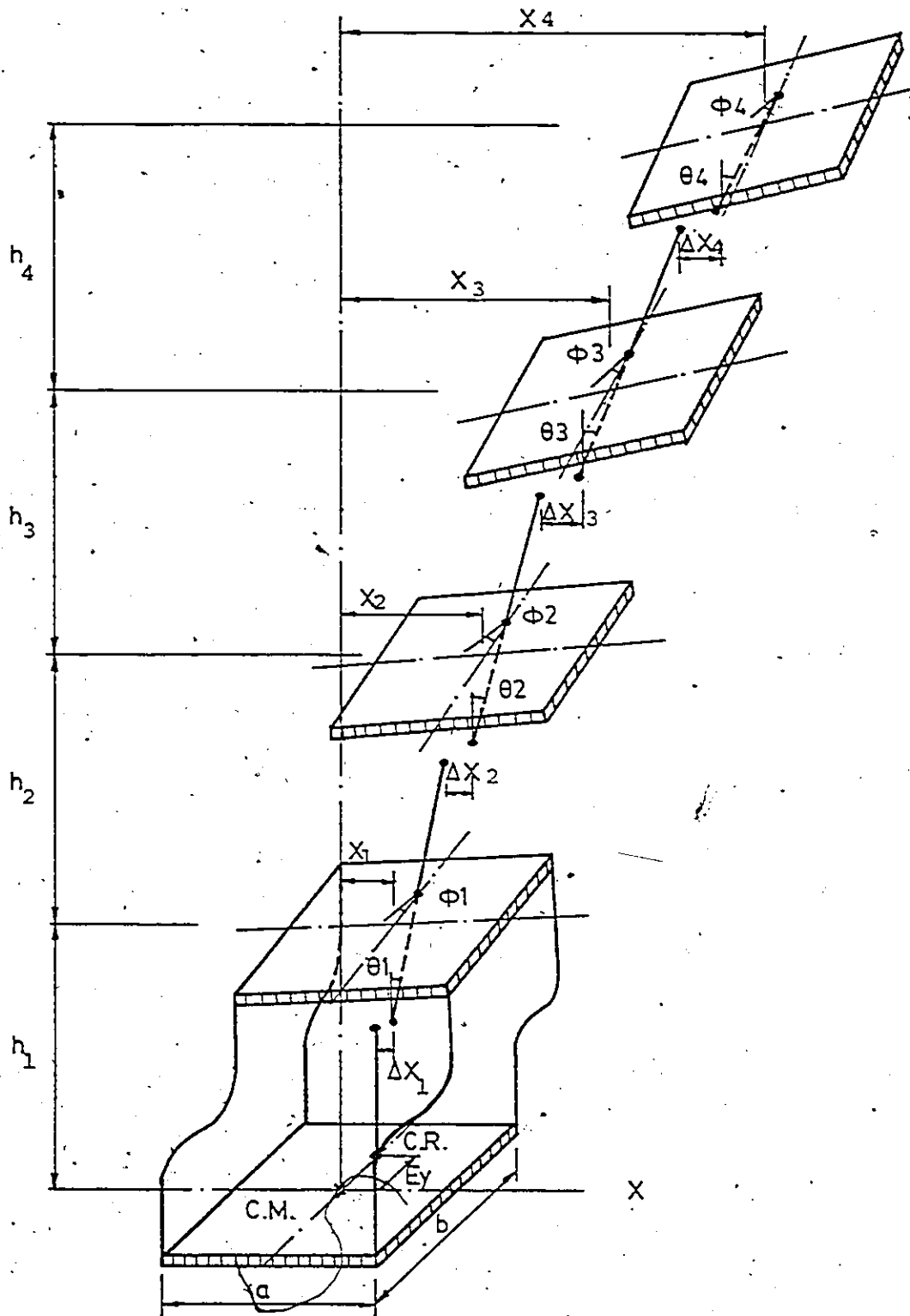


Fig.2.10 Multi-unit Spatial Model

Substituting ΔX_i into Eq. 2.16 yields,

$$\begin{aligned}
 & M_i \ddot{X}_i - (K_{sx_i}) \cdot X_{i-1} + (K_{sx_i} + K_{sx_{i+1}}) \cdot X_i - (K_{sx_{i+1}}) \cdot X_{i+1} \\
 & - (K_{sx_i} \cdot \frac{h_i}{2}) \cdot \theta_{i-1} - (K_{sx_i} \cdot \frac{h_i}{2} - K_{sx_{i+1}} \cdot \frac{h_{i+1}}{2}) \cdot \theta_i \\
 & + (K_{sx_{i+1}} \cdot \frac{h_{i+1}}{2}) \cdot \theta_{i+1} + (K_{sx_i} \cdot e_{y_i}) \cdot \phi_{i-1} \\
 & - (K_{sx_i} \cdot e_{y_i} + K_{sx_{i+1}} \cdot e_{y_{i+1}}) \cdot \phi_i + (K_{sx_{i+1}} \cdot e_{y_{i+1}}) \cdot \phi_{i+1} \\
 & = -M_i \bar{g}_x(t)_i
 \end{aligned} \tag{2.17}$$

In matrix form, it is shown in Eq. 2.18.

The equilibrium equation of torsional motion at the center of mass is

$$\begin{aligned}
 & I_{\phi} \ddot{\phi} + K_{\phi_i} \Delta \phi_i - K_{\phi_{i+1}} \cdot \Delta \phi_{i+1} - K_{sx_i} \cdot \Delta X_i \cdot e_{y_i} \\
 & + K_{sx_{i+1}} \cdot \Delta X_{i+1} \cdot e_{y_{i+1}} = -M_i \bar{y}_i^2 \bar{g}_i(t)
 \end{aligned} \tag{2.19}$$

Substituting Eq. 2.15 into Eq. 2.19 yields:

$$\begin{aligned}
 & I_{\phi} \ddot{\phi} + (K_{sx_i} \cdot e_{y_i}) X_{i-1} - (K_{sx_i} \cdot e_{y_i} + K_{sx_{i+1}} \cdot e_{y_{i+1}}) X_i \\
 & + (K_{sx_{i+1}} \cdot e_{y_{i+1}}) X_{i+1} + (K_{sx_i} \cdot e_{y_i} \cdot \frac{h_i}{2}) \theta_{i-1} \\
 & + (K_{sx_i} \cdot e_{y_i} \cdot \frac{h_i}{2} - K_{sx_{i+1}} \cdot e_{y_{i+1}} \cdot \frac{h_{i+1}}{2}) \theta_i \\
 & - (K_{sx_{i+1}} \cdot e_{y_{i+1}} \cdot \frac{h_{i+1}}{2}) \theta_{i+1} - (K_{\phi_i} + K_{sx_i} \cdot e_{y_i}^2) \phi_{i-1}
 \end{aligned}$$

$$\begin{aligned}
 &+ (K_{\phi_i} + K_{\phi_{i+1}} + K_{sx_i} \cdot e_{y_i}^2 + K_{sx_{i+1}} \cdot e_{y_{i+1}}^2) \phi_i \\
 &- (K_{\phi_{i+1}} + K_{sx_{i+1}} \cdot e_{y_{i+1}}^2) \cdot \phi_{i+1} = - I_{\phi} \ddot{g}_{\phi}(t)
 \end{aligned}
 \tag{2.20}$$

Also, Eq. 2.20 can be rewritten into a matrix form as Eq. 2.21.

$$\begin{bmatrix} M_1 & 0 & 0 & \dots & 0 \\ & M_2 & 0 & 0 & \\ & & \ddots & & \\ & & & 0 & \\ \text{sym} & & & & M_n \end{bmatrix} \begin{Bmatrix} \bar{x}_1 \\ \bar{x}_2 \\ \vdots \\ \vdots \\ \bar{x}_n \end{Bmatrix} + [K_{xx} \mid K_{x\theta} \mid K_{x\phi}] \begin{Bmatrix} x_1 \\ x_2 \\ \theta_1 \\ \theta_2 \\ \vdots \\ \phi_1 \\ \phi_2 \\ \vdots \end{Bmatrix} = -[M][I] \ddot{g}_x(t)
 \tag{2.18}$$

where

$$[K_{xx}] = \begin{bmatrix} K_{11} & K_{12} & 0 & \dots & 0 \\ & K_{22} & K_{23} & 0 & \dots & 0 \\ & & \ddots & & & \vdots \\ & & & & & K_{n-1, n} \\ & & & & & K_{nn} \end{bmatrix}$$

and

$$\begin{aligned}
 K_{11} &= K_{sx_1} + K_{sx_2} \\
 K_{12} &= -K_{sx_2} \\
 K_{22} &= K_{sx_2} + K_{sx_3} \\
 K_{23} &= -K_{sx_3} \\
 \vdots & \\
 K_{n-1, n} &= -K_{sx_n} \\
 K_{nn} &= K_{sx_n}
 \end{aligned}$$

$$[K_{x\theta}] = \begin{bmatrix} K_{11} & K_{12} & 0 & \dots & 0 \\ K_{21} & K_{22} & K_{23} & 0 & \dots & 0 \\ 0 & & & & & \vdots \\ \vdots & & & & & K_{n-1, n} \\ 0 & & & & & K_{n, n-1} & K_{nn} \end{bmatrix}$$

and

$$K_{11} = \frac{1}{2} (-K_{sx1} \cdot h_1 + K_{sx2} \cdot h_2)$$

$$K_{12} = \frac{1}{2} \cdot K_{sx2} \cdot h_2$$

$$K_{21} = -\frac{1}{2} \cdot K_{sx2} \cdot h_2$$

$$K_{22} = \frac{1}{2} (-K_{sx2} \cdot h_2 + K_{sx3} \cdot h_3)$$

$$K_{23} = \frac{1}{2} \cdot K_{sx3} \cdot h_3$$

$$\vdots$$

$$K_{n-1, n} = \frac{1}{2} K_{sxn} \cdot h_n$$

$$K_{n, n-1} = -\frac{1}{2} \cdot K_{sxn} \cdot h_n$$

$$K_{nn} = -\frac{1}{2} \cdot K_{sxn} \cdot h_n$$

$$[K_{x\phi}] = \begin{bmatrix} K_{11} & K_{12} & 0 & \dots & 0 \\ & K_{22} & K_{23} & \dots & 0 \\ \text{sym} & & & & \vdots \\ & & & & K_{n-1, n} \\ & & & & & K_{nn} \end{bmatrix}$$

and

$$K_{11} = -(K_{sx1} \cdot e_{y1} + K_{sx2} \cdot e_{y2})$$

$$K_{12} = K_{sx2} \cdot e_{y2}$$

$$K_{22} = -(K_{sx2} \cdot e_{y2} + K_{sx3} \cdot e_{y3})$$

$$K_{23} = K_{sx3} \cdot e_{y3}$$

$$\vdots$$

$$K_{n-1, n} = K_{sxn} \cdot e_{yn}$$

$$K_{nn} = -K_{sxn} \cdot e_{yn}$$

$$\begin{bmatrix} I_{\phi_1} & 0 & \dots & 0 \\ & I_{\phi_2} & 0 & \dots & 0 \\ & & \ddots & & \\ & & & I_{\phi_n} & \\ \text{sym} & & & & \end{bmatrix} \begin{Bmatrix} \ddot{\phi}_1 \\ \ddot{\phi}_2 \\ \vdots \\ \ddot{\phi}_n \end{Bmatrix} + [K_{\phi x} \mid K_{\phi \theta} \mid K_{\phi \phi}] \begin{Bmatrix} X_1 \\ X_2 \\ \vdots \\ \theta_1 \\ \theta_2 \\ \vdots \\ \phi_1 \\ \phi_2 \end{Bmatrix}$$

$$= - [I_{\phi}] \{I\} \ddot{g}_{\phi}(t) \quad (2.21)$$

where

$$[K_{\phi x}] = \begin{bmatrix} K_{11} & K_{12} & 0 & \dots & 0 \\ & K_{22} & K_{23} & 0 & \dots & 0 \\ & & & \ddots & & \\ & & & & K_{n-1,n} \\ \text{sym} & & & & & K_{nn} \end{bmatrix}$$

and

$$K_{11} = - (K_{sx_1} \cdot e_{y_1} + K_{sx_2} \cdot e_{y_2})$$

$$K_{12} = K_{sx_2} \cdot e_{y_2}$$

$$K_{22} = - (K_{sx_2} \cdot e_{y_2} + K_{sx_3} \cdot e_{y_3})$$

$$K_{23} = K_{sx_3} \cdot e_{y_3}$$

$$\vdots$$

$$K_{n-1,n} = K_{sx_n} \cdot e_{y_n}$$

$$K_{nn} = - K_{sx_n} \cdot e_{y_n}$$

$$[K_{\phi \theta}] = \begin{bmatrix} K_{11} & K_{12} & 0 & \dots & 0 \\ K_{21} & K_{22} & K_{23} & 0 & \dots & 0 \\ 0 & & & \ddots & & \\ \vdots & & & & K_{n-1,n} \\ 0 & & & & & K_{n,n-1} & K_{nn} \end{bmatrix}$$

and

$$K_{11} = \frac{1}{2} (K_{sx_1} \cdot e_{y_1} \cdot h_1 - K_{sx_2} \cdot e_{y_2} \cdot h_2)$$

$$K_{12} = -\frac{1}{2} \cdot K_{sx_2} \cdot e_{y_2} \cdot h_2$$

$$K_{21} = \frac{1}{2} \cdot K_{sx_2} \cdot e_{y_2} \cdot h_2$$

$$K_{22} = \frac{1}{2} (K_{sx_2} \cdot e_{y_2} \cdot h_2 - K_{sx_3} \cdot e_{y_3} \cdot h_3)$$

$$K_{23} = -\frac{1}{2} \cdot K_{sx_3} \cdot e_{y_3} \cdot h_3$$

$$\vdots$$

$$K_{n-1,n} = -\frac{1}{2} \cdot K_{sx_n} \cdot e_{y_n} \cdot h_n$$

$$K_{n,n-1} = \frac{1}{2} \cdot K_{sx_n} \cdot e_{y_n} \cdot h_n$$

$$K_{nn} = \frac{1}{2} \cdot K_{sx_n} \cdot e_{y_n}$$

$$[K_{\phi\phi}] = \begin{bmatrix} K_{11} & K_{12} & 0 & \dots & 0 \\ & K_{22} & K_{23} & 0 & \dots & 0 \\ \text{sym} & & & & & K_{n-1,n} \\ & & & & & & & & & K_{nn} \end{bmatrix}$$

and

$$K_{11} = K_{\phi_1} + K_{\phi_2} + K_{sx_1} \cdot e_{y_1}^2 + K_{sx_2} \cdot e_{y_2}^2$$

$$K_{12} = - (K_{\phi_2} + K_{sx_2} \cdot e_{y_2}^2)$$

$$K_{22} = K_{\phi_2} + K_{\phi_3} + K_{sx_2} \cdot e_{y_2}^2 + K_{sx_3} \cdot e_{y_3}^2$$

$$K_{23} = - (K_{\phi_3} + K_{sx_3} \cdot e_{y_3}^2)$$

$$\vdots$$

$$K_{n-1,n} = - (K_{\phi_n} + K_{sx_n} \cdot e_{y_n}^2)$$

$$K_{nn} = K_{\phi_n} + K_{sx_n} \cdot e_{y_n}^2$$

In Fig. 2.10, θ_i denotes rocking angle of unit i . The equilibrium equation of rocking motion can be written as,

$$I_{\theta_i} \ddot{\theta}_i - K_{X_{i+1}} (\theta_{i+1} - \theta_i) \cdot \frac{a_{i+1}^2}{2} + K_{X_i} (\theta_i - \theta_{i-1}) \cdot \frac{a_i^2}{2} - K_{S_{X_{i+1}}} \cdot \Delta X_{i+1} \cdot \frac{h_{i+1}}{2} - K_{S_{X_i}} \cdot \Delta X_i \cdot \frac{h_i}{2} = -I_{\theta_i} \cdot \ddot{g}_{\theta_i}(t) \quad (2.22)$$

Again, substituting ΔX_i in Eq. 2.15 into Eq. 2.22, one obtains:

$$I_{\theta_i} \ddot{\theta}_i + \left(\frac{K_{S_i} h_i}{2} \right) X_{i-1} - \left(\frac{K_{S_i} h_i - K_{S_{i+1}} h_{i+1}}{2} \right) X_i - \frac{K_{S_{i+1}} h_{i+1}}{2} X_{i+1} - \left(\frac{K_{X_i} \cdot a_i^2}{2} + \frac{K_{S_i} \cdot h_i^2}{4} \right) \theta_{i-1} + \left(\frac{K_{X_i} \cdot a_i^2 + K_{i+1} \cdot a_{i+1}^2}{2} + \frac{K_{S_i} h_i^2 + K_{S_{i+1}} h_{i+1}^2}{4} \right) \theta_i + \left(-\frac{K_{X_{i+1}} \cdot a_{i+1}^2}{2} + \frac{K_{S_{i+1}} \cdot h_{i+1}^2}{4} \right) \theta_{i+1} - \left(\frac{K_{S_i} h_i e_{y_i}}{2} \right) \phi_{i-1} + \left(\frac{K_{S_i} h_i e_{y_i} - K_{S_{i+1}} h_{i+1} e_{y_{i+1}}}{2} \right) \phi_i + \left(\frac{K_{S_{i+1}} h_{i+1} e_{y_{i+1}}}{2} \right) \phi_{i+1} = -I_{\theta_i} \cdot \ddot{g}_{\theta_i}(t) \quad (2.23)$$

or, Eq. 2.23 can be formed into a matrix as Eq. 2.24.

The assembly of equations 2.18, 2.21 and 2.24 leads to the undamped general equation of the motion in x direction, when the reference point is at the center of mass namely,

$$\begin{bmatrix} M & 0 & 0 \\ 0 & I_{\theta} & 0 \\ 0 & 0 & I_{\phi} \end{bmatrix} \begin{Bmatrix} \ddot{X} \\ \ddot{\theta} \\ \ddot{\phi} \end{Bmatrix} + [K] \begin{Bmatrix} X \\ \theta \\ \phi \end{Bmatrix} = - \begin{bmatrix} M & 0 & 0 \\ 0 & I_{\theta} & 0 \\ 0 & 0 & I_{\phi} \end{bmatrix} \cdot \begin{Bmatrix} \ddot{g}_x \\ \ddot{g}_{\theta} \\ \ddot{g}_{\phi} \end{Bmatrix} \quad (2.25)$$

where the generalized stiffness matrix $[K]$ is

$$[K] = \begin{bmatrix} K_{xx} & K_{x\theta} & K_{x\phi} \\ K_{\theta x} & K_{\theta\theta} & K_{\theta\phi} \\ K_{\phi x} & K_{\phi\theta} & K_{\phi\phi} \end{bmatrix} \quad (2.26)$$

By eliminating rocking moment response, assuming $I_\theta = 0$, the overturning rotation θ can be written as

$$\theta = -K_{\theta\theta}^{-1} (K_{\theta x} \cdot X + K_{\theta\phi} \cdot \phi) \quad (2.27)$$

Therefore, a condensed stiffness matrix $[\bar{K}]$ results,

$$[\bar{K}] = \begin{bmatrix} (K_{xx} - K_{x\theta} \cdot K_{\theta\theta}^{-1} \cdot K_{\theta x}) & (K_{x\phi} - K_{x\theta} \cdot K_{\theta\theta}^{-1} \cdot K_{\theta\phi}) \\ (K_{\phi x} - K_{\phi\theta} \cdot K_{\theta\theta}^{-1} \cdot K_{\theta x}) & (K_{\phi\phi} - K_{\phi\theta} \cdot K_{\theta\theta}^{-1} \cdot K_{\theta\phi}) \end{bmatrix} \quad (2.28)$$

This condensed matrix $[\bar{K}]$ is still a symmetrical matrix, because

$$(K_{x\phi} - K_{x\theta} \cdot K_{\theta\theta}^{-1} \cdot K_{\theta\phi})^T = (K_{\phi x} - K_{\phi\theta} \cdot K_{\theta\theta}^{-1} \cdot K_{\theta x})$$

since

$$(A-B)^T = A^T - B^T$$

$$(ABC)^T = C^T \cdot B^T \cdot A^T$$

Using the same procedure, the general dynamic equation of motion in Y axis for the spatial modelling can be obtained. The condensed stiffness matrix $[\bar{K}]$ to an asymmetrical structure, in which the reference point is the center of mass, can be written as

$$[\bar{K}] = \begin{bmatrix} (K_{xx} - K_{x\theta} \cdot K_{\theta\theta}^{-1} \cdot K_{\theta x}) & 0 & (K_{x\phi} - K_{x\theta} \cdot K_{\theta\theta}^{-1} \cdot K_{\theta\phi}) \\ 0 & (K_{yy} - K_{y\theta} \cdot K_{\theta\theta}^{-1} \cdot K_{\theta y}) & (K_{y\phi} - K_{y\theta} \cdot K_{\theta\theta}^{-1} \cdot K_{\theta\phi}) \\ (K_{\phi x} - K_{\phi\theta} \cdot K_{\theta\theta}^{-1} \cdot K_{\theta x}) & (K_{\phi y} - K_{\phi\theta} \cdot K_{\theta\theta}^{-1} \cdot K_{\theta y}) & (K_{\phi\phi} - K_{\phi\theta} \cdot K_{\theta\theta}^{-1} \cdot K_{\theta\phi}) \\ \cdot K_{\theta x}) & \cdot K_{\theta y}) & -K_{\phi\theta} \cdot K_{\theta\theta}^{-1} \cdot K_{\theta\phi}) \end{bmatrix}$$

$$\begin{bmatrix} I_{e_1} & 0 & \dots & 0 \\ I_{e_2} & 0 & \dots & 0 \\ \vdots & \vdots & \ddots & \vdots \\ \text{sym} & & & I_{e_n} \end{bmatrix} \begin{Bmatrix} \ddot{\theta}_1 \\ \ddot{\theta}_2 \\ \vdots \\ \ddot{\theta}_n \end{Bmatrix} + [K_{\theta x} \mid K_{\theta \theta} \mid K_{\theta \phi}] \begin{Bmatrix} x_1 \\ x_2 \\ \vdots \\ \theta_1 \\ \theta_2 \\ \vdots \\ \phi_1 \\ \phi_2 \end{Bmatrix}$$

$$= - [I_{\theta}] \{I\} \ddot{g}_{\theta}(t) \quad (2.24)$$

where

$$[K_{\theta x}] = \begin{bmatrix} K_{11} & K_{12} & 0 & \dots & 0 \\ K_{21} & K_{22} & K_{23} & 0 & \dots & 0 \\ \vdots & \vdots & \vdots & \ddots & \vdots & \vdots \\ & & & & K_{n-1,n} & \\ & & & & & K_{nn} \end{bmatrix}$$

and

$$K_{11} = \frac{1}{2} (-K_{sx_1} \cdot h_1 + K_{sx_2} \cdot h_2)$$

$$K_{12} = -\frac{1}{2} \cdot K_{sx_2} \cdot h_2$$

$$K_{21} = \frac{1}{2} \cdot K_{sx_2} \cdot h_2$$

$$K_{22} = \frac{1}{2} (-K_{sx_2} \cdot h_2 + K_{sx_3} \cdot h_3)$$

$$K_{23} = -\frac{1}{2} \cdot K_{sx_3} \cdot h_3$$

$$\vdots$$

$$K_{n-1,n} = -\frac{1}{2} \cdot K_{sx_n} \cdot h_n$$

$$K_{n,n-1} = \frac{1}{2} \cdot K_{sx_n} \cdot h_n$$

$$K_{nn} = -\frac{1}{2} \cdot K_{sx_n} \cdot h_n$$

$$[K_{\theta \theta}] = \begin{bmatrix} K_{11} & K_{12} & 0 & \dots & 0 \\ & K_{22} & K_{23} & 0 & \dots & 0 \\ \text{sym} & & & & & K_{n-1,n} \\ & & & & & & K_{nn} \end{bmatrix}$$

2.3.3 The General Equation of Motion

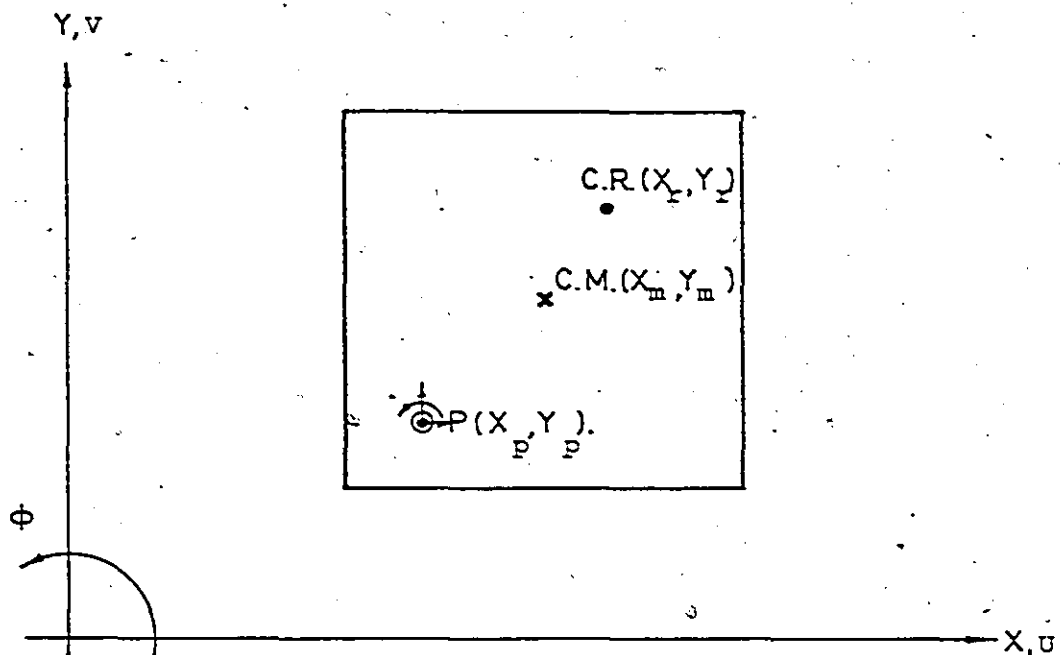
Eq. 2.25 represents the general equation of motion where the reference point is at the center of mass. While the reference point of motion is arbitrary in the spatial modelling, the mass matrix will no longer be a diagonal matrix.

Fig. 2.11 shows that in the X and Y coordinate system, an arbitrary point p and centers of mass and rigidity are located at (X_p, Y_p) , (X_m, Y_m) and (X_r, Y_r) respectively. The translational displacements in the X and Y axes of any point (i) of the unit are defined as U_i and V_i and the rotation of the unit as counter-clockwise direction as positive sign is indicated by ϕ . The general equation of undamped motion in terms of the displacements of an arbitrary point p for a single unit is

$$\begin{aligned}
 & \begin{bmatrix} M & 0 & M(Y_p - Y_m) \\ 0 & M & -M(X_p - X_m) \\ -M(Y_p - Y_m) & -M(X_p - X_m) & I_p \end{bmatrix} \begin{Bmatrix} \ddot{U}_p \\ \ddot{V}_p \\ \ddot{\phi} \end{Bmatrix} \\
 + & \begin{bmatrix} K_x & 0 & K_x(Y_p - Y_r) \\ 0 & K_y & -K_y(X_p - X_r) \\ K_x(Y_p - Y_r) & -K_y(X_p - X_r) & K_p^\phi \end{bmatrix} \begin{Bmatrix} U_p \\ V_p \\ \phi \end{Bmatrix} \\
 = & \begin{bmatrix} M & 0 & 0 \\ 0 & M & 0 \\ 0 & 0 & I_\phi \end{bmatrix} \begin{Bmatrix} \ddot{g}_x \\ \ddot{g}_y \\ \ddot{\phi} \end{Bmatrix}
 \end{aligned}$$

where $I_p = I_m + M[(X_p - X_m)^2 + (Y_p - Y_m)^2]$

$$K_p^\phi = K_R + K_x (Y_p - Y_r)^2 + K_y (X_p - X_r)^2 \quad (2.30)$$



POINT	POSITION	DISPLACEMENTS
P	(X_p, Y_p)	U_p, V_p, ϕ
CM	(X_m, Y_m)	U_m, V_m, ϕ
CR	(X_r, Y_r)	U_r, V_r, ϕ

Fig. 2.11 Geometric Relations of Arbitrary Point and Centers of Mass, and Rigidity

In equation 2.30, I_m is mass polar moment of inertia of the unit referred to the mass center. The elements of stiffness matrix can be expressed by the torsional (K_ϕ) and shear (K_s), flexural (K) spring stiffness in both X and Y directions of the model:

$$K_x = K_{sx} - \left(-\frac{K_{sx} \cdot h}{2}\right) \cdot \left(\frac{K_x \cdot a^2}{2} + \frac{K_{sx} \cdot h^2}{4}\right)^{-1} \cdot \left(-\frac{K_{sx} \cdot h}{2}\right)$$

$$K_y = K_{sy} - \left(-\frac{K_{sy} \cdot h}{2}\right) \cdot \left(\frac{K_y \cdot b^2}{2} + \frac{K_{sy} \cdot h^2}{4}\right)^{-1} \cdot \left(-\frac{K_{sy} \cdot h}{2}\right)$$

$$K_x(Y_p - Y_r) = -K_{sx} \cdot (Y_p - Y_r) - \left(-\frac{K_{sx} \cdot h}{2}\right) \cdot \left(\frac{K_x \cdot a^2}{2} + \frac{K_{sx} \cdot h^2}{4}\right)^{-1} \cdot \left[\frac{K_{sx} \cdot h}{2} \cdot (Y_p - Y_r)\right]$$

$$K_y(X_p - X_r) = -K_{sy} \cdot (X_p - X_r) - \left(-\frac{K_{sy} \cdot h}{2}\right) \cdot \left(\frac{K_y \cdot b^2}{2} + \frac{K_{sy} \cdot h^2}{4}\right)^{-1} \cdot \left[\frac{K_{sy} \cdot h}{2} \cdot (X_p - X_r)\right]$$

and $K_R = K_\phi$ is the torsional stiffness of the unit referred to its center of rigidity. To arbitrary point p, the term K_p^ϕ can be expressed as

$$K_p^\phi = [K_\phi + K_{sx} \cdot (Y_p - Y_r)^2 + K_{sy} \cdot (X_p - X_r)^2 - \{[K_{sx} \cdot \frac{h}{2}(Y_p - Y_r)] \cdot \left(\frac{K_x \cdot a^2}{2} + \frac{K_{sx} \cdot h^2}{4}\right)^{-1} \cdot \left[\frac{K_{sx} \cdot h}{2} \cdot (Y_p - Y_r)\right] - [K_{sy} \cdot \frac{h}{2}(X_p - X_r)] \cdot \left(\frac{K_y \cdot b^2}{2} + \frac{K_{sy} \cdot h^2}{4}\right)^{-1} \cdot \left[\frac{K_{sy} \cdot h}{2} \cdot (X_p - X_r)\right]\}]$$

When Eq. 2.30 applies to a multi-unit model, each element of the mass matrix in Eq. 2.30 becomes a diagonal matrix. Let $EMY_i = Y_{p_i} - Y_{m_i}$ and $EMX_i = X_{p_i} - X_{m_i}$, the mass matrix for a multi-unit model can be written as

$$\begin{array}{c}
 \left[\begin{array}{ccc|ccc|ccc}
 m_1 & 0 & \dots & 0 & m_1 E M Y_1 & 0 & \dots & 0 \\
 & m_2 & & 0 & 0 & m_2 E M Y_2 & & 0 \\
 & & \ddots & & \vdots & & \ddots & \\
 & & & m_n & 0 & & & m_n E M Y_n \\
 \hline
 & m_1 & 0 & \dots & 0 & -m_1 E M X_1 & 0 & \dots & 0 \\
 & & m_2 & & 0 & 0 & -m_2 E M X_2 & 0 & \dots & 0 \\
 & & & \ddots & & \vdots & & \ddots & \\
 & & & & m_n & 0 & & & -m_n E M X_n \\
 \hline
 & & & & & I_{p1} & 0 & \dots & 0 \\
 & & & & & & I_{p2} & & 0 \\
 & & & & & & & \ddots & \\
 & & & & & & & & I_{pn} \\
 \hline
 & & & & & & & & & \text{sym}
 \end{array} \right]
 \end{array}$$

where $I_{p_i} = I_{m_i} + m_i [EMX_i^2 + EMY_i^2]$

The stiffness matrix in Eq. 2.30 for a multi-unit model is replaced by the condensed stiffness matrix $[K]$ (Eq. 2.29) while the eccentricities of center of rigidity to the arbitrary point (p) applied into Eq. 2.29 are defined as $ERY_i = Y_{p_i} - Y_{r_i}$ and $ERX_i = X_{p_i} - X_{r_i}$. Symbolically, the stiffness matrix is

$$\begin{bmatrix} (K_{xx} - K_{x\theta} \cdot K_{\theta\theta}^{-1} \cdot K_{\theta x}) & 0 & (K_{x\phi} - K_{x\theta} \cdot K_{\theta\theta}^{-1} \cdot K_{\theta x\phi}) \\ & (K_{yy} - K_{y\theta} \cdot K_{\theta\theta}^{-1} \cdot K_{\theta y}) & (K_{y\phi} - K_{y\theta} \cdot K_{\theta\theta}^{-1} \cdot K_{\theta y\phi}) \\ \text{sym} & & (K_{\phi\phi} - K_{\phi\theta} \cdot K_{\theta\theta}^{-1} \cdot K_{\theta\phi}) \\ & & -K_{\phi\theta} \cdot K_{\theta\theta}^{-1} \cdot K_{\theta\phi} \end{bmatrix}$$

The terms of K_{xx} , $K_{x\theta}$, $K_{\theta\theta}$, $K_{x\phi}$, K_{yy} , $K_{\phi\phi}$ are all matrices which have been shown in Eq. 2.18, 2.21 and 2.24 but the eccentricities e_{y_i} and e_{x_i} shall be substituted by ERY_i and ERX_i respectively.

For example,

$$[K_{xx}] = \begin{bmatrix} K_{11} & K_{12} & 0 & \dots & 0 \\ & K_{22} & K_{23} & 0 & \dots & 0 \\ & & & & & \\ \text{sym} & & & & & K_{n-1,n} \\ & & & & & K_{nn} \end{bmatrix}$$

where,

$$K_{11} = K_{sx_1} + K_{sx_2}$$

$$K_{12} = -K_{sx_2}$$

$$K_{22} = K_{sx_2} + K_{sx_3}$$

$$K_{23} = -K_{sx_3}$$

$$K_{n-1,n} = -K_{sx_n}$$

$$K_{nn} = K_{sx_n}$$

$$[K_{\theta x}]^T = [K_{x\theta}] = \begin{bmatrix} K_{11} & K_{12} & 0 & \dots & 0 \\ K_{21} & K_{22} & K_{23} & 0 & \dots & 0 \\ & & & & & \vdots \\ & & & & & K_{n-1,n} \\ & & & & K_{n,n-1} & K_{nn} \end{bmatrix}$$

where

$$K_{11} = \frac{1}{2}(-K_{sx_1} \cdot h_1 + K_{sx_2} \cdot h_2)$$

$$K_{12} = \frac{1}{2} \cdot K_{sx_2} \cdot h_2$$

$$K_{21} = -\frac{1}{2} \cdot K_{sx_2} \cdot h_2$$

$$K_{22} = \frac{1}{2}(-K_{sx_2} \cdot h_2 + K_{sx_3} \cdot h_3)$$

$$K_{23} = \frac{1}{2} \cdot K_{sx_3} \cdot h_3$$

$$\vdots$$

$$K_{n-1,n} = \frac{1}{2} \cdot K_{sx_n} \cdot h_n$$

$$K_{n,n-1} = -\frac{1}{2} \cdot K_{sx_n} \cdot h_n$$

$$K_{nn} = -\frac{1}{2} \cdot K_{sx_n} \cdot h_n$$

$$[K_{\phi x}]^T = [K_{x\phi}] = \begin{bmatrix} K_{11} & K_{12} & 0 & \dots & 0 \\ & K_{22} & K_{23} & 0 & \dots & 0 \\ & & & & & \vdots \\ & & & & & K_{n-1,n} \\ & & & & & K_{nn} \end{bmatrix}$$

sym

where

$$K_{11} = -(K_{sx_1} \cdot ERY_1 + K_{sx_2} \cdot ERY_2)$$

$$K_{12} = K_{sx_2} \cdot ERY_2$$

$$K_{22} = -(K_{sx_2} \cdot ERY_2 + K_{sx_3} \cdot ERY_3)$$

$$K_{23} = K_{sx_3} \cdot ERY_3$$

$$K_{n-1,n} = K_{sx_n} \cdot ERY_n$$

$$K_{nn} = -K_{sx_n} \cdot ERY_n$$

$$[K_{\theta\theta_x}] = \begin{bmatrix} K_{11} & K_{12} & 0 & \dots & 0 \\ & K_{22} & K_{23} & 0 & \dots & 0 \\ & & & \ddots & & \\ \text{sym} & & & & & K_{n-1,n} \\ & & & & & K_{nn} \end{bmatrix}$$

and

$$K_{11} = \frac{1}{2} (K_{x_1} \cdot a_1^2 + K_{x_2} \cdot a_2^2) + \frac{1}{4} (K_{sx_1} \cdot h_1^2 + K_{sx_2} \cdot h_2^2)$$

$$K_{12} = -\frac{1}{2} \cdot K_{x_2} \cdot a_2^2 + \frac{1}{4} \cdot K_{sx_2} \cdot h_2^2$$

$$K_{22} = \frac{1}{2} (K_{x_2} \cdot a_2^2 + K_{x_3} \cdot a_3^2) + \frac{1}{4} (K_{sx_2} \cdot h_2^2 + K_{sx_3} \cdot h_3^2)$$

$$K_{23} = -\frac{1}{2} K_{x_3} \cdot a_3^2 + \frac{1}{4} \cdot K_{sx_3} \cdot h_3^2$$

$$K_{n-1,n} = -\frac{1}{2} \cdot K_{x_n} \cdot a_n^2 + \frac{1}{4} \cdot K_{sx_n} \cdot h_n^2$$

$$K_{nn} = \frac{1}{2} \cdot K_{x_n} \cdot a_n^2 + \frac{1}{4} K_{sx_n} \cdot h_n^2$$

$$K_{12} = -(K_{\phi_2} + K_{sx_2} \cdot ERY_2^2 + K_{sy_2} \cdot ERX_2^2)$$

$$K_{22} = K_{\phi_2} + K_{\phi_3} + K_{sx_2} \cdot ERY_2^2 + K_{sx_3} \cdot ERY_3^2 \\ + K_{sy_2} \cdot ERX_2^2 + K_{sy_3} \cdot ERX_3^2$$

$$K_{23} = -(K_{\phi_3} + K_{sx_3} \cdot ERY_3^2 + K_{sy_3} \cdot ERX_3^2)$$

$$K_{n-1,n} = -(K_{\phi_n} + K_{sx_n} \cdot ERY_n^2 + K_{sy_n} \cdot ERX_n^2)$$

$$K_{nn} = K_{\phi_n} + K_{sx_n} \cdot ERY_n^2 + K_{sy_n} \cdot ERX_n^2$$

Substituting K_{sx_i} , K_{x_i} , ERY_i , a_i by K_{sy_i} , K_{y_i} , ERX_i and b_i , matrices

$[K_{yy}]$, $[K_{y\theta}]$, $[K_{y\phi}]$, $[K_{\theta\theta y}]$ and $[K_{\theta y \phi}]$ can be shown to have similar forms.

Consequently, the detailed description of Eq. 2.30 applied to multi-unit model is complicated. However, this equation is very useful, particularly when the dynamic analysis is applied to offset buildings in Chapter 4.

CHAPTER 3

THE EFFECTS OF COUPLED TRANSLATIONAL AND TORSIONAL MOTION IN MONOSYMMETRICAL FRAME BUILDING

3.1 Introduction

Completely symmetrical structures do not exist. Owing to inevitable eccentricity, it is necessary to take coupled response into account for buildings which are subjected to earthquake excitation. In Chapter 1, a review of many investigations on the effects of seismic coupled lateral-torsional response on buildings is presented. The general conclusions are as follows:

- (1) Coupled lateral and torsional motions cause torque and reduce base shear.
- (2) The effect of torsional coupling depends strongly on ω_ϕ / ω_x , the ratio of uncoupled torsional frequency to uncoupled lateral fundamental frequency.

A parametric study on the effect of coupled motions is made in this Chapter. Particular attention is given to the circumstance when the phenomenon of sympathetic coupled torsional-translational resonance occurs. Three groups of monosymmetrical uniform frame structures are studied in this Chapter. They are a six-storey building with uncoupled translational period $T_x=0.5$ sec, a twelve-storey building with $T_x=1.0$ sec and a twenty four-storey structure with $T_x=2.0$ sec. (shown in Fig. 1.3)

Different ratios of uncoupled torsional periods to uncoupled translational periods related to small eccentricity ($e/D = 0.03$), moderate eccentricity

($e/D = 0.10$) and exceptional large eccentricity($e/D = 0.50$) in each building group are considered. A dynamic analysis by applying the response spectrum method according to Commentary K of National Building Code of Canada(NBC 77) is carried out. As a comparison, the static shear force and torsional calculations based on NBC 77 are also calculated for each building.

3.2 Uncoupled Fundamental Translational and Torsional Periods

The study of general equation of motion in Chapter 2 presents equation (2.30) of which the reference point can be arbitrary. In a monosymmetrical structure, when the reference point is at the center of rigidity(shown in Fig.2.9), the terms of X_p and X_r of Eq.2.30 are equal to X_m , and y_p is equal to y_r . Therefore, the off-diagonal elements of stiffness matrix are all equal to zero. Let $e_y = y_p$ (or y_r) - y_m represent the monosymmetrical structure's eccentricity in y axis direction, the undamped free vibration equation of motion in terms of the displacements at the center of rigidity is

$$\begin{bmatrix} M & Me_y \\ Me_y & I_\phi \end{bmatrix} \begin{Bmatrix} \ddot{x} \\ \ddot{\phi} \end{Bmatrix} + \begin{bmatrix} K_x & 0 \\ 0 & K_\phi \end{bmatrix} \begin{Bmatrix} x \\ \phi \end{Bmatrix} = 0$$

in which $I_\phi = I_m + M \cdot e_y^2$

Based on the above equation, the uncoupled translational periods (T_x) can be defined by the condition that the torsional rotation (ϕ) is set to zero. i.e.

$$[M] \{\ddot{x}\} + [K_x] \{x\} = 0 \quad - (3.1)$$

Analogously, when the structure is only rotated around the center of rigidity, the inertia torque occurs at center of mass is $I_m \cdot \ddot{\phi}$. An additional translational inertia force occurred at center of mass, due to the eccentricity (e_y), is $M \cdot e_y \cdot \ddot{\phi}$. Hence, the uncoupled torsional fundamental period T_ϕ can be obtained by equation

$$[I_\phi] \{ \ddot{\phi} \} + [K_\phi] \{ \phi \} = 0 \quad - (3.2)$$

where $I_\phi = I_m + M \cdot e_y^2$.

3.3 The Comparison of Base Shear Between Stiff and Flexible Structure

Due to seismic excitation, a stiff(short period) structure may develop larger base shear than a flexible(long period) structure. In NBC 77, the formulation of static base shear $V = ASFKIW$, in which $S = \frac{0.5}{\sqrt{T}}$ is the seismic coefficient and T is the fundamental period of the structure, has reflected this fact. According to Commentary K of NBC 77, the lateral dynamic storey forces P_i for any mode i are computed from equation

$$\{ P_i \} = [M] \cdot \{ \phi \} \cdot \gamma_i \cdot S_{ai} \quad - (3.3)$$

where $[M]$ is the mass matrix of the structure, column vector $\{ \phi \}$ is the mode shapes, γ_i is the modal participation factor and S_{ai} is the spectral acceleration. As shown in the peak ground motion bounds and elastic average response spectrum (shown in Fig.3.1), the spectral acceleration S_a increases when the fundamental periods and damping ratio decrease.

Table(3.1) lists the base shears by equivalent static calculation

Poor Copy

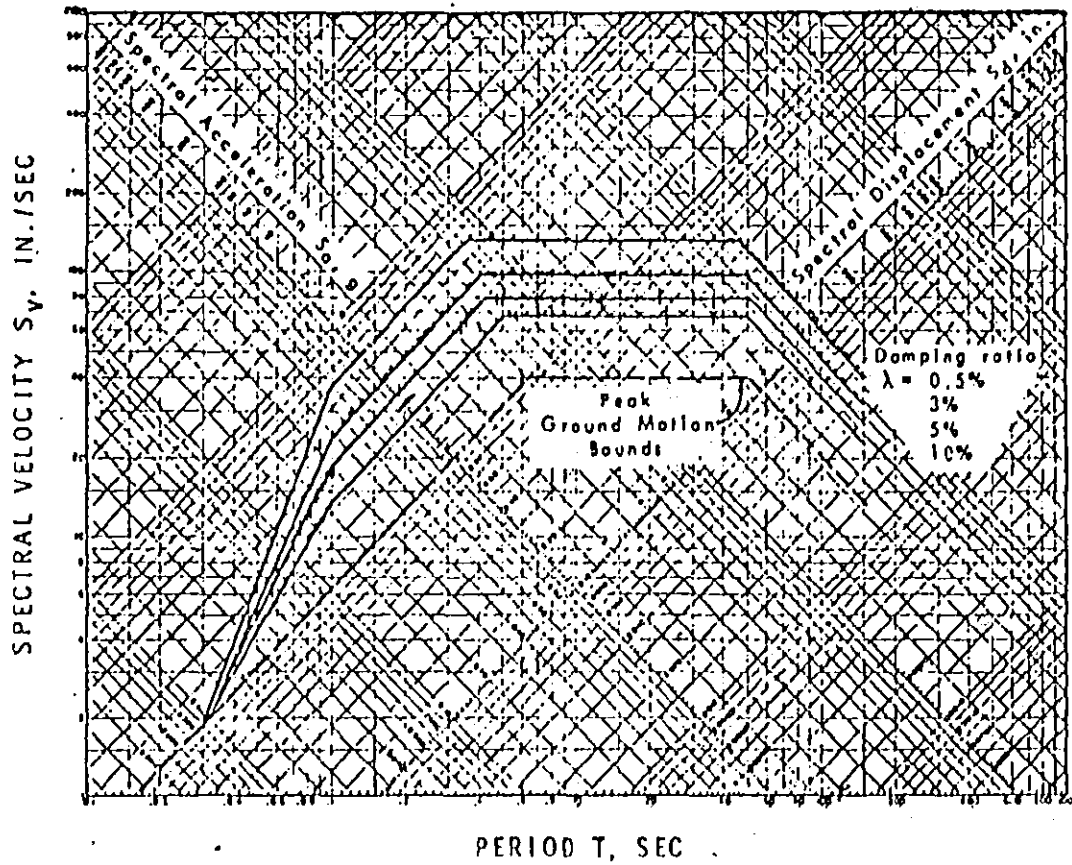


Fig.3.1 Peak Ground Motion Bounds and Elastic Average Response Spectrum for 1.0g Max. Ground Acceleration

Building	I	II	III
T_x	0.5 (sec)	1.0 (sec)	2.0 (sec)
Total Height	6 x 11' - 0"	12 x 11' - 0"	24 x 11' - 0"
Total Weight (W)	8,400 ^k	16,800 ^k	33,600 ^k
Static Calculation $V=ASF\sum W_i$ **	423.33 ^k	672.0 ^k	1066.73 ^k
$S = \frac{0.5}{\sqrt{T_x}}$	0.63	0.5	0.40
R.S.S. Dynamic Analysis $\xi = 0.05$ $\{P\}_i = [M] \{\phi\}_i \gamma_i \int a$	762.6 ^k	757.0 ^k	790.60 ^k
$\int a_1$	0.10g	0.05g	0.03g

Table 3.1 Base Shear Comparison Between Static Calculation and Dynamic Analysis

** A = 0.04
 F = 1
 I = 1
 K = 2

and dynamic analysis combined by root-sum-square(RSS) method for the three frame buildings under the assumption that the buildings are symmetric structures. (i.e. $e_x = e_y = 0$) It is interesting to notice that the dynamic base shear for the six-storey($T_x = 0.5\text{sec}$) building with total weight $8,400^k$ is larger than the twelve-storey($T_x = 1.0\text{sec}$) building with total weight $16,800^k$. Tables 3.2 (a) to (d) display the contribution of spectral acceleration and mode shapes to the shear force calculation. For example, in the first mode, the largest base shear occurs at the six-storey building due to the higher spectral acceleration S_{a1} and larger magnitudes of mode shapes $\{ \phi \}$.

Commentary J and K of NBC 77 limit the base shear computed from a dynamic analysis to be not less than 90 per cent of that obtained by the static procedure. The base shear study mentioned above shows that for short period stiff structures, the static base shear underestimates the dynamic analysis by a factor of 1.8. Therefore, the necessity of dynamic analysis for earthquake engineering is more apparent..

Dynamic analysis by response spectrum method is adopted in this thesis. Due to the assumption of linear elastic structure behaviour in the Duhamel integral^[19] equation, the numerical coefficient K in the static procedure is chosen as equal to two to exclude the consideration of ductility for the frame structure.

3.4 The Consequence of Coupled Translational and Torsional Motion to Base Shear

The equivalent static base shear formulation of NBC 77 does not reflect the contribution of eccentricity and coupled motion to the seismic response of structure. However, the comparison of dynamic base shear to

U N I T (i)	T _{x1} = 0.5 SEC					T _{x1} = 1.0 SEC					T _{x1} = 2.0 SEC						
	[W]	φ ₁	r ₁	Sa ₁	V ₁ (Shear)	[W]	φ ₁	r ₁	Sa ₁	V ₁ (Shear)	[W]	φ ₁	r ₁	Sa ₁	V ₁ (Shear)		
1	1400 ^k	0.1303	↑	↑	756.30 ^k	1400	0.0465	↑	↑	723.79	2800	0.0420	↑	↑	711.62		
2	1400	0.2544	↑	↑	713.07	1400	0.0932	↑	↑	713.13	2800	0.0869	↑	↑	702.08		
3	1400	0.3648	2.2793	0.10	628.67	1400	0.1393	↑	↑	691.74	2800	0.1314	↑	↑	682.31		
4	1400	0.4551	↑	↑	507.62	1400	0.1841	↑	↑	659.76	2800	0.1755	↑	↑	652.40		
5	1400	0.5197	↑	↑	356.62	1400	0.2268	3.1538	0.05	617.50	2800	0.2183	3.1269	0.03	612.45		
6	1400	0.5550	↑	↑	184.16	1400	0.2666	↑	↑	565.45	2800	0.2592	↑	↑	562.75		
7						1400	0.3028	↑	↑	504.27	2800	0.2972	↑	↑	503.74		
8						1400	0.3349	↑	↑	434.78	2800	0.3318	↑	↑	436.08		
9						1400	0.3622	↑	↑	357.92	2800	0.3623	↑	↑	360.54		
10						1400	0.3844	↑	↑	274.79	2800	0.3882	↑	↑	270.06		
11						1400	0.4011	↑	↑	186.56	2800	0.4090	↑	↑	189.69		
12						1400	0.4119	↑	↑	94.52	2800	0.4243	↑	↑	96.60		
R.S.S. V base =					762.6	R.S.S. V base =					757.0	R.S.S. V base =					790.60

Table 3.2 (a) 1st Mode Dynamic Shear Forces Comparison for Building with T_{x1} = 0.5 sec. (e_x = e_y = 0)
 1.0
 2.0 ξ = 0.05

U n i t(1)	T _{x1} = 0.5 SEC					T _{x1} = 1.0 SEC					T _{x1} = 2.0 SEC						
	[W]	φ ₂	γ ₂	Sa ₂	V ₁ (Shear)	[W]	φ ₂	γ ₂	Sa ₂	V ₁ (Shear)	[W]	φ ₂	γ ₂	Sa ₂	V ₁ (Shear)		
1	1400	-0.3668			93.29	1400	0.1456			208.61	2800	0.1440			307.28		
2	1400	-0.5502			47.30	1400	0.2709			181.35	2800	0.2682			269.80		
3	1400	-0.4593	-0.7452	0.12	-21.58	1400	0.3591			130.62	2800	0.3566			199.99		
4	1400	-0.1392			-79.01	1400	0.3984			63.39	2800	0.3978			107.16		
5	1400	0.2514			-96.43	1400	0.3834			-11.19	2800	0.3865			3.60		
6	1400	0.5188			-64.95	1400	0.3163	1.1143	0.12	-82.97	2800	0.3240	1.1804	0.08	-97.00		
7						1400	0.2058			-142.18	2800	0.2182			-191.34		
8						1400	0.0669			-180.71	2800	0.0827			-238.14		
9						1400	-0.0819			-193.24	2800	-0.0653			-259.67		
10						1400	-0.2208			-177.90	2800	-0.2068			-242.68		
11						1400	-0.3312			-136.56	2800	-0.3239			-188.85		
12						1400	-0.3983			-74.56	2800	-0.4016			-104.54		
R.S.G. V base =					762.6	R.S.S. V base =					757.0	R.S.S. V base =					790.6

Table 3.2 (b) 2nd Mode Dynamic Shear Forces Comparison for Building with T_{x1} = 0.5 sec (a_x = a_y = 0)
 1.0
 2.0 ξ = 0.05

U n i t (L)	T _{x1} = 0.5 Sec					T _{x1} = 1.0 Sec					T _{x1} = 2.0 Sec						
	[W]	φ ₃	γ ₃	s _{a3}	V (Shear)	[W]	φ ₃	γ ₃	s _{a3}	V (Shear)	[W]	φ ₃	γ ₃	s _{a3}	V (Shear)		
1	1400	-0.5193			27.37	1400	-0.2350			65.45	2800	-0.2349			134.83		
2	1400	-0.3710			-7.85	1400	-0.3820			40.81	2800	-0.3833			84.84		
3	1400	0.2539	-0.4036	0.12	-33.00	1400	-0.3053			0.75	2800	-0.3896			3.25		
4	1400	0.5505			-15.79	1400	-0.2436			-39.65	2800	-0.2514			-79.68		
5	1400	0.1368			21.54	1400	-0.0107	-0.624	0.12	65.20	2800	-0.0205	-0.6335	0.12	-133.54		
6	1400	-0.4544			30.81	1400	0.2254			-66.32	2800	0.2162			-137.54		
7						1400	0.3752			42.68	2800	-0.3700			-91.51		
8						1400	0.3819			-3.34	2800	0.3829			-12.77		
9						1400	0.2431			36.71	2800	0.2501			68.72		
10						1400	0.0113			62.20	2800	0.0214			121.94		
11						1400	-0.2259			63.38	2800	-0.2175			126.49		
12						1400	-0.3785			39.69	2800	-0.3768			80.21		
R.S.B. V base =					762.6	R.S.B. V base =					757.0	R.S.B. V base =					790.6

Table 3.2 (c) 3rd Mode Dynamic Shear Forces Comparison for Buildings with T_{x1} = 0.5 Sec (e_x = e_y = 0)
1.0
2.0 ξ = 0.05

Unit (f)	T _{x1} = 0.5 Sec					T _{x1} = 1.0 Sec					T _{x1} = 2.0 Sec						
	[W]	φ ₄	γ ₄	S _{a4}	V (Shear)	[W]	φ ₄	γ ₄	S _{a4}	V (Shear)	[W]	φ ₄	γ ₄	S _{a4}	V (Shear)		
1	1400	0.5507	↑	↑	7.83	1400	-0.3077	↑	↑	30.97	2800	-0.3073	↑	↑	63.21		
2	1400	-0.1321			-9.66	1400	-0.3929	↑	↑	8.78	2800	-0.3932	↑	↑	18.43		
3	1400	-0.5205	0.2466	0.09	-5.46	1400	-0.1943			-19.57	2800	-0.1961			-38.07		
4	1400	0.2550			11.06	1400	0.1451			-33.58	2800	0.1429			-67.45		
5	1400	0.4585	↓	↓	3.96	1400	0.3808	-0.4294	0.12	-23.11	2800	0.3809	-0.4337	0.12	-46.63		
6	1400	-0.3652			-11.60	1400	0.3430			4.36	2800	0.3477			8.88		
7						1400	0.0590			29.11	2800	0.0670			59.56		
8						1400	-0.2667			33.36	2800	0.2600			69.32		
9						1400	-0.3993			14.12	2800	-0.3991			-31.44		
10						1400	-0.2434			-14.68	2800	-0.2505			-26.73		
11						1400	0.0889			-32.24	2800	0.0794			-63.24		
12						1400	0.3581			-25.83	2800	0.3545			-51.67		
R.S.S. V base =					762.6	R.S.S. V base =					757.0	R.S.S. V base =					790.6

Table 3.2 (d) 4th Mode Dynamic Shear Forces Comparison for Buildings with T_{x1} = 0.5 Sec (e_x = e_y = 0)
 T_{x1} = 1.0 ξ = 0.05
 T_{x1} = 2.0

static base shear for the three monosymmetrical frame structures (shown in Fig.3.2) exhibits that the dynamic base shear will decrease when the eccentricity increases. Fig.3.2 also shows that the dynamic base shear drops abruptly when the center of rigidity is close to the center of mass and the uncoupled torsional period is equal to the uncoupled translational period. Actually, this is one of the phenomena of sympathetic torsional and translational resonance which occurs in structures with small eccentricities. Further study of this particular aspect will be discussed in Section 3.6.

3.5 The Study of Dynamic Torque Affected by Eccentricity and Coupled Motion

Based on the root-sum-square rule, dynamic torsions are shown in Figs.3.3 to 3.11 for buildings with small, medium and exceptionally large eccentricities associated with uncoupled torsional periods which vary in the neighbourhood of uncoupled translational periods.

Because the equivalent static base shear (V_s) is not a function of structural eccentricity and coupled motion, the dynamic torques (M_t) are normalized by a factor of V_s/V_d in each circumstance before it is compared with the static torque calculation of NBC 77 in this thesis.

The distribution of dynamic torque envelopes for the three frame buildings are similar. For simplicity, the study of the twelve-storey building is used for discussion in detail. The following comments can be made:

- (1) Sympathetic coupled torsional-lateral resonance occurs in buildings with small eccentricities when the uncoupled torsional period is equal to uncoupled lateral period. Fig. 3.3 displays the fact that the RSS dynamic torque is four times the

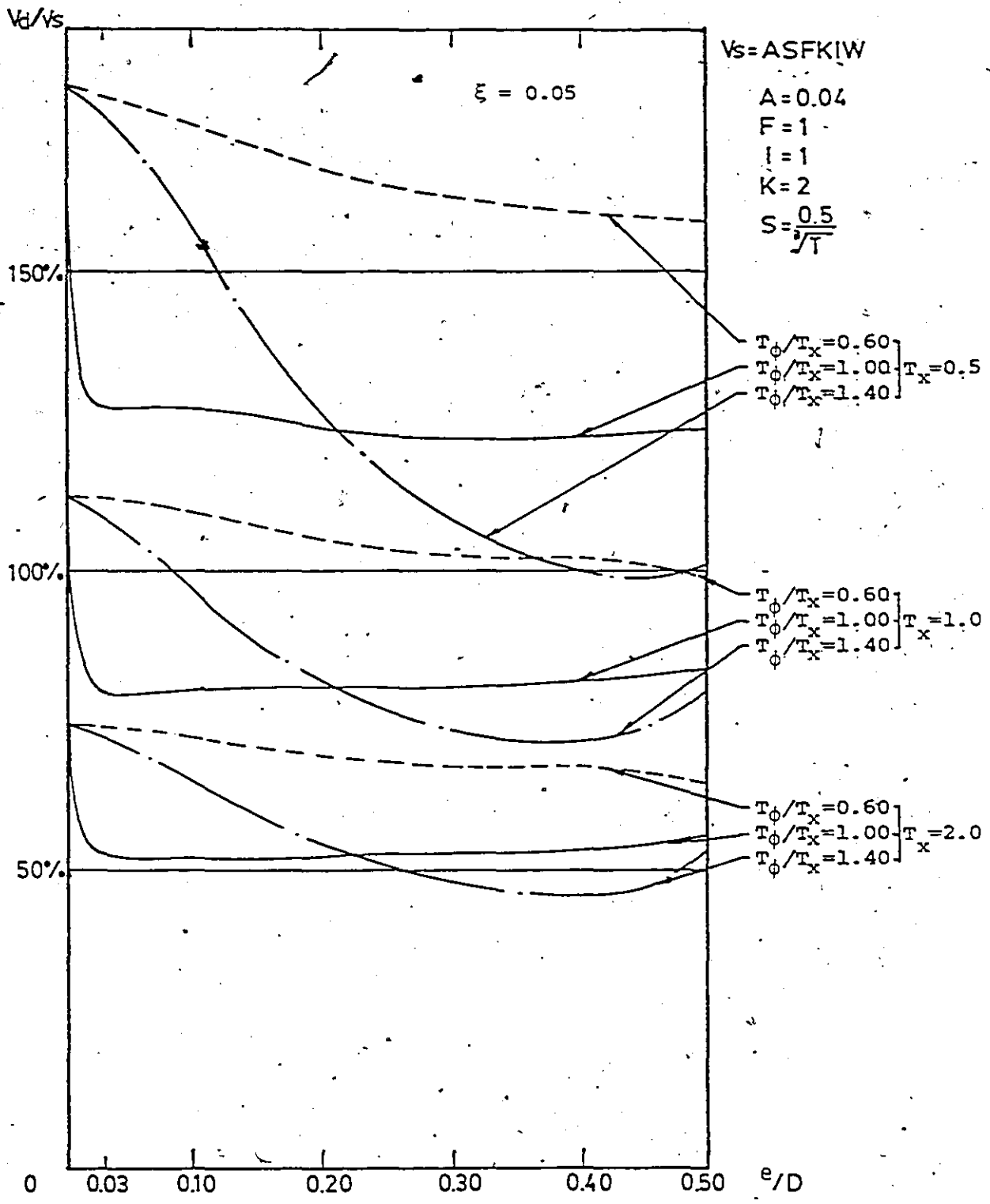


Fig.3.2 The Comparison of Dynamic and Static Base Shear Due to Eccentricities and Coupled Motions



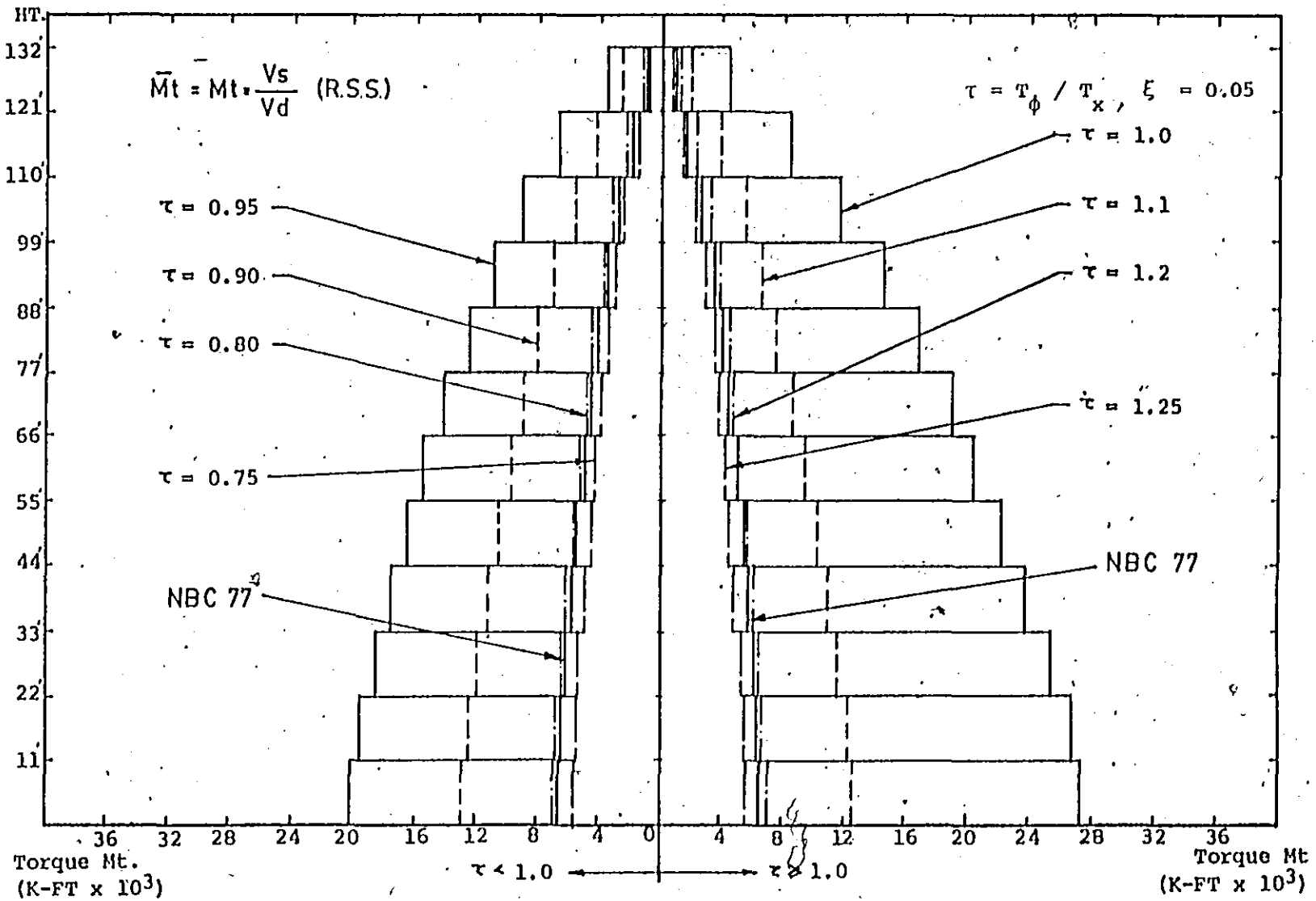


FIG. 3.3 COMPARISON OF TORQUE FOR BUILDING $T_x=1.00$ (SEC), $e/D=0.03$

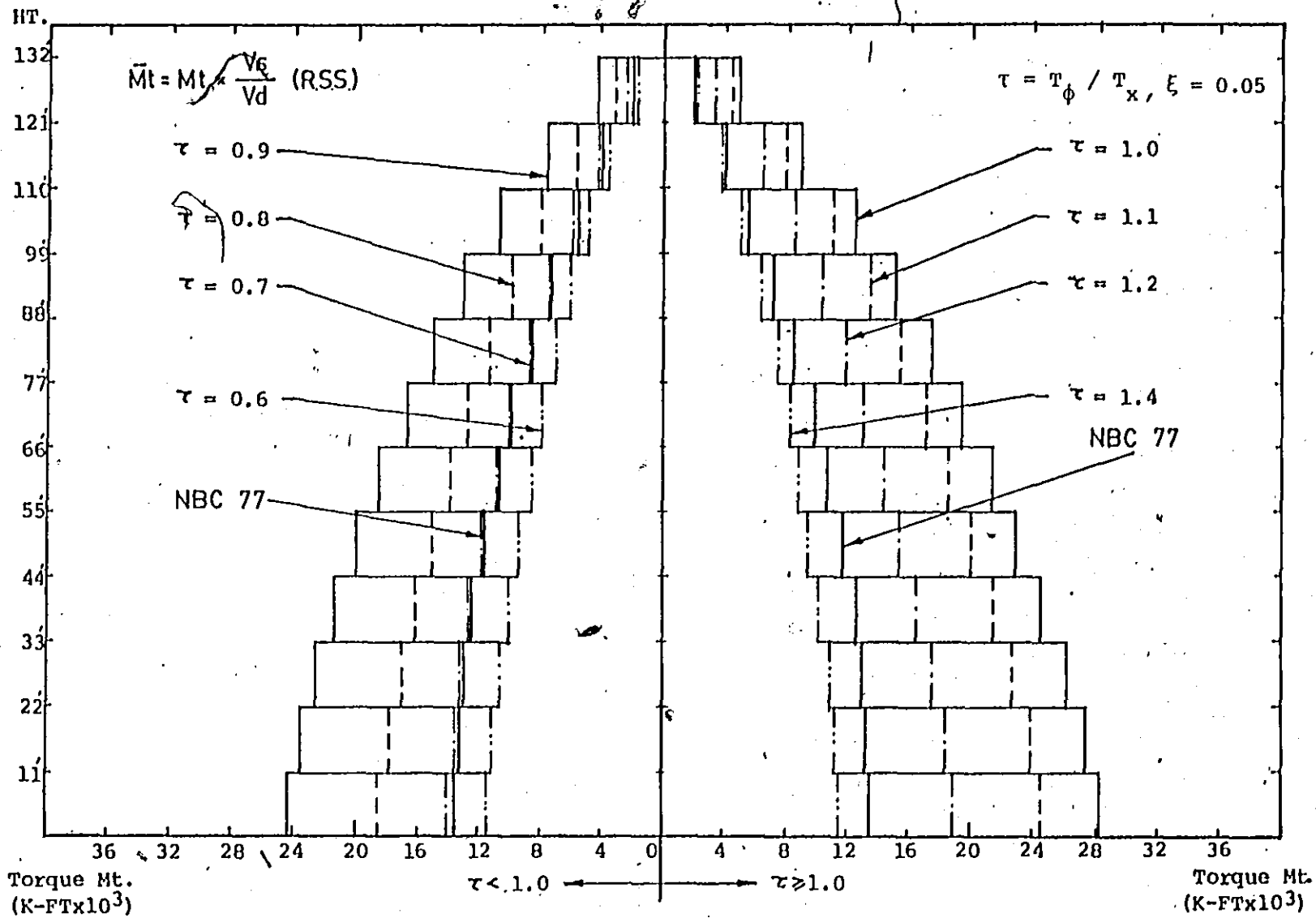


FIG. 3.4 COMPARISON OF TORQUE FOR BUILDING $T_x=1.00$ (SEC), $e/D=0.10$

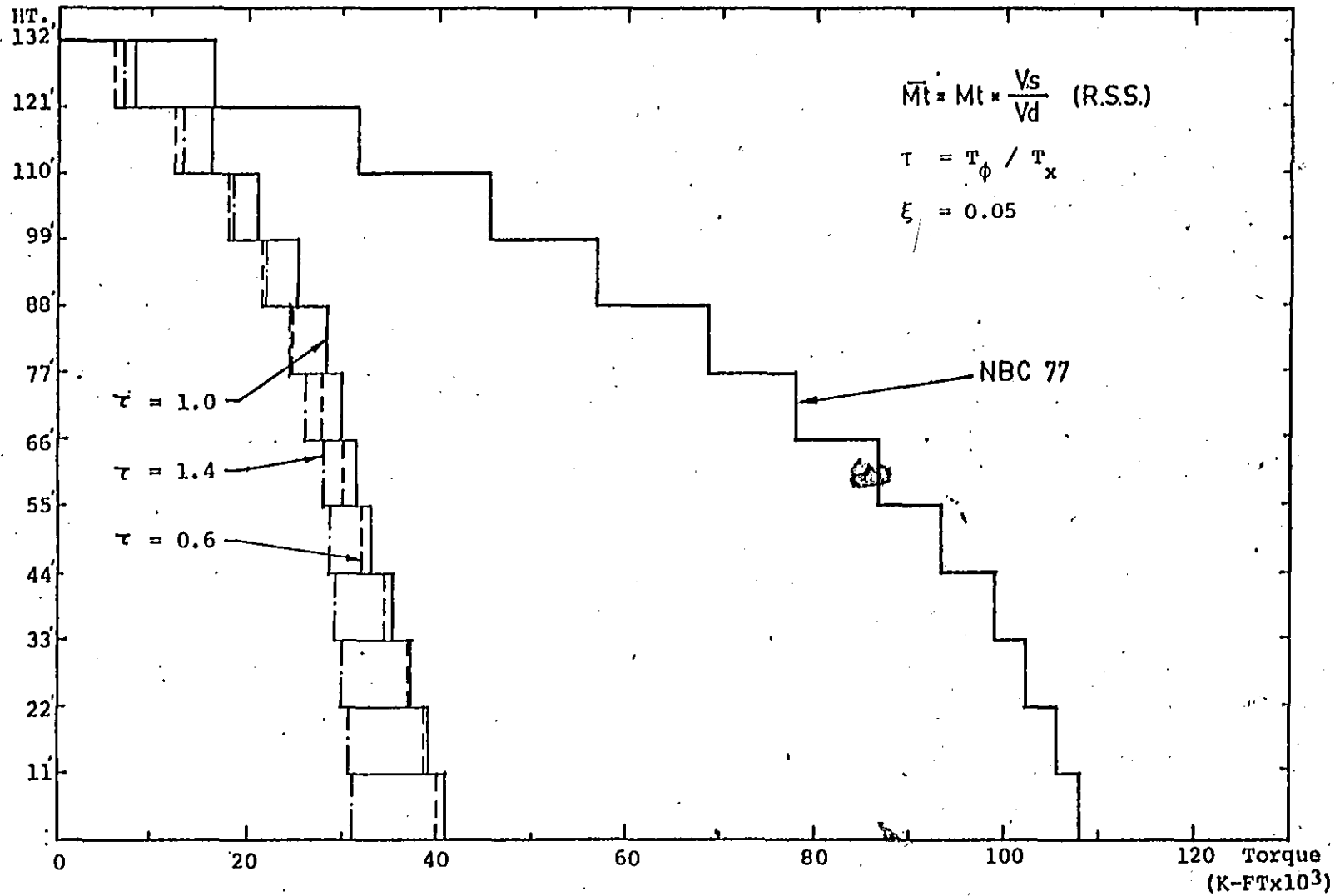


FIG. 3.5 COMPARISON OF TORQUE FOR BUILDING $T_x=1.00(\text{SEC})$, $e/D=0.50$

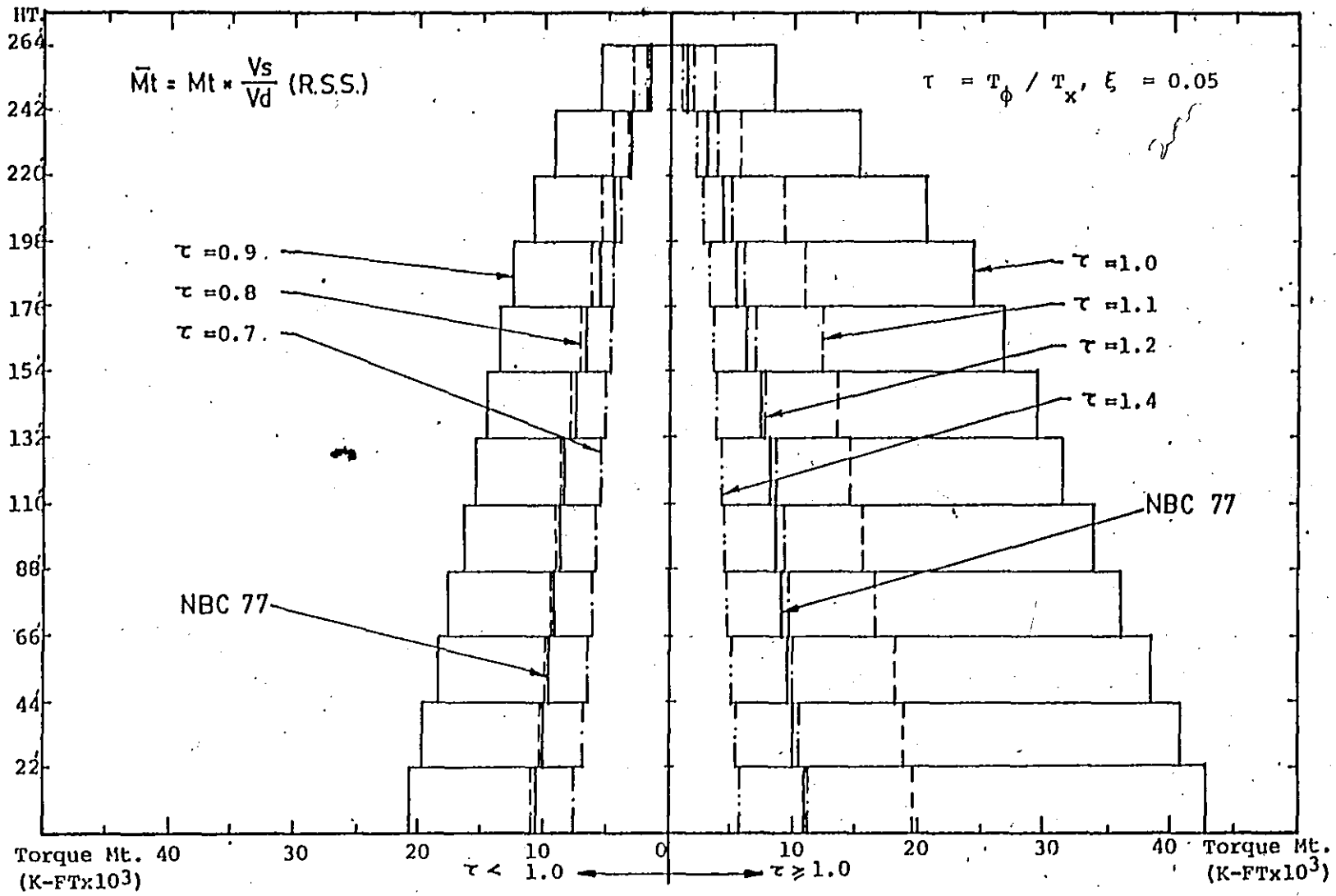


FIG. 3.6 COMPARISON OF TORQUE FOR BUILDING $T_x=2.00(\text{SEC})$, $e/D=0.03$

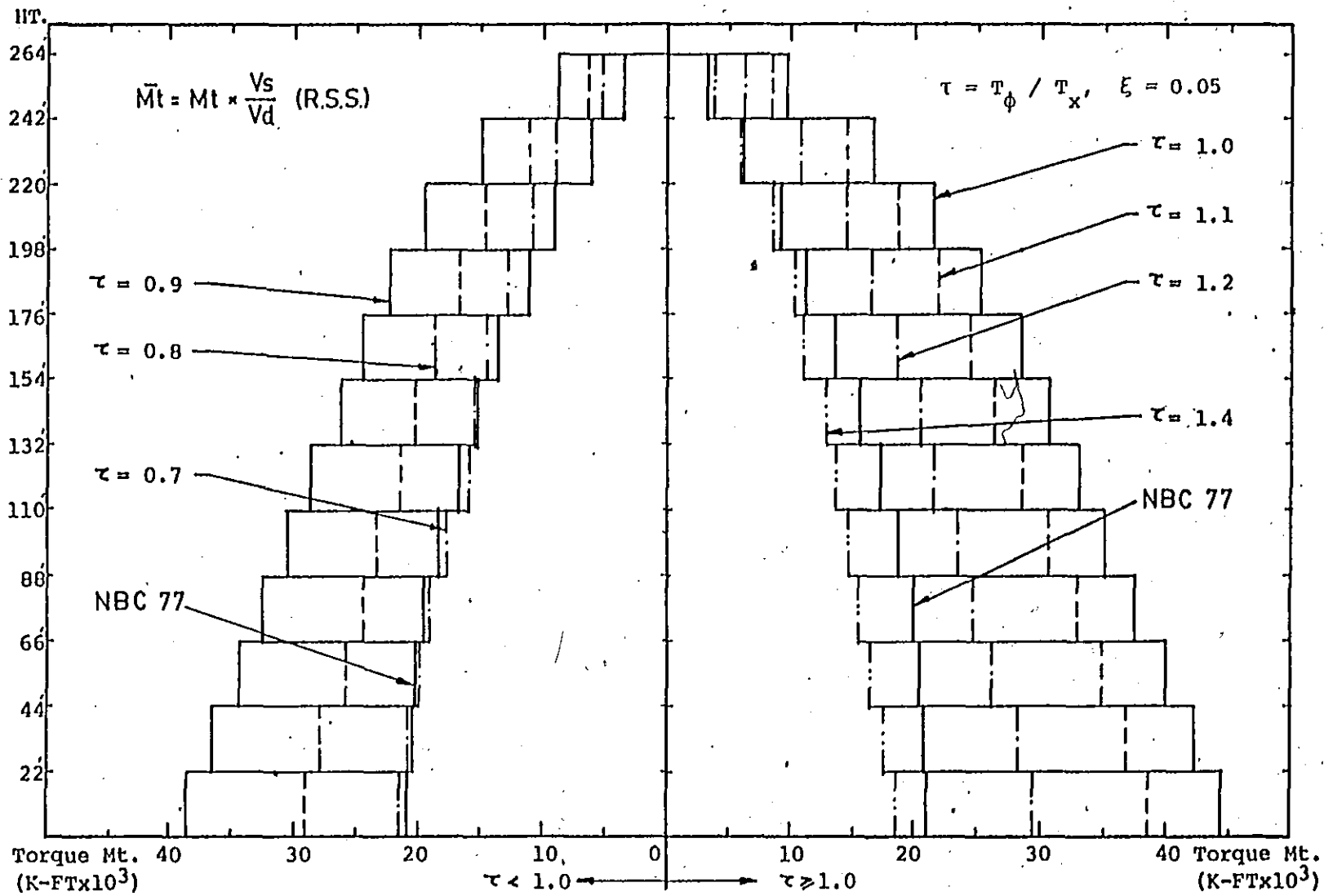


FIG. 3.7 COMPARISON OF TORQUE FOR BUILDING $T_x=2.00$ (SEC), $e/D=0.1$

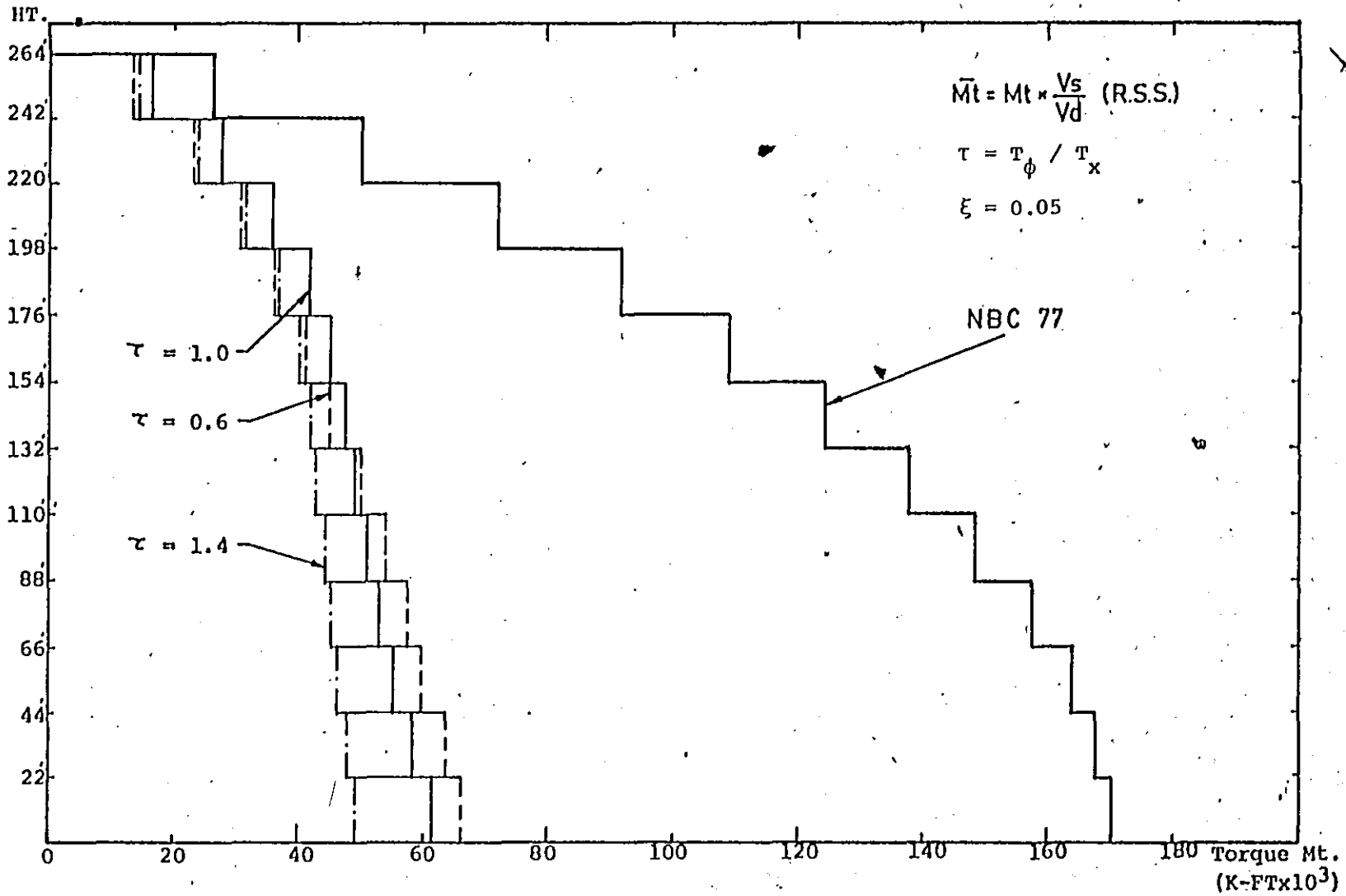


FIG. 3.8 COMPARISON OF TORQUE FOR BUILDING $T_x=2.00$ (SEC), $e/D=0.50$

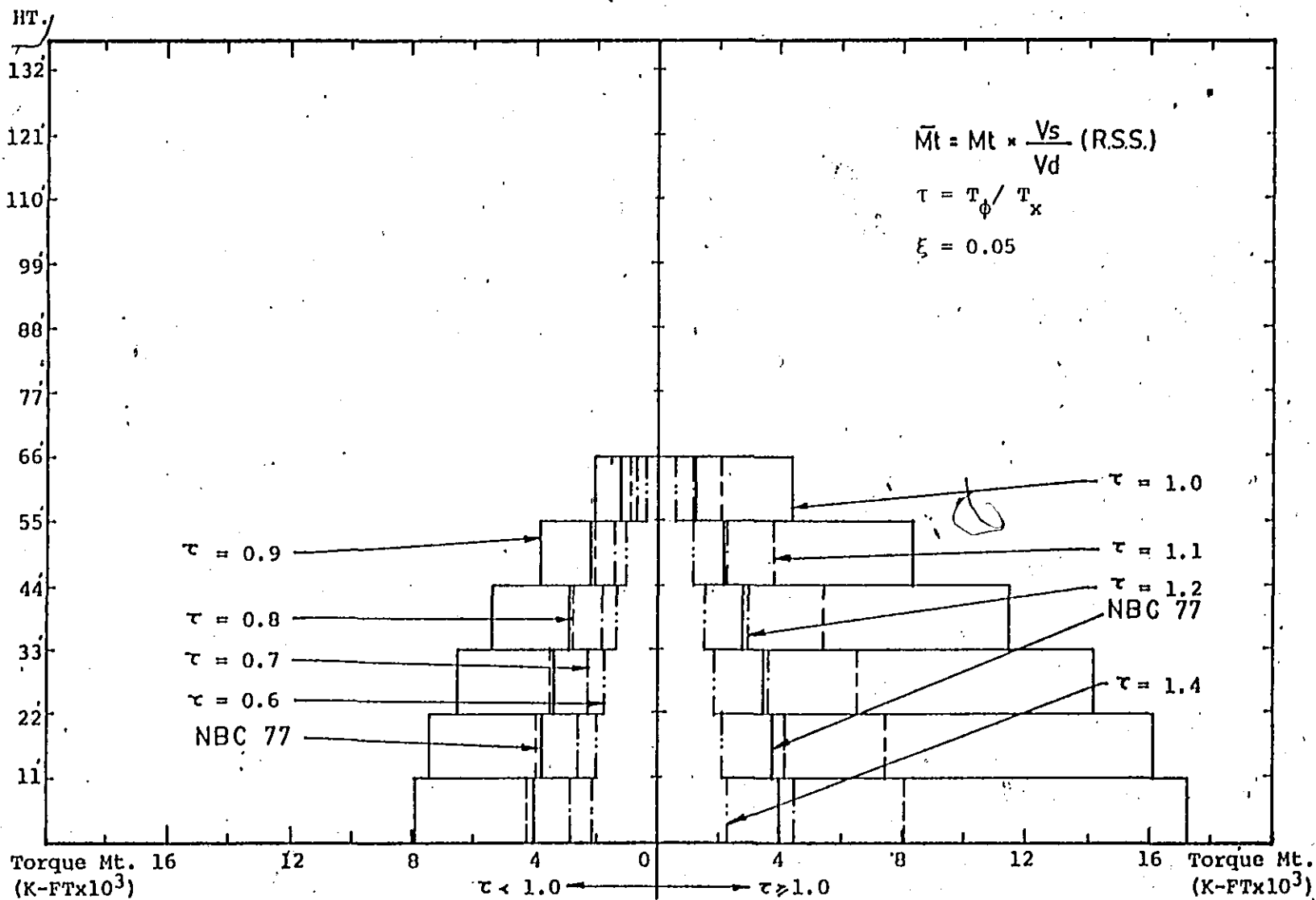


FIG. 3.9 COMPARISON OF TORQUE FOR BUILDING $T_x=0.5$ SEC, $e/d=0.03$

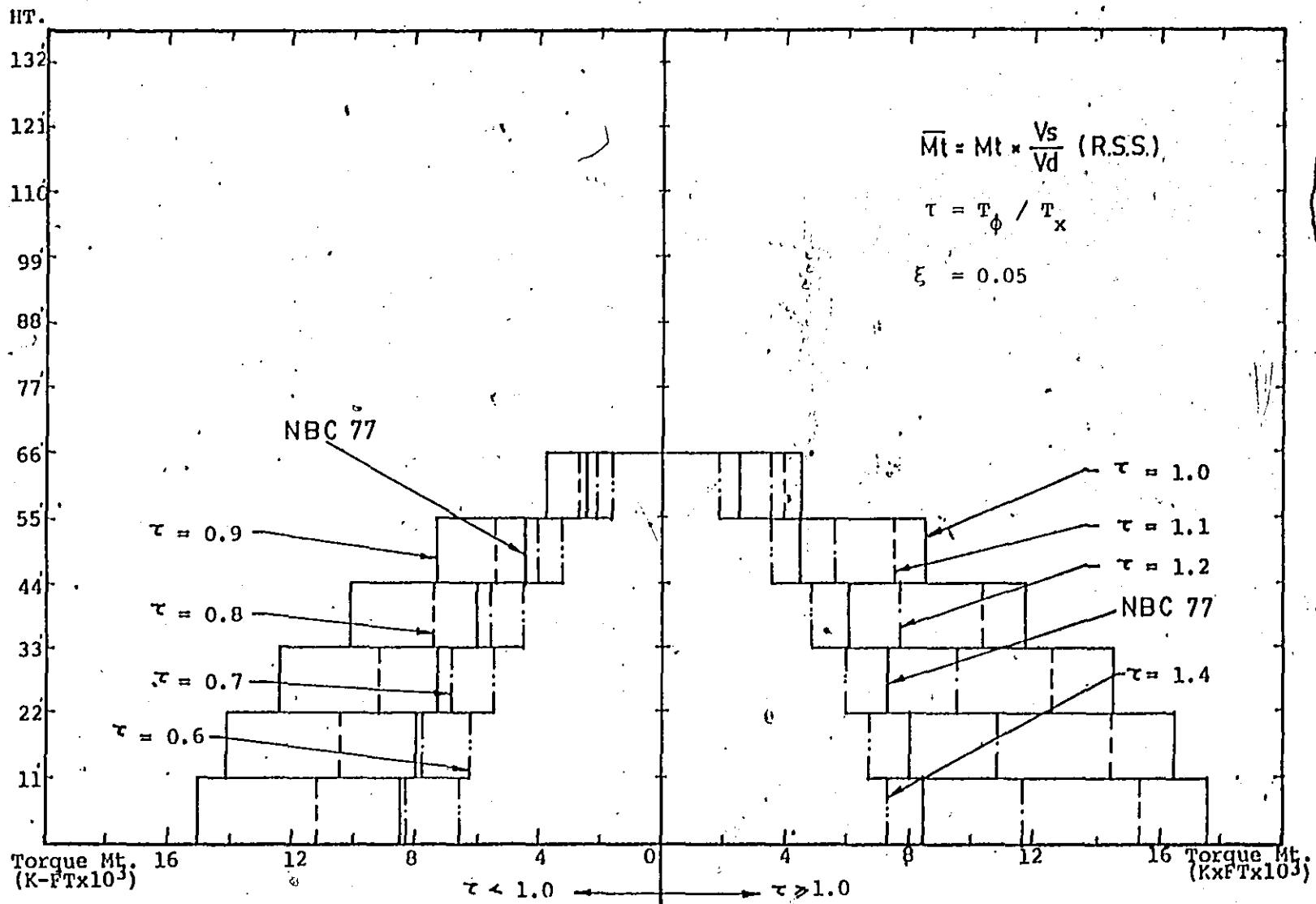


FIG. 3.10 COMPARISON OF TORQUE FOR BUILDING $T_x=0.5$ SEC, $e/D=0.10$

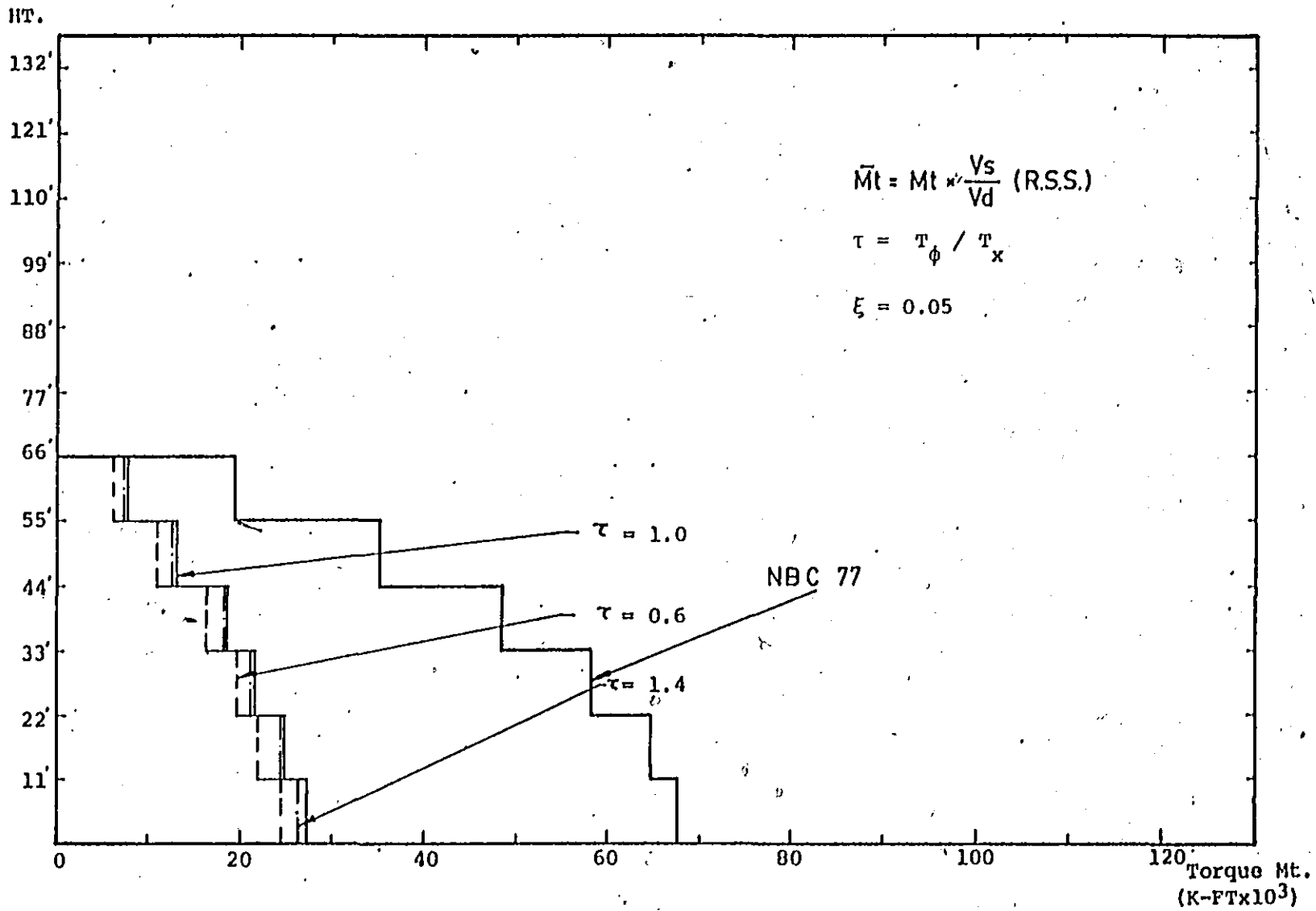


FIG. 3.11 COMPARISON OF TORQUE FOR BUILDING $T_x=0.5$ SEC, $e/D=0.5$

static torque when the eccentricity is small (i.e. $e/D = 0.03$).

In the case of building with moderate eccentricity (say $e/D = 0.10$), the ratio of dynamic torque to static torque is about two.

- (2) The current static torsion design criterion in NBC 77 requires the doubling of the torque when the design eccentricity e_x exceeds one-quarter of the dimension of the structural plan in the direction of computed eccentricity. However, the dynamic torsion for the structure with exceptionally large eccentricity (i.e. $e/D = 0.5$) is only one-third of static torque. Therefore, the sympathetic resonance is not significant when the building possesses large eccentricity and the criterion of the present building code to double the design torque for such cases is a conservative requirement.
- (3) In general, the static design torque in NBC 77 is a good estimate when the fundamental uncoupled torsional period is removed ± 20 per cent from the uncoupled fundamental translational period.

3.6 The Study of Sympathetic Resonance

The frequencies of the three monosymmetrical frame buildings with small ($e/D = 0.03$), moderate ($e/D = 0.10$) and exceptionally large ($e/D = 0.5$) eccentricities associated with different ratios of uncoupled torsional periods to uncoupled translational periods are tabulated in Tables 3.3 (a) to (c).

One can observe from the tables that for structures with small eccentricities, the frequencies are distributed in pairs. Within each pair, the frequencies are close to one another. For visualization, the first four modal frequencies for the building with $T_x = 1.0$ sec are

$\xi = 0.03 D$

$\tau = T \phi / T_x$	$\omega 1$	$\omega 2$	$\omega 3$	$\omega 4$	$\omega 5$	$\omega 6$
0.8	12.498	15.817	36.817	46.534	59.424	74.562
0.9	12.427	14.740	36.606	41.602	59.051	66.695
1.0	12.118	13.050	35.676	38.419	57.357	61.799
1.1	11.289	12.735	33.215	37.513	53.250	60.514
1.2	10.405	12.666	30.611	37.313	49.050	60.221

 $\xi = 0.10 D$

$\tau = T \phi / T_x$	$\omega 1$	$\omega 2$	$\omega 3$	$\omega 4$	$\omega 5$	$\omega 6$
0.8	12.066	16.830	35.538	49.523	57.300	75.557
0.9	11.757	15.353	34.622	45.186	55.759	72.557
1.0	11.278	14.404	33.203	42.405	53.391	68.199
1.1	10.656	13.859	31.363	40.811	50.362	65.727
1.2	9.984	13.559	29.381	39.934	47.137	62.120

 $\xi = 0.50 D$

$\tau = T \phi / T_x$	$\omega 1$	$\omega 2$	$\omega 3$	$\omega 4$	$\omega 5$	$\omega 6$
0.8	10.367	30.177	30.575	49.141	64.787	76.674
0.9	9.894	28.135	29.147	46.869	61.788	73.121
1.0	9.420	26.599	27.745	44.596	58.788	69.567
1.1	8.956	25.432	26.377	42.374	55.856	66.095
1.2	8.509	24.528	25.069	40.241	53.042	62.763

Table 3.3 (a) Frequencies for Building $T_x = 0.5$ Sec., $\xi = 0.05$

$\xi = 0.03 D$

$\tau = T \phi / T_x$	$\omega 1$	$\omega 2$	$\omega 3$	$\omega 4$	$\omega 5$	$\omega 6$	$\omega 7$	$\omega 8$	$\omega 9$	$\omega 10$	$\omega 11$	$\omega 12$
0.8	6.246	7.887	18.733	23.541	31.694	38.853	43.792	53.539	55.255	65.774	67.384	75.273
0.9	6.210	7.052	18.618	21.055	31.422	34.836	43.400	48.020	54.741	60.459	65.157	71.930
1.0	6.058	6.524	18.124	19.519	30.194	32.716	41.639	45.170	52.441	56.954	62.896	67.787
1.1	5.631	6.364	16.814	19.078	27.786	32.237	38.292	44.539	48.197	56.192	57.338	65.575
1.2	5.189	6.330	15.489	18.984	25.564	32.119	35.226	44.329	44.385	52.740	55.999	60.315

 $\xi = 0.10 D$

$\tau = T \phi / T_x$	$\omega 1$	$\omega 2$	$\omega 3$	$\omega 4$	$\omega 5$	$\omega 6$	$\omega 7$	$\omega 8$	$\omega 9$	$\omega 10$	$\omega 11$	$\omega 12$
0.8	6.031	8.414	18.076	25.129	30.468	41.626	42.088	53.067	57.399	63.164	72.251	72.298
0.9	5.877	7.675	17.602	22.939	29.547	38.161	40.787	51.412	52.639	61.190	66.306	70.010
1.0	5.639	7.201	16.871	21.544	28.164	36.037	38.855	48.948	49.741	58.249	62.690	66.635
1.1	5.328	6.928	15.925	20.745	26.462	34.862	36.488	45.948	48.141	54.670	60.704	62.534
1.2	4.992	6.777	14.912	20.307	24.709	34.046	34.240	43.881	47.272	51.018	58.351	59.625

 $\xi = 0.50 D$

$\tau = T \phi / T_x$	$\omega 1$	$\omega 2$	$\omega 3$	$\omega 4$	$\omega 5$	$\omega 6$	$\omega 7$	$\omega 8$	$\omega 9$	$\omega 10$	$\omega 11$	$\omega 12$
0.8	5.183	15.009	15.621	26.012	35.905	45.089	45.360	53.872	61.635	68.414	74.116	75.239
0.9	4.946	14.014	14.866	24.770	34.183	42.082	43.102	51.276	58.662	65.113	70.229	70.542
1.0	4.710	13.252	14.143	23.534	32.470	39.795	40.933	48.696	55.708	61.832	66.527	66.986
1.1	4.477	12.667	13.447	22.331	30.806	38.059	38.833	46.190	52.839	58.648	63.529	63.741
1.2	4.254	12.205	12.790	21.183	29.217	36.665	36.887	43.800	50.103	55.609	60.240	61.595

Table 3.3 (b) Frequencies for Building - $T_x = 1.00$ Sec., $\xi = 0.05$

$\xi = 0.03 D$

$T = \phi / T_x$	$\omega 1$	$\omega 2$	$\omega 3$	$\omega 4$	$\omega 5$	$\omega 6$	$\omega 7$	$\omega 8$	$\omega 9$	$\omega 10$	$\omega 11$	$\omega 12$
0.8	3.125	3.954	9.463	11.805	16.400	19.505	22.731	26.884	28.749	33.841	34.247	39.217
0.9	3.107	3.535	9.399	10.564	16.172	17.582	22.383	24.269	28.269	30.592	33.662	36.410
1.0	3.030	3.263	9.104	9.816	15.221	16.813	20.992	23.288	26.438	29.440	31.457	35.066
1.1	2.822	3.184	8.435	9.632	13.954	16.673	19.231	23.110	24.207	28.798	29.231	32.936
1.2	2.601	3.167	7.767	9.589	12.825	16.629	17.673	22.242	23.053	26.460	29.161	30.261

 $\xi = 0.10 D$

$T = \phi / T_x$	$\omega 1$	$\omega 2$	$\omega 3$	$\omega 4$	$\omega 5$	$\omega 6$	$\omega 7$	$\omega 8$	$\omega 9$	$\omega 10$	$\omega 11$	$\omega 12$
0.8	3.017	4.207	9.118	12.584	15.674	20.963	21.702	27.411	28.936	32.645	36.459	37.375
0.9	2.940	3.838	8.866	11.505	15.103	19.341	20.883	26.346	26.732	31.375	33.710	35.910
1.0	2.820	3.601	8.479	10.827	14.285	18.402	19.727	24.863	25.466	29.596	32.153	33.863
1.1	2.664	3.464	7.989	10.446	13.347	17.902	18.418	23.195	24.797	27.603	31.334	31.577
1.2	2.496	3.390	7.472	10.237	12.423	17.125	17.641	21.570	24.433	25.666	29.356	30.889

 $\xi = 0.50 D$

$T = \phi / T_x$	$\omega 1$	$\omega 2$	$\omega 3$	$\omega 4$	$\omega 5$	$\omega 6$	$\omega 7$	$\omega 8$	$\omega 9$	$\omega 10$	$\omega 11$	$\omega 12$
0.8	2.593	7.422	7.951	13.288	18.376	22.659	23.237	27.633	31.627	35.111	38.034	38.155
0.9	2.474	6.944	7.546	12.620	17.444	21.139	22.039	26.220	30.006	33.310	35.699	36.093
1.0	2.356	6.570	7.171	11.961	16.526	20.003	20.872	24.829	28.412	31.539	33.898	34.174
1.1	2.240	6.276	6.818	11.326	15.643	19.139	19.755	23.493	26.880	29.837	32.323	32.551
1.2	2.128	6.038	6.491	10.724	14.807	18.451	18.721	22.228	25.431	28.229	30.581	31.512

Table 3.3 (c) Frequencies for Building $T_x = 2.00$ Sec. , $\xi = 0.05$

depicted in Fig.3.12.

The study of mode shapes and modal participation factors for a building with $T_x = 1.0$ sec at $\tau = T_\phi / T_x = 1.0$ is indicated in Figs.3.13 to 3.15 and Tables 3.4 to 3.6 .

Attention is drawn to the buildings with small eccentricities. The mode shapes, modal participation factors and periods of six modes for the small eccentric building with $\tau = T_\phi / T_x = 1.0$ are shown in Fig.3.13 and Table 3.4 . It is interesting to notice that in the first four modes, the periods, the magnitudes of translational and torsional mode shapes, and modal participation factors are close in each pair of modes. According to the dynamic force equation(Eq.3.3), pairwise modal contributions consist of nearly identical modal shear forces(both magnitudes and signs), but the modal torques have the same magnitudes with opposite signs.

In another words, in a building with small eccentricity under sympathetic resonance condition, the pairwise modal contributions are out of phase (phase angle $\theta = \pi$) for torques and in phase ($\theta = 0$) for shear forces.

Moreover, owing to the periods being close in the lower two pairs of modes, the root-sum-square(RSS) rule in combining the modal contributions will exaggerate the design torsions and underestimate the response of shear force for the small eccentric buildings with equal uncoupled translational and torsional periods (i.e. $\tau = T_\phi / T_x = 1.0$). The mode shapes and modal participation factors for structures with moderate eccentricities at $\tau = 1.0$, generally appear in the same patterns and characters (shown in Fig.3.14 and Table 3.5). However, owing to the difference in pairwise mode periods, the cross modal torque interference, as mentioned before to the small eccentric building, is not so significant

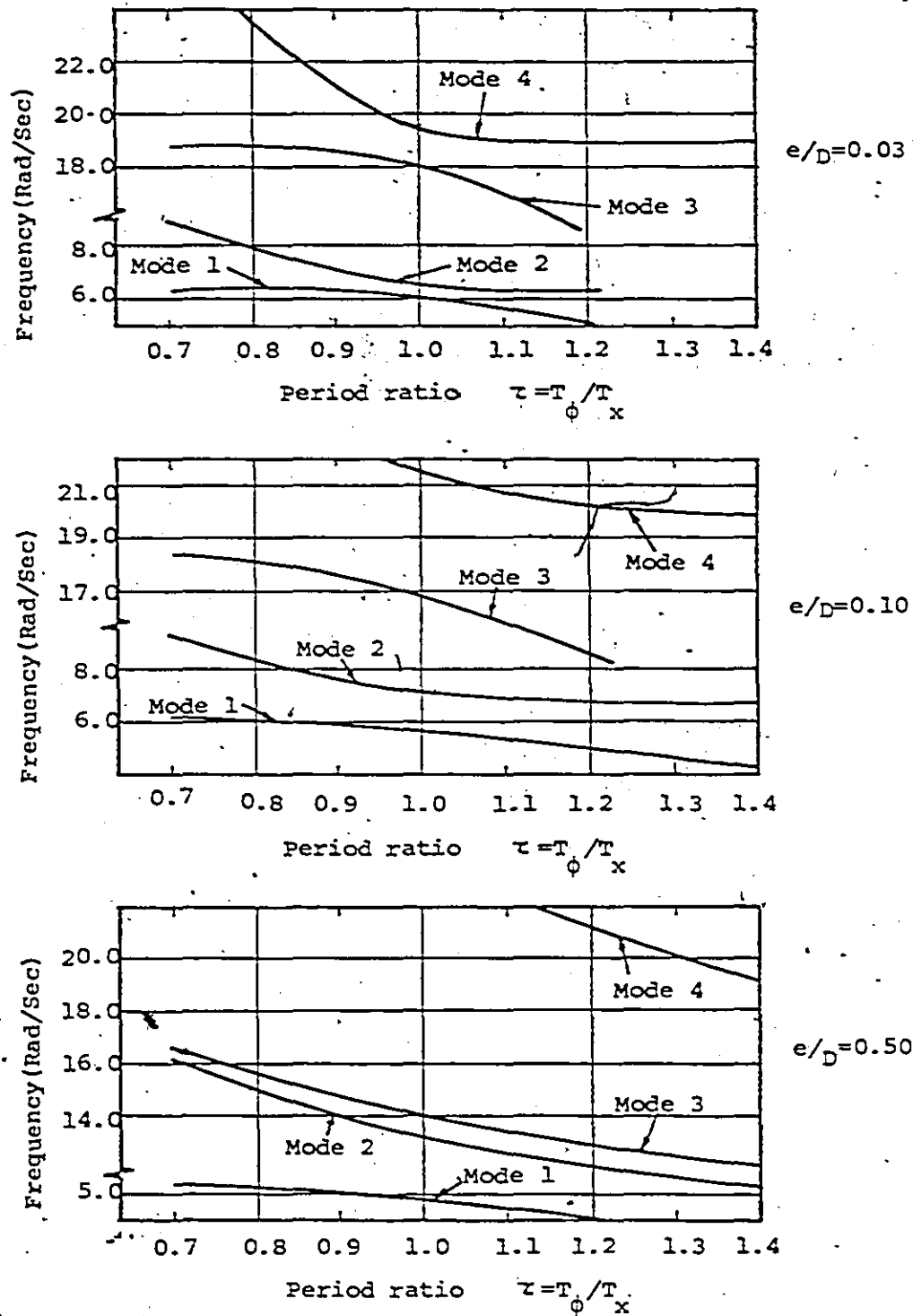


Fig.3.12 Effect of Eccentricity and Uncoupled Periods Ratios to Frequencies of Building ($T_x=1.0\text{Sec}$), $\xi = 0.05$

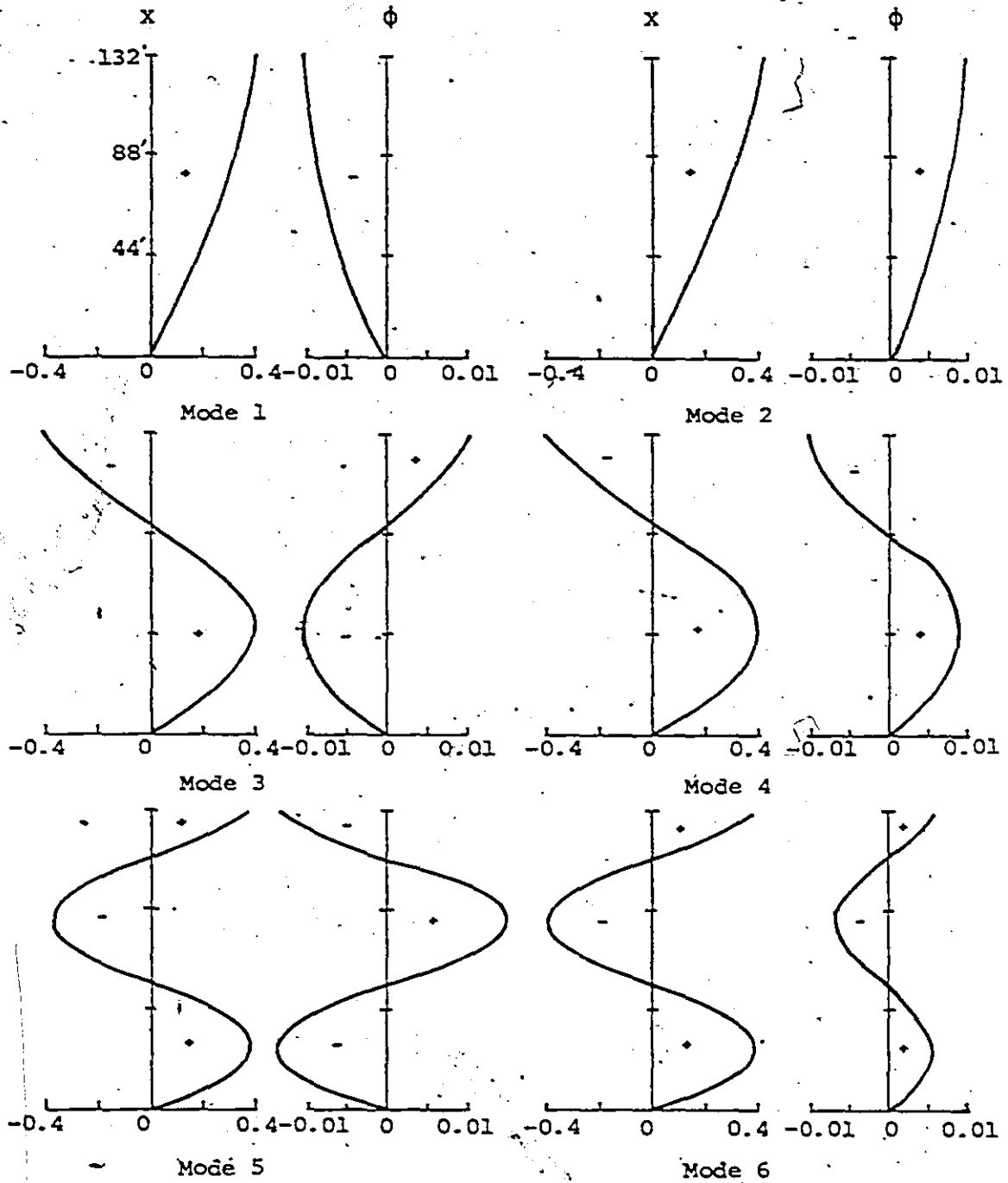


Fig.3.13 Mode Shapes for Building $T_x=1.0$ Sec. ($e/D=0.03$, $\tau=1.0$), $\xi_x=0.05$

Period	T1= 1.037 $\gamma_1 = 1.591$		T3= 0.347 $\gamma_3 = 0.5248$		T5= 0.208 $\gamma_5 = 0.1927$		
Mode shape	X	Theta	X	Theta	X	Theta	
Level	1	.4649E-01	-.1224E-02	.1458E+00	-.3863E-02	.2358E+00	-.8948E-02
	2	.9322E-01	-.2428E-02	.2713E+00	-.7184E-02	.3632E+00	-.1448E-01
	3	.1394E+00	-.3594E-02	.3596E+00	-.9496E-02	.3867E+00	-.1447E-01
	4	.1842E+00	-.4704E-02	.3989E+00	-.1047E-01	.2449E+00	-.8938E-02
	5	.2268E+00	-.5740E-02	.3839E+00	-.9982E-02	.1179E-01	.2832E-04
	6	.2666E+00	-.6685E-02	.3167E+00	-.8087E-02	-.2244E+00	.8979E-02
	7	.3028E+00	-.7525E-02	.2062E+00	-.5853E-02	-.3743E+00	.1451E-01
	8	.3348E+00	-.8247E-02	.6736E-01	-.1307E-02	-.3812E+00	.1451E-01
	9	.3621E+00	-.8839E-02	-.8131E-01	.2627E+02	-.2429E+00	.8963E-02
	10	.3843E+00	-.9291E-02	-.2199E+00	.6197E-02	-.1194E-01	-.1322E-04
	11	.4009E+00	-.9597E-02	-.3300E+00	.8900E-02	.2241E+00	-.8993E-02
	12	.4117E+00	-.9751E-02	-.3968E+00	.1036E-01	.3759E+00	-.1454E-01
Period	T2= 0.963 $\gamma_2 = 1.563$		T4= 0.322 $\gamma_4 = 0.5898$		T6= 0.192 $\gamma_6 = 0.4316$		
Mode shape	X	Theta	X	Theta	X	Theta	
Level	1	.4643E-01	.1245E-02	.1453E+00	.3438E-02	.2346E+00	.3996E-02
	2	.9318E-01	.2471E-02	.2704E+00	.6393E-02	.3813E+00	.6465E-02
	3	.1392E+00	.3657E+02	.3585E+00	.8449E-02	.3846E+00	.6464E-02
	4	.1840E+00	.4785E-02	.3977E+00	.9317E-02	.2432E+00	.3996E-02
	5	.2266E+00	.5838E-02	.3829E+00	.8876E-02	.1049E-01	.7439E-05
	6	.2664E+00	.6796E-02	.3159E+00	.7189E-02	-.2254E+00	-.3976E-02
	7	.3027E+00	.7651E-02	.2056E+00	.4495E-02	-.3752E+00	-.6434E-02
	8	.3348E+00	.8383E-02	.6672E-01	.1173E-02	-.3821E+00	-.6430E-02
	9	.3622E+00	.8983E-02	-.8223E-01	-.2310E-02	-.2433E+00	-.3972E-02
	10	.3844E+00	.9441E-02	-.2213E+00	-.5463E-02	-.1118E-01	-.3925E-05
	11	.4010E+00	.9750E-02	-.3320E+00	-.7845E-02	.2264E+00	.3957E-02
	12	.4118E+00	.9906E-02	-.3993E+00	-.9125E-02	.3794E+00	.6401E-02

γ_i = Modal Participation Factor

Table 3.4 Mode Shapes for Building $T=1.0$ Sec. $e/D=0.03$, $\tau=1.0$, $\xi=0.05$

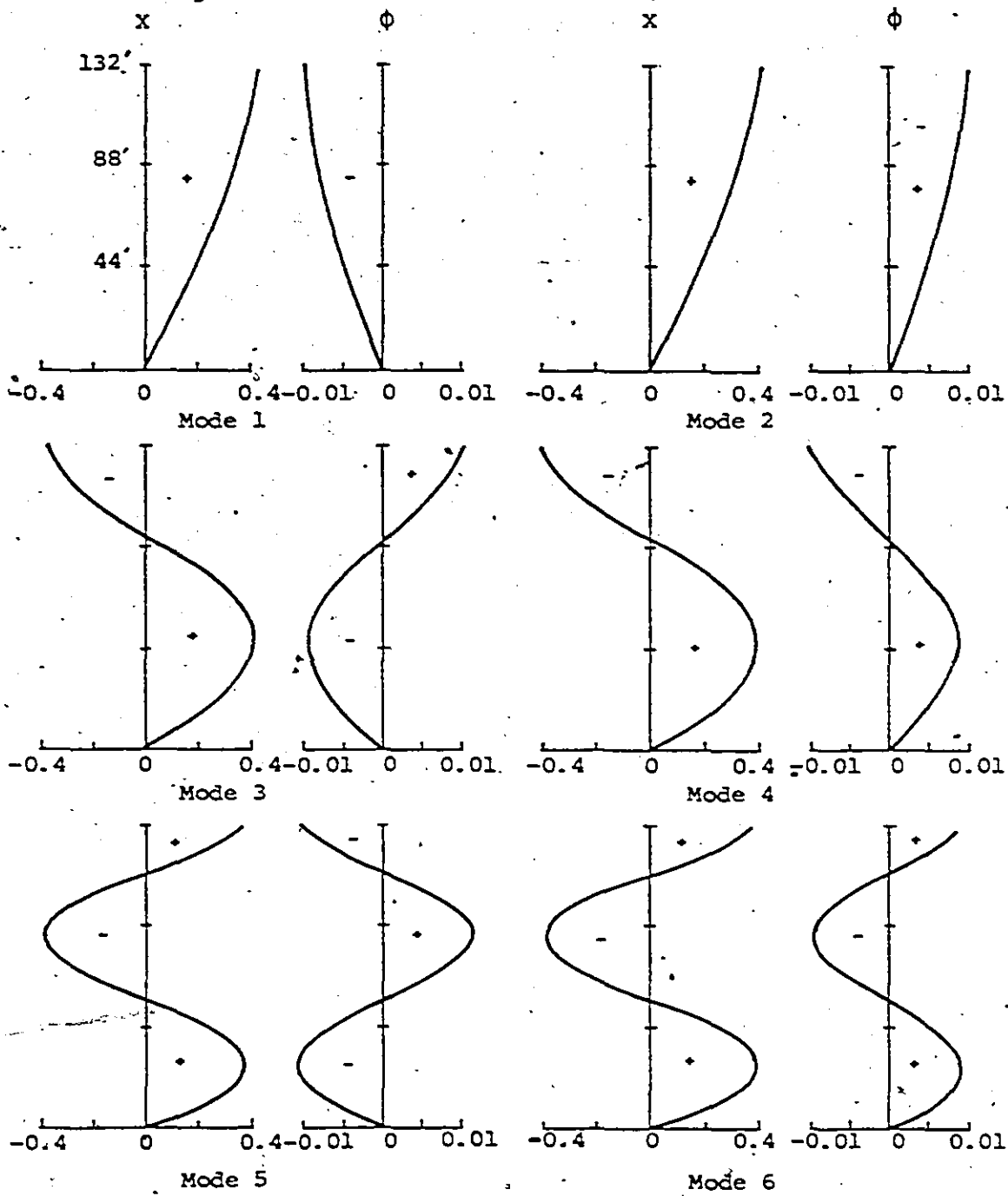


Fig. 3.14 Mode Shapes for Building $T_x = 1.0$ Sec. ($e/D = 0.1$, $\tau = 1.0$), $\xi = 0.05$

Period	$\#1= 1.114$	$\gamma_1 = 1.584$	$T3= 0.372$	$\gamma_3 = 0.5499$	$T5= 0.223$	$\gamma_5 = 0.2760$	
Mode Shape	X	Theta	X	Theta	X	Theta	
Level	1	.4654E-01	-.1197E-02	.1464E+00	-.3594E-02	.2380E+00	-.6541E-02
	2	.0331E-01	-.2175E-02	-.2723E+00	-.6682E-02	-.3872E+00	-.1057E-01
	3	.1395E+00	-.3516E-02	.3609E+00	-.8833E-02	.3916E+00	-.1055E-01
	4	.1843E+00	-.4602E-02	-.4004E+00	-.9741E-02	-.2601E+00	-.6450E-02
	5	.2269E+00	-.5616E-02	.3856E+00	-.9273E-02	.1646E-01	.1321E-03
	6	.2667E+00	-.6542E-02	-.3184E+00	-.7589E-02	-.2207E+00	-.6711E-02
	7	.3029E+00	-.7369E-02	.2080E+00	-.4676E-02	.3728E+00	.1076E-01
	8	.3348E+00	-.8073E-02	-.6027E-01	-.1174E-02	-.3805E+00	-.1872E-01
	9	.3621E+00	-.8654E-02	-.7912E-01	.2506E-02	.2440E+00	.6581E-02
	10	.3842E+00	-.9098E-02	-.2173E+00	-.5850E-02	-.1492E+01	-.8729E-04
	11	.4008E+00	-.9398E-02	-.3269E+00	.8365E-02	.2193E+00	-.6755E-02
	12	.4116E+00	-.9549E-02	-.3934E+00	-.9753E-02	-.3608E+00	-.1088E-01
Period	$T2= 0.872$	$\gamma_2 = 1.568$	$T4= 0.292$	$\gamma_4 = 0.5626$	$T6= 0.174$	$\gamma_6 = 0.3455$	
Mode Shape	X	Theta	X	Theta	X	Theta	
Level	1	.4631E-01	.1206E-02	.1443E+00	.3516E-02	.2387E+00	.5237E-02
	2	.0289E-01	-.2397E-02	-.2686E+00	-.6533E-02	-.3760E+00	-.8444E-02
	3	.1389E+00	.3547E-02	.3564E+00	.8625E-02	.3812E+00	.8398E-02
	4	.1837E+00	-.4640E-02	-.4060E+00	-.9497E-02	-.2435E+00	-.5110E-02
	5	.2263E+00	.5658E-02	.3819E+00	.9030E-02	.1369E-01	-.8234E-04
	6	.2662E+00	-.6587E-02	-.3168E+00	-.7294E-02	-.2222E+00	-.5200E-02
	7	.3025E+00	.7410E-02	.2062E+00	.4543E-02	.3747E+00	-.8281E-02
	8	.3347E+00	-.8116E-02	-.6746E-01	-.1161E-02	-.3858E+00	-.8182E-02
	9	.3622E+00	.8694E-02	-.8202E-01	-.2351E-02	.2477E+00	.4985E-02
	10	.3845E+00	-.9135E-02	-.2223E+00	-.5522E-02	-.1367E+01	-.6023E-04
	11	.4013E+00	.9432E-02	-.3342E+00	-.7905E-02	.2284E+00	.5034E-02
	12	.4122E+00	-.9581E-02	-.4026E+00	-.9178E-02	-.3853E+00	-.8076E-02

γ_i = Modal Participation Factor

Table 3.5 Mode Shapes for Building $T_x=1.0$ Sec., $e/D=0.10$, $\tau=1.0$, $\xi=0.05$

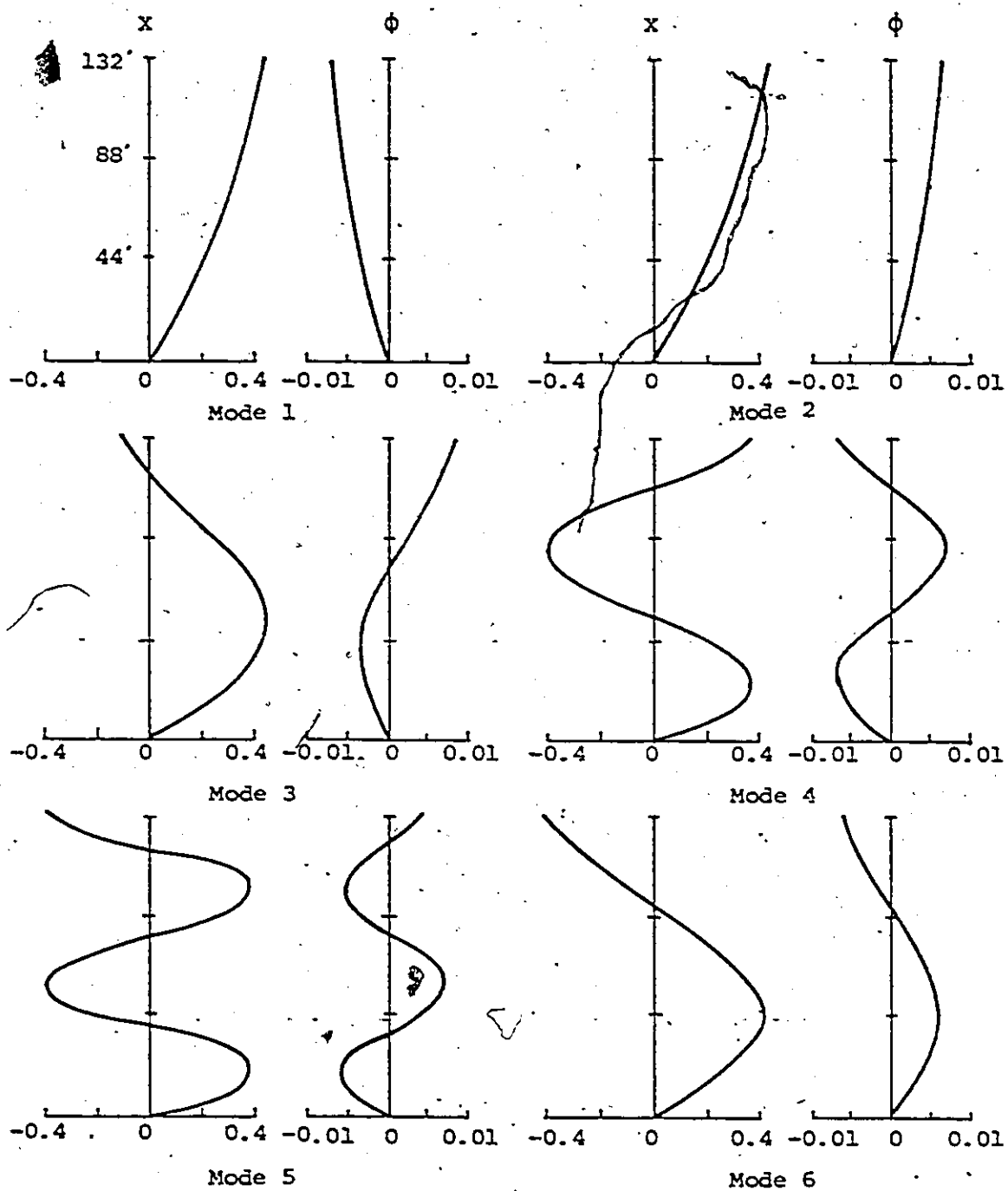


Fig.3.15 Mode Shapes for Building $T_x=1.0$ Sec. ($e/D=0.5$, $\tau=1.0$), $\xi=0.05$

Period	T1= 1.333	$\gamma_1 = 1.584$	T3= 0.444	$\gamma_3 = 0.7946$	T5= 0.193	$\gamma_5 = 0.2114$	
Mode shape	X	Theta	X	Theta	X	Theta	
Level	1	.4664E-01	-.7756E-03	.1459E+00	-.1414E-02	.3153E+00	-.5035E-02
	2	.9349E-01	-.1539E-02	.2752E+00	-.2575E-02	.4077E+00	.6340E-02
	3	.1397E+00	-.2279E-02	.3739E+00	-.3263E-02	.2155E+00	-.4896E-02
	4	.1846E+00	-.2984E-02	.4317E+00	-.3329E-02	-.1187E+00	.2867E-02
	5	.2272E+00	-.3643E-02	.4439E+00	-.2712E-02	-.3512E+00	.6817E-02
	6	.2669E+00	-.4245E-02	.4119E+00	-.1448E-02	-.3138E+00	.6103E-02
	7	.3030E+00	-.4780E-02	.3429E+00	.3294E-03	-.3508E-01	.1218E-02
	8	.3350E+00	-.5241E-02	.2486E+00	.2412E-02	.2803E+00	-.4359E-02
	9	.3621E+00	-.5620E-02	.1440E+00	.4542E-02	.3996E+00	-.6671E-02
	10	.3841E+00	-.5909E-02	.4497E-01	.6448E-02	.2309E+00	-.4135E-02
	11	.4006E+00	-.6105E-02	-.3383E-01	.7881E-02	-.1102E+00	.1320E-02
	12	.4113E+00	-.6205E-02	-.8108E-01	.8652E-02	-.3832E+00	.5658E-02
Period	T2= 0.474	$\gamma_2 = 1.117$	T4= 0.267	$\gamma_4 = 0.2924$	T6= 0.158	$\gamma_6 = 0.5068$	
Mode shape	X	Theta	X	Theta	X	Theta	
Level	1	.3479E-01	.9584E-03	.2290E+00	-.4010E-02	.1330E+00	.2495E-02
	2	.7144E-01	.1879E-02	.3702E+00	-.6520E-02	.2600E+00	.4428E-02
	3	.1105E+00	.2728E-02	.3688E+00	-.6595E-02	.3627E+00	.5546E-02
	4	.1520E+00	.3480E-02	.2242E+00	-.4222E-02	.4136E+00	.5928E-02
	5	.1957E+00	.4116E-02	-.9279E-02	-.3143E-03	.3937E+00	.5720E-02
	6	.2406E+00	.4629E-02	-.2431E+00	.3638E-02	.3088E+00	.4903E-02
	7	.2854E+00	.5021E-02	-.3882E+00	.6134E-02	.1847E+00	.3344E-02
	8	.3283E+00	.5303E-02	-.3885E+00	.6233E-02	.4896E-01	.1081E-02
	9	.3674E+00	.5491E-02	-.2439E+00	.3911E-02	-.8498E-01	-.1492E-02
	10	.4006E+00	.5605E-02	-.7279E-02	.6998E-04	-.2136E+00	-.3770E-02
	11	.4281E+00	.5665E-02	.2326E+00	-.3806E-02	-.3287E+00	-.5296E-02
	12	.4423E+00	.5689E-02	.3863E+00	-.6227E-02	-.4056E+00	-.5977E-02

γ_1 = Modal Participation Factor

Table 3.6 Mode Shapes for Building $T_x=1.0$ Sec., $e/D=0.05$, $\tau=1.0$, $\xi=0.05$

in this case.

Fig. 3.15 and Table 3.6 exhibit the mode shapes, modal participation factors and periods for the building with exceptional large eccentricities when $\tau = 1.0$. It is observed that the mode periods are well separated and the cross modal torque interference does not affect the dynamic response for this building, even though the uncoupled torsional and translational periods are equal.

In order to display the effect of cross modal torque interference, the dynamic modal base shears and base torques for the twelve-storey buildings with small, moderate and large eccentricities at $\tau = T_\phi / T_x = 1.0$ are listed in Table 3.7.

3.7 The Discussion of the RSS Role for Modal Contribution

The maximum elastic force in mode i is given in equation 3.3, in which S_{a_i} is the spectral acceleration for i th mode. Because the maxima in each mode usually do not occur at the same time, the method of square root of the sum of the squares of the modal response is proposed to obtain the maximum total response. For instance, the maximum total shear force (P) is approximated by

$$P_{\max} = \sqrt{(P_1)_{\max}^2 + (P_2)_{\max}^2 + \dots} \quad (3.4)$$

In a system with two degrees of freedom having classical modes, when the two natural frequencies are close to each other, that is, when $\frac{\omega_2 - \omega_1}{\omega_2 + \omega_1} \ll 1$ the response functions exhibit beating and behave as a sine or cosine wave of frequency $\omega_2 + \omega_1$ modulated by a trigonometric function of

α/D	MODE	1	2	3	4	5	6	7	8	9	10	11	12	R.B.B.	Hewmark & Rosen- bluth	STATIC
0.03	Base Shear	378 ^k	345	106	103	23	43	10	21	5	12	3	6	535.7	691	672
	Base Torque	-15350 ^{k-ft}	14250	-4270	3682	-1309	1115	-613	521	-332	281	-194	154	21770	12990	6383
0.10	Base Shear	405 ^k	313	129	80	38	28	10	8	15	5	8	3	537	579	672
	Base Torque	-16940 ^{k-ft}	13260	-5070	3112	-1662	1017	-790	-416	466	-251	261	-142	22430	20760	13440
0.50	Base Shear	406 ^k	90	257	55	29	19	19	8	5	3	8	1	562	597	672
	Base Torque	-31300 ^{k-ft}	9696	-9535	-3681	-1755	1388	-943	-562	-340	-203	427	-105	34420	32480	107500

Table 3.7 Base Shear and Torque for Building

$T_x = 1.0$ Sec, $\tau = 1.0$

frequency $\omega_2 - \omega_1$. This phenomenon may illustrate the situations described in previous section. However, to obtain the total maximum response of a structure, Newmark and Rosenblueth presented an equation [20] to modify the approximated RSS method. i.e.

$$Q^2 = \sum_i Q_i^2 + \sum_{i \neq j} \frac{Q_i \cdot Q_j}{1 + \epsilon_{ij}} \quad - (3.6)$$

where $\epsilon_{ij} = \frac{\omega'_i - \omega'_j}{\xi'_i \omega_i + \xi'_j \omega_j}$

and $\omega'_i = \omega_i \sqrt{1 - \xi_i^2}$ is the damped frequency,

In this thesis, 5 per cent damping ratio (ξ) is adopted for all the examples, so $\xi'_i = \xi'_j = \xi = 0.05$ and $\omega'_i = \omega_i$, $\omega'_j = \omega_j$ are used for simplicity. Therefore, the simplified results lead to $\epsilon_{ij} = \frac{\omega_i - \omega_j}{\xi(\omega_i + \omega_j)}$

Based on this form, the dynamic design base shear and torque are computed once more for the twelve-storey monosymmetrical building with different eccentricities. The comparison of the difference of base shear and torque between equations (3.4) and (3.6) are shown in Figs. 3.16 to 3.19 under the condition that the uncoupled torsional period is equal to uncoupled translational period.

Intuitively, equation 3.6 drops the torque and increases the shear forces dramatically when the eccentricity is small. For instance, the RSS rule underestimates the base shear to the structures with small and moderate eccentricities by the factors of 0.78 and 0.93 respectively,

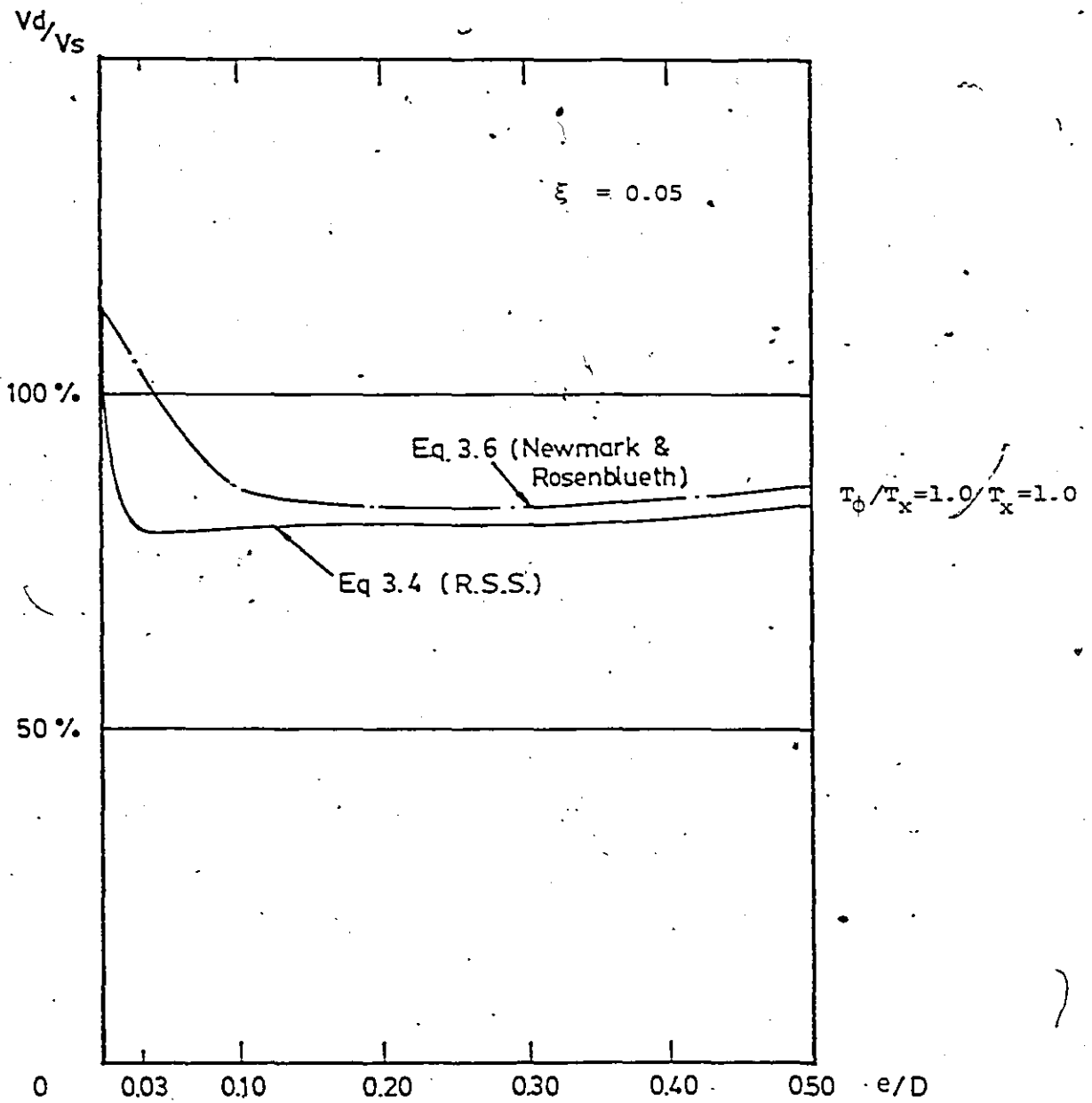


Fig.3.16 Dynamic Base Shear Comparison Between Eq.3.4 and Eq.3.6

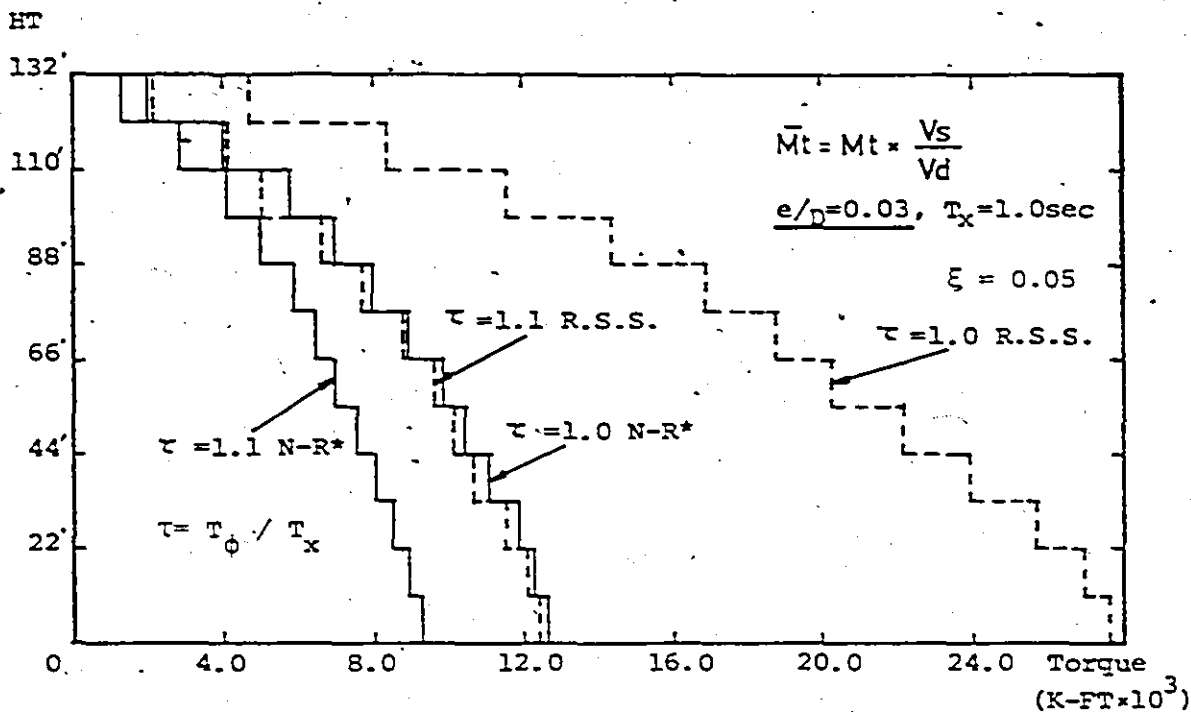


Fig. 3.17 Normalized Torque Comparison Between R.S.S. and N-R^{*} Equation

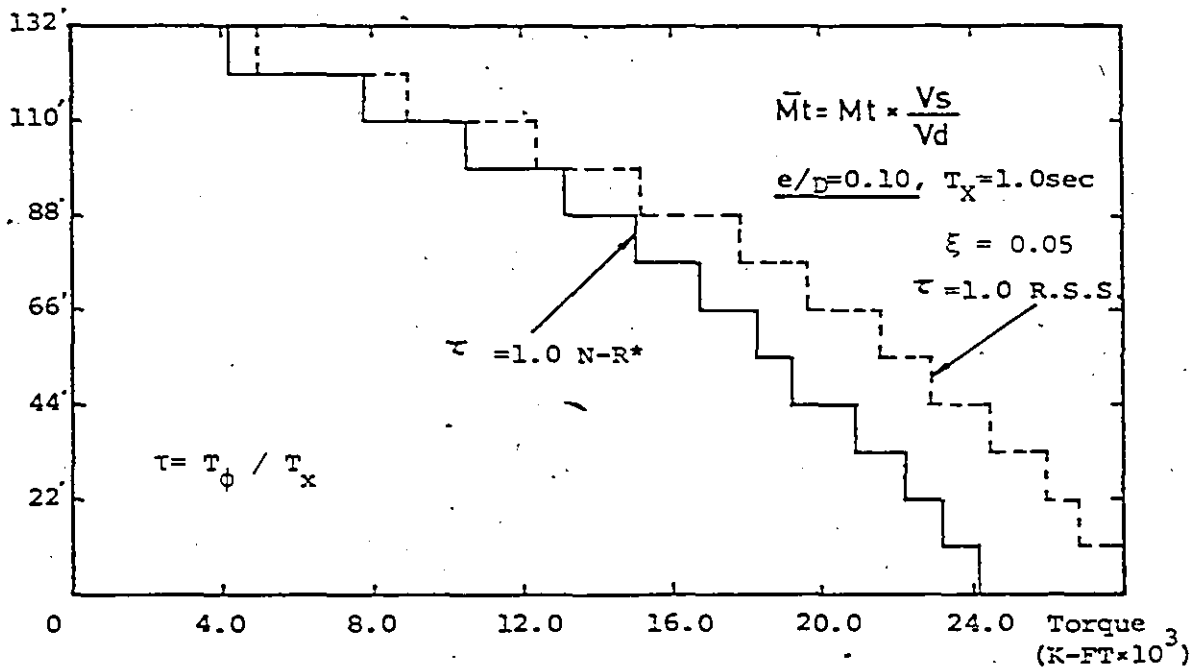


Fig. 3.18 Normalized Torque Comparison Between R.S.S. and N-R^{*} Equation

* N-R = Newmark & Rosenblueth Equation

HT.

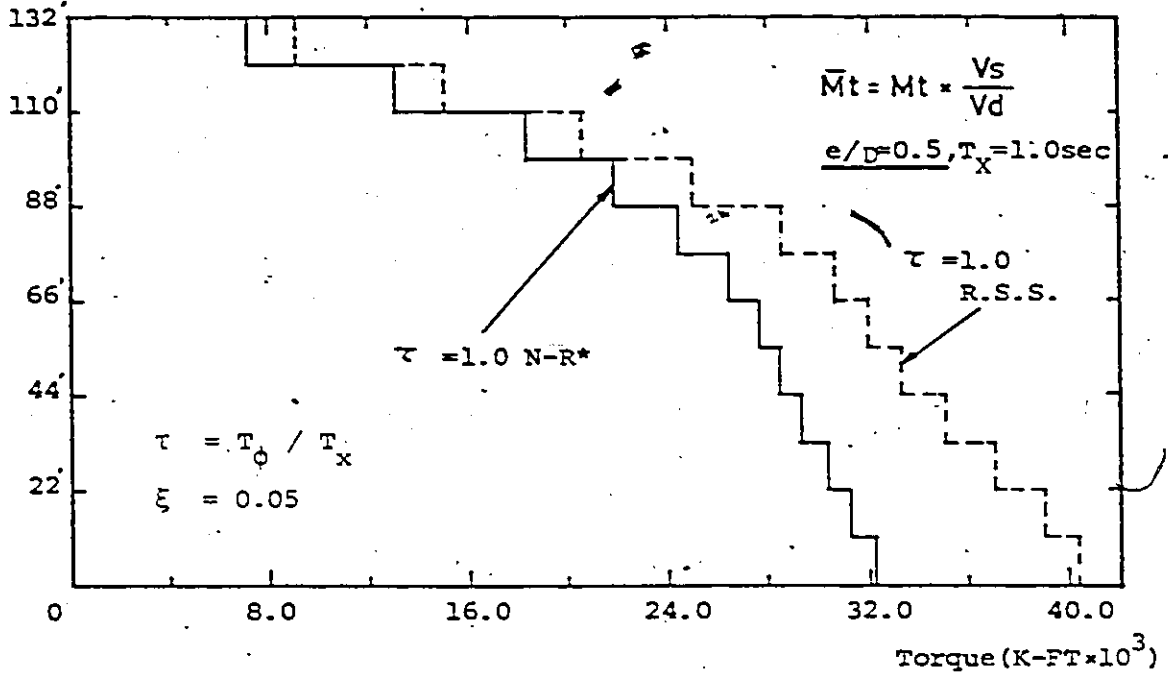


Fig. 3.19 Normalized Torque Comparison Between R.S.S. and N-R* Equation

* N-R = Newmark & Rosenblueth Equation


if the calculations are compared between Eq.3.4 and Eq.3.6 . On the other hand, the RSS rule overestimates the base torque of these two structures by the factors of 1.67 and 1.08 respectively. Consequently, the normalized dynamic torques ($\bar{M}_t = M_t \times \frac{V_s}{V_d}$) by equation 3.6 differ from the calculation of equation 3.4 by a factor of 2.14 for the structure with $e/D = 0.03$ and 1.16 for the structure with $e/D = 0.10$. ✓

3.8 Conclusions

The study of dynamic base shear and torque in the coupled translational and torsional response in monosymmetrical frame buildings leads to the following conclusions:

- (1) The coupled torsional-translational sympathetic resonance occurs in the structures with small eccentricities. The closeness of the coupled periods is the governing factor to the phenomenon of torsional coupling.
- (2) For the structures with large eccentricities, the ratio of uncoupled torsional to translational periods does not reflect the effect of the closeness of coupled periods. For instance, the first and second periods are 1.33 sec and 0.47 sec respectively for the building with exceptionally large eccentricities ($e/D = 0.5$), even when the uncoupled torsional and translational periods are both 1 second . The cross modal torque interference in this case is indeed very small.
- (3) The current static torque calculation in NBC 77 defines that the torsion should be doubled when the design

eccentricity (e_y) exceeds $0.25 D_n$ is a conservative requirement.

- (4) The conventional RSS rule exaggerates the torsion and diminishes shear force responses when the center of mass is close to the center of resistance of the structure and the uncoupled translational and torsional periods are approximately equal. The equation (3.6) is believed to be the 'best' estimate of maximum total response, particularly to the structures with coupled motions' periods are not well separated.
- 

CHAPTER 4

TORSIONAL PROVISIONS IN BUILDING CODES

4.1 Introduction

Subsection 4.1.9 'Effects of Earthquakes' of NBC 77 defines the static formulation of torsional moments (M_{tx}) and design eccentricity (e_x). When the design eccentricity (e_x) exceeds $0.25 D_n$, Building Code (NBC 77) requires that a dynamic analysis shall be made or the torsion shall be doubled. Commentary J and K of NBC 77 allow the use of analysis by response spectrum method and limit the dynamic base shear such that it can not be less than 90 per cent of static base shear.

In order to study the accuracy of the static code provision on torsional effect, the normalized dynamic torques studied in Chapter 3 are compared to the static calculations according to NBC 77. Mono-symmetrical frame buildings with uncoupled translational period (T_x) equals one second and various eccentricities are taken as examples. Moreover, the static torsional provisions supplied by another four countries building codes (i.e. Germany, Mexico, U.S.A. and New Zealand codes) are investigated at the same time.

For irregular buildings with eccentric offset (or setback), NBC 80 modifies the formulation of static eccentricity (e). Also, it is studied and discussed in this chapter.

4.2 Torsional Provisions in Building Codes

Most seismic Building Codes formulate the static torsional moment

at each storey by multiplying the storey shear and a quantity termed 'design eccentricity' (e_x). As tabulated in Table 4.1 most building codes, except the German code, define the design eccentricity into two parts. Generally, the first part is a function of the eccentricity defined as the distance between the mass center and the resistance center. This part accounts for the complex motion of torsion and the effect of the simultaneous action of the two horizontal ground motion. NBC 77, Mexican and New Zealand codes introduce a magnification factor by 50 per cent to 70 per cent. The second term is called ~~accidental~~ eccentricity to attribute other factors such as the variations in the estimates of the relative rigidities, uncertain estimates of dead and live loads at the floor levels, addition of wall panels and partitions after completion of the building, variation of the stiffness with time and inelastic or plastic action. The effect of possible torsional motion of the ground is also considered. In general, this term is a function of D — the maximum dimension of the storey measured perpendicular to the direction of lateral ground motion.

Canadian Code (NBC) is one of the few codes in which dynamic analysis by using response spectrum technique can be applied as an alternative for design calculation. For combining the maximum response from different modes, the root-sum-square rule is utilized.

As well as indicated in Commentary K of NBC 77, the study of effects of coupled motion in Chapter 3 has demonstrated that the static torsional moment is a good estimation when τ is out of the range of ± 20 per cent. Because the envelopes of floor torques for both static and dynamic analysis to the three frame buildings are similar, only the base torques (M_{t0}) of the 12-storey buildings are chosen to study the accuracy of building codes.

Country	Design Eccentricity	Comment
Canada [1]	$e_x = 1.5e + 0.05D$ or $e_x = 0.5e - 0.05D$	Torsional shear on member based on worse of two cases
Germany [21]	$e_x = e + e_1 + 0.05D$ or $e_x = e - 0.05D$	Torsional shear on member based on worse of two cases
Mexico [22]	$e_x = 1.5e + 0.10D$ or $e_x = e - 0.10D$	Torsional shear on member based on worse of two cases
New Zealand [23]	$e_x = 1.7e - e^2/D + 0.10D$ or $e_x = e - 0.10D$	Torsional shear on member based on worse of two cases
Turkey [24]	$e_x = e + 0.05D$	--
U.S.A. [25]	$e_x = e + 0.05D$	Negative torsional shear on member neglected.
U.S.A. (ATC 3-06) [26]	$e_x = e + 0.05D$ or $e_x = e - 0.05D$	Torsional shear on member based on worse of two cases.

e = structural eccentricity

e_1 = eccentricity factor to allow for sympathetic resonance effect [15]

D = plan dimension of floor

Table 4.1 The Formulations of Design Eccentricity of Different Countries

As shown in Figs. 4.1 and 4.2, the normalized dynamic base torques by RSS rule according to Commentary K of NBC 77 and Newmark and Rosenblueth equation (Eq. 3.6) are presented with various ratios (τ) of uncoupled torsional periods to translational periods. It can be seen again, the dynamic RSS torques are substantially reduced in the buildings with small eccentricities due to the cross modal torque interference. The other torsional moments of five seismic codes are also presented. The results show that the German code provides a good estimate, particularly when the uncoupled torsional and translational periods are equal. This is because there is an additional term e_1 in the German code's design eccentricity which takes into account the effect of sympathetic coupled resonance^[15]. The other four seismic codes have no provision for this effect. In decreasing order of underestimation, they are the New Zealand code, Mexican code, Canadian code and the U.S. code.

For a building in which the design eccentricity exceeds 25 per cent of plan dimension, NBC 77 requires the static torque to be doubled. Fig. 4.3 shows the normalized dynamic and static torques for the 12-storey frame building with exceptionally large eccentricity ($e/D = 0.5$). As a comparison, a curve marked 1/2 NBC is also presented to show if the requirement of doubling torque is ignored. It can be seen that the static torque curve without doubling has conservatively enveloped the dynamic torque curve. It shows further that the doubling static torque as currently specified in NBC 77 is a very conservative requirement for buildings with large eccentricity.

4.3 Buildings with Eccentric Offset

The design eccentricity e_x defined in NBC 77 is a local measurement in each storey of the building. To an irregular building with the

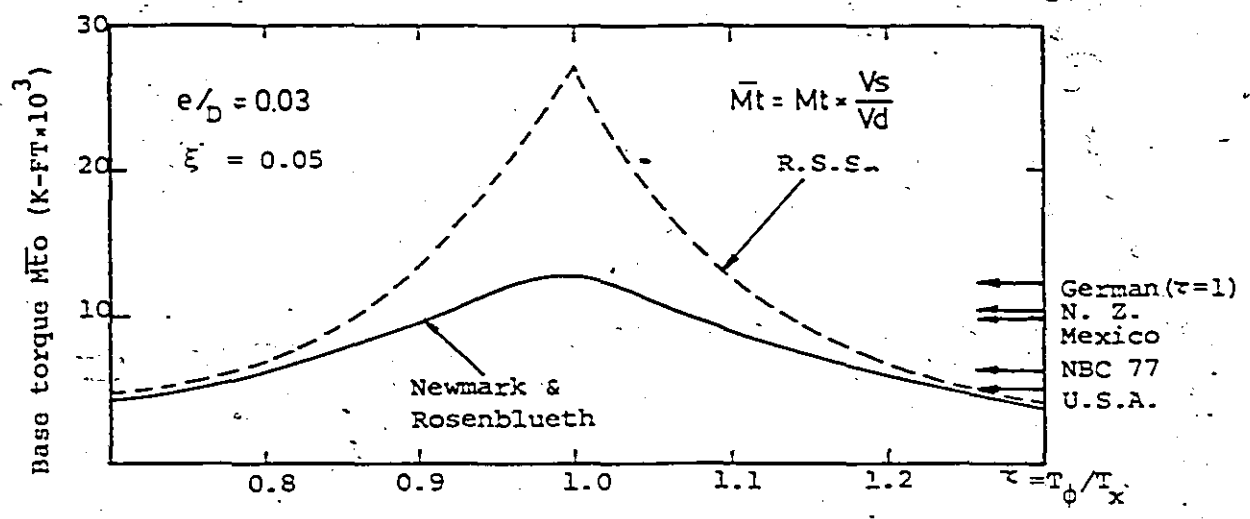


Fig. 4.1 The Effect of Torsional Period for Building $T_x = 1.0$ Sec.

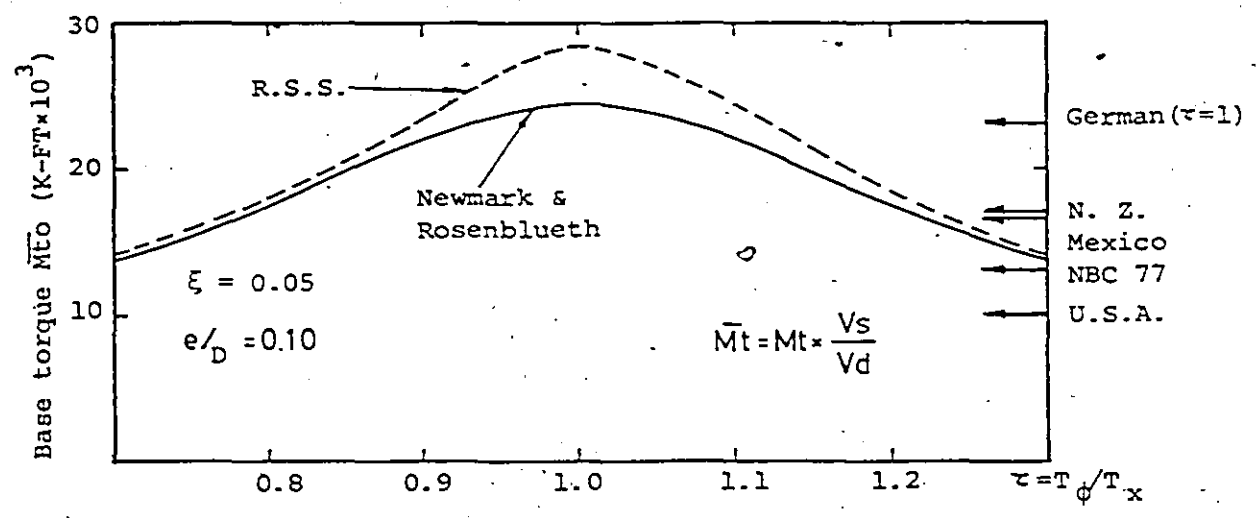


Fig. 4.2 The Effect of Torsional Period for Building $T_x = 1.0$ Sec.

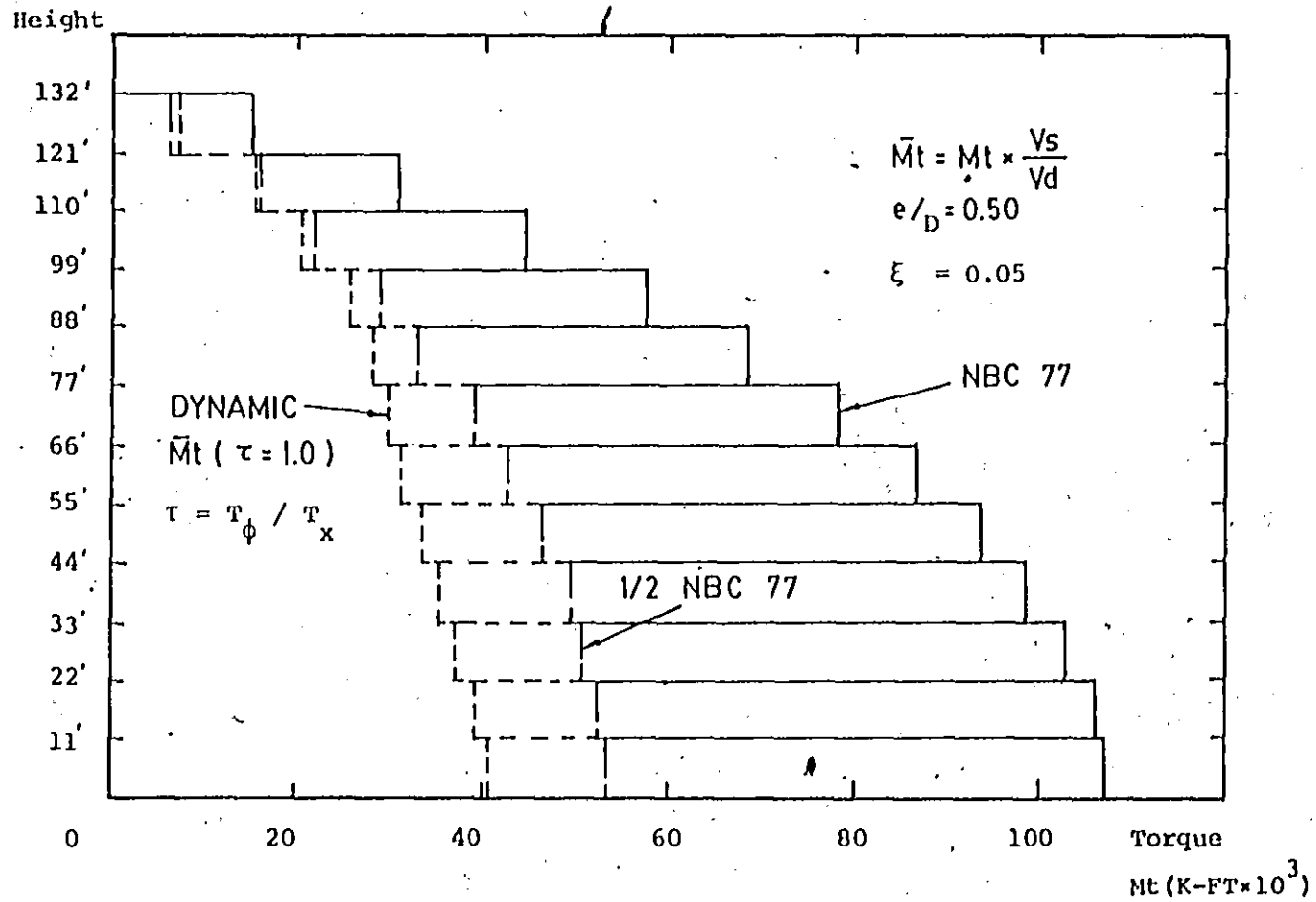


Fig. 4.3 Comparison of Torque for Building $T_x = 1.0$ Sec.

feature of eccentrical offset (shown in Fig.4.4), NBC 80 provides a modification on the definition of structural eccentricity (e). For floor x , e is given by equation

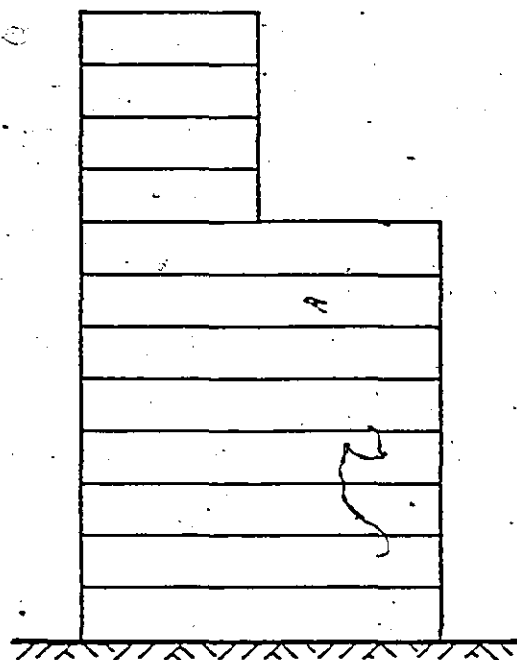
$$e = \frac{\sum_{i=x}^N P_i e_{ix}}{\sum_{i=x}^N P_i} \quad (4.1)$$

where e_{ix} = distance between the center of mass at floor i to the center of resistance at floor x and N is the total number of floor. Equation(4.1) essentially establishes an equivalent structural eccentricity for floor x by considering all the torques caused by shear forces in and above floor x . Therefore, the effect of eccentric offset of the upper stories can be taken into consideration.

The establishment of general equation of motion in Chapter 2(Eq.2.30) allows the dynamic analysis for a building to be referred to an arbitrary point conveniently. In order to clarify the applicability of new equation(4.1), a comparison of dynamic and static analysis according to Canadian Building Code is made to buildings with the features of eccentrical offset. Within each floor, the floor plan is assumed symmetrical.

As shown in Fig.4.4, the eccentric offset floor plan is arranged to reduce half of the floor dimensions in Y axis (half number of floor columns are reduced in the same time). Therefore, the centers of mass or rigidity of the offset floors and centers of mass or rigidity of the floors of the lower portion of the building do not lie on one vertical axis, and the structural eccentricity is entirely due to the eccentric offset.

Three frame buildings with two, four and six eccentric offset top stories are considered (shown in Fig.4.6). Assuming that the



Section A-A



Lumped mass modelling

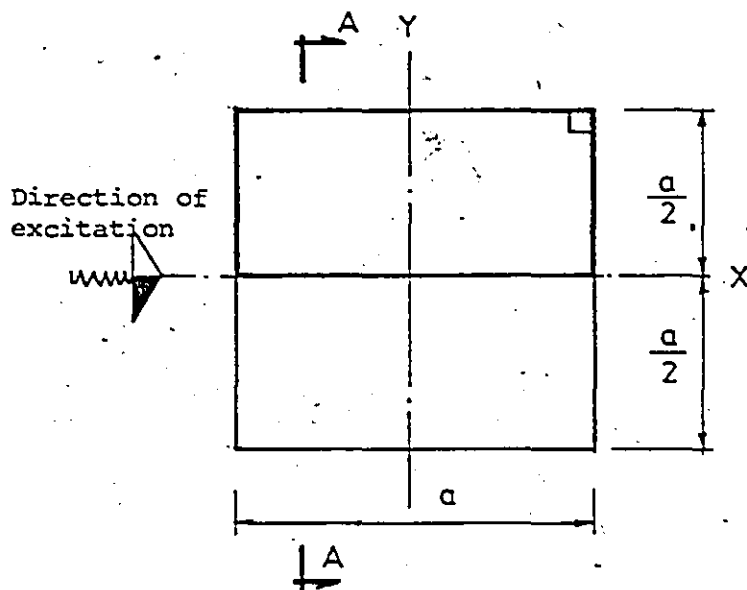


Fig. 4.4 The Configuration of Eccentric Offset Building

columns in each floor are regularly symmetrically spaced, half of mass and interstorey lateral stiffness are taken for the offset floor, because the translational stiffnesses in X and Y directions are

$$K_x = \sum_{i=1}^m k_{xi}$$

$$\text{and } K_y = \sum_{i=1}^m k_{yi}$$

in which k_{xi} and k_{yi} are the lateral stiffness of each column in X and Y axes respectively, and m is the total number of columns in the lower portion of building's floor plan.

By further assuming that the lateral stiffness of each column in both X and Y axes are equal, i.e. $k_{xi} = k_{yi}$, 31% of floor torsional stiffness and mass polar moment of inertia at the regular lower portion of the building can be taken for the offset floors. Since the floor torsional stiffness ($K_{\phi 1}$) in the lower portion of the building is

$$K_{\phi 1} = \sum_{i=1}^m k_{yi} \cdot x_i^2 + \sum_{i=1}^m k_{xi} \cdot y_i^2$$

and the torsional stiffness ($K_{\phi 2}$) in the offset floor is

$$K_{\phi 2} = \frac{1}{2} \left[\sum_{i=1}^m k_{yi} \cdot x_i^2 + \sum_{i=1}^m k_{xi} \cdot \left(\frac{y_i}{2}\right)^2 \right]$$

let $x_i = y_i = c_i$ and $k_{xi} = k_{yi} = k_{ci}$

$$K_{\phi 1} = 2 \sum_{i=1}^m k_{ci} \cdot c_i^2$$

$$\text{and } K_{\phi 2} = \frac{1}{2} \left(\sum_{i=1}^m \frac{5}{4} k_{ci} \cdot c_i^2 \right)$$

therefore

$$\frac{K_{\phi 2}}{K_{\phi 1}} = \frac{\frac{5}{8} \sum_{i=1}^m k_{ci} \cdot c_i^2}{2 \sum_{i=1}^m k_{ci} \cdot c_i^2} = \frac{5}{16} = 0.31$$

Mass polar moment of inertia for the floor in the lower portion of the building refer to the center of mass is

$$\begin{aligned} I_{\phi 1} &= I_{xx} + I_{yy} \\ &= \rho \frac{a^2}{12} \cdot 2a^2 \end{aligned}$$

where ρ is the floor area mass density. And the mass polar moment of inertia for the offset floor is

$$I_{\phi 2} = \frac{1}{2} \cdot \rho \cdot \frac{a^2}{12} \cdot \frac{5a^2}{4}$$

Hence

$$\frac{I_{\phi 2}}{I_{\phi 1}} = \frac{5}{16} = 0.31$$

As shown in Fig. 4.5, the reference points for the lower portion of the building are chosen as the floor center of mass (or rigidity). The reference points for the eccentric offset floors are located on the vertical axis through the floor centers of mass (or rigidity) of the lower portion of the building. After the dynamic analysis is completed for each mode, the dynamic shear forces and torques occurred at these fictitious reference points are transferred back to the 'real' center of mass (or rigidity) for the eccentric floors. It can be seen from the figure, the torque (free vectors) are unrestricted moving to center of mass of the offset floor while transfer shear force (sliding vector) to the center of mass (or rigidity) involves an additional torque at the center of mass of the offset floors.

Figs. 4.7 to 4.9 show the comparison of storey torques occurred at floor mass centers to the three irregular buildings. The calculations are based on NBC 77, NBC 80 and dynamic response spectrum analysis. The final dynamic torque envelope is the result of the RSS combination of twelve modal response. The natural frequencies of these buildings are shown

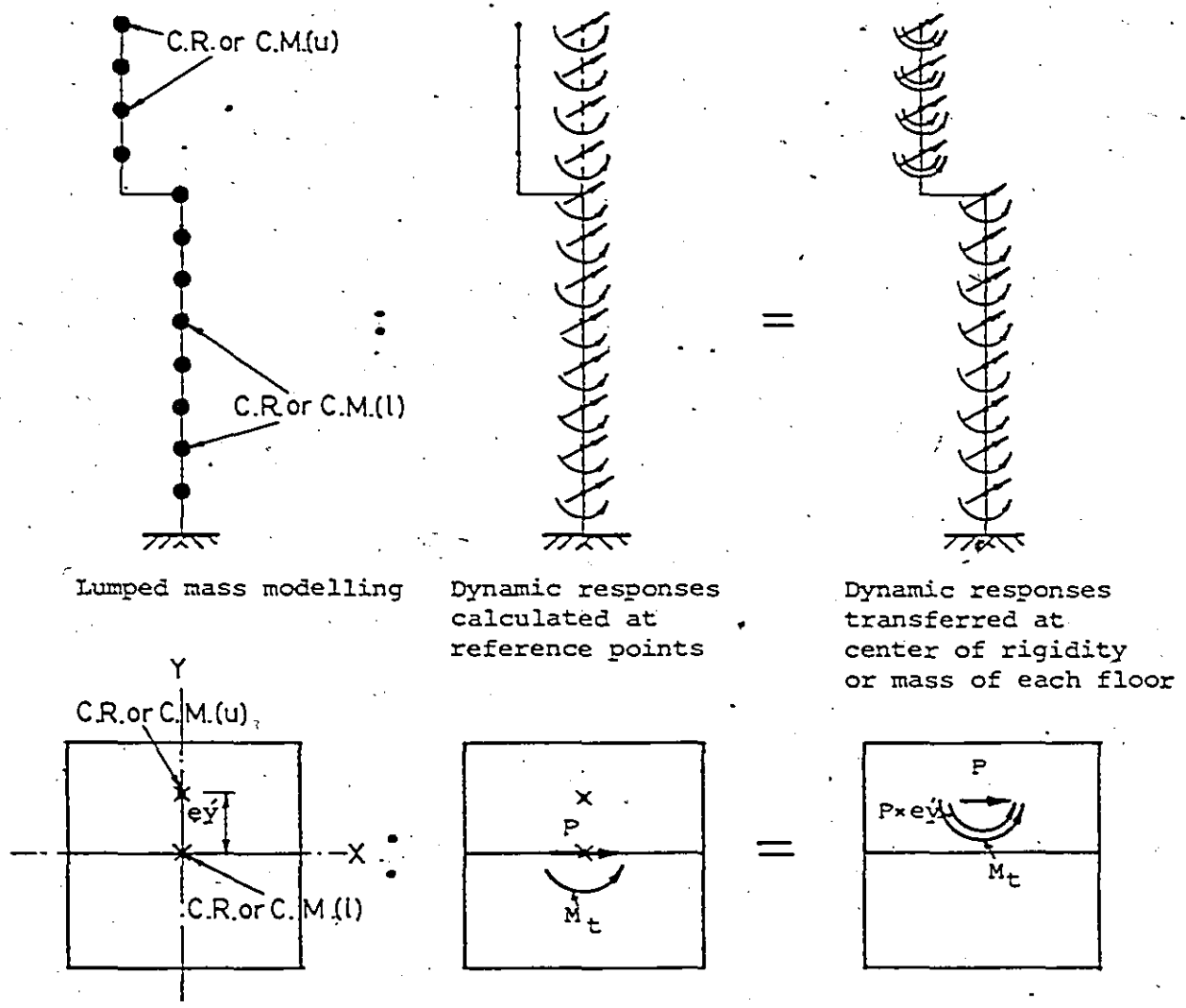
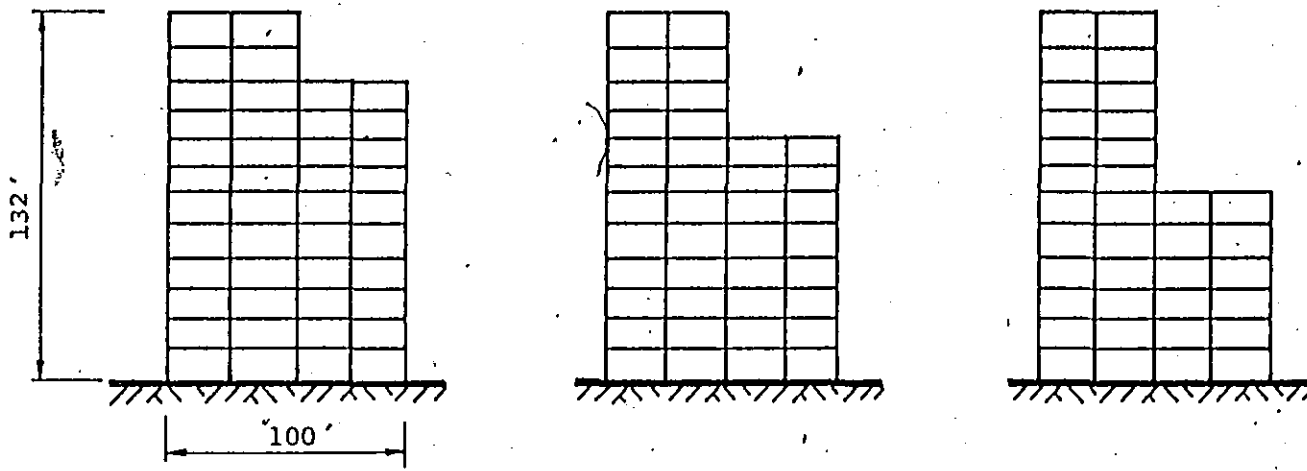


Fig. 4.5 The Transfer of Dynamic Responses from Reference Point to Floor Center of Rigidity or Mass for Eccentric Offset Building



STRUCTURE A

STRUCTURE B

STRUCTURE C

Fig. 4.6 Buildings with Eccentric Offset Floors

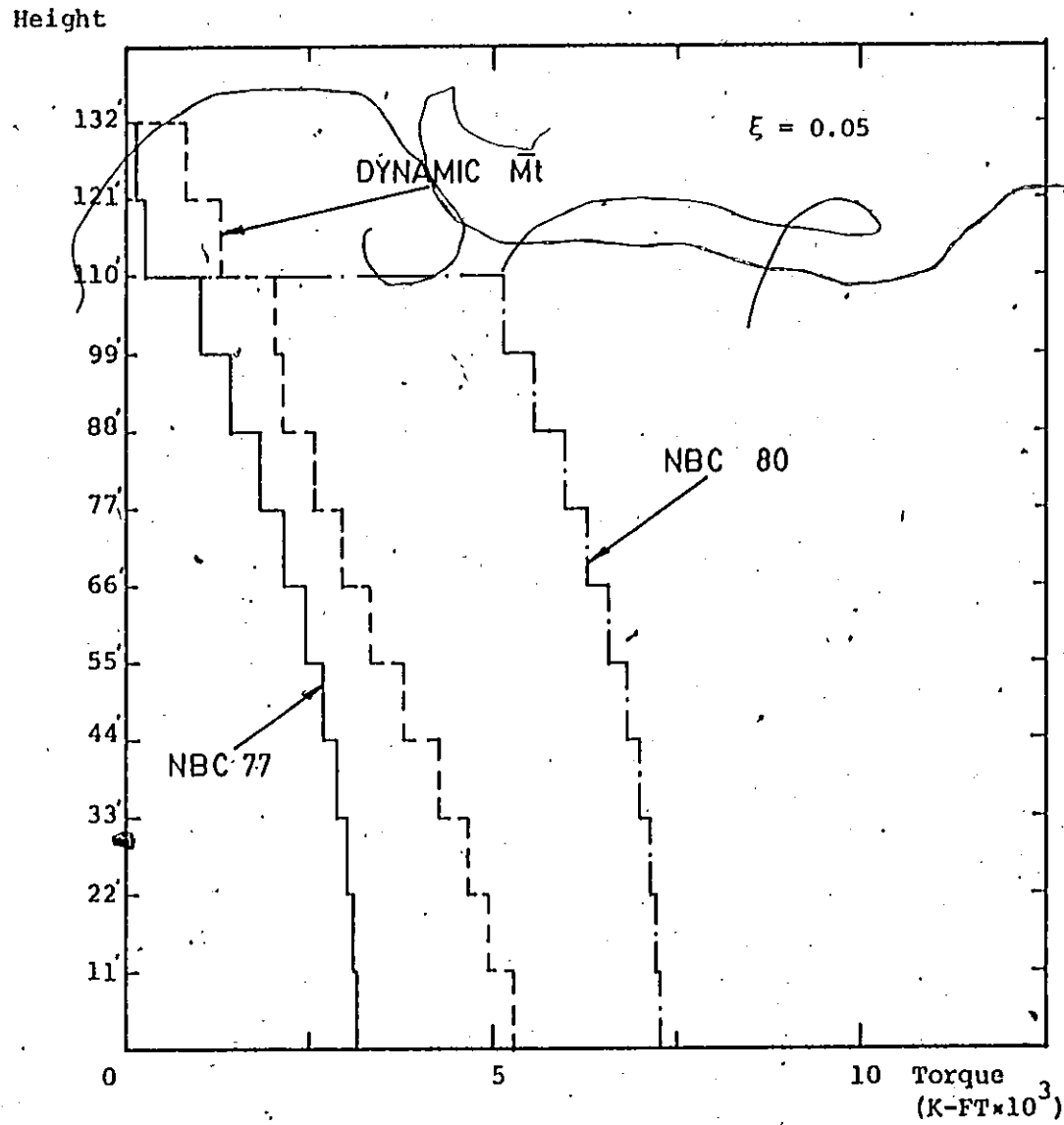
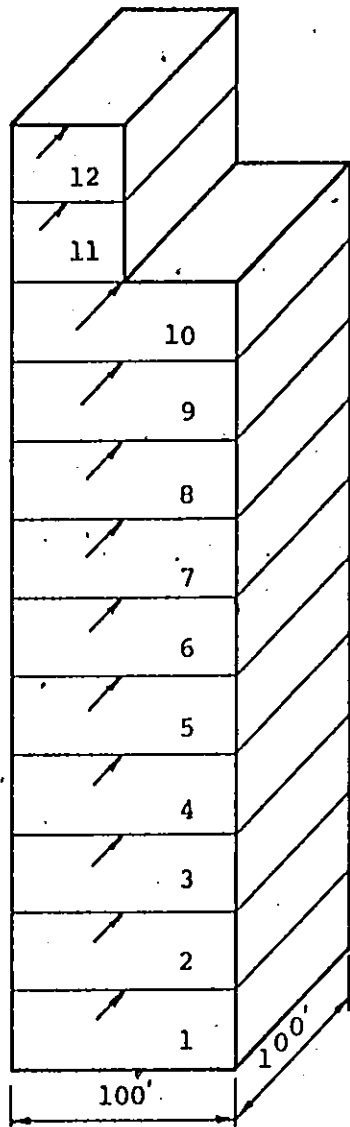


Fig. 4.7 Torque Envelope for Structure A

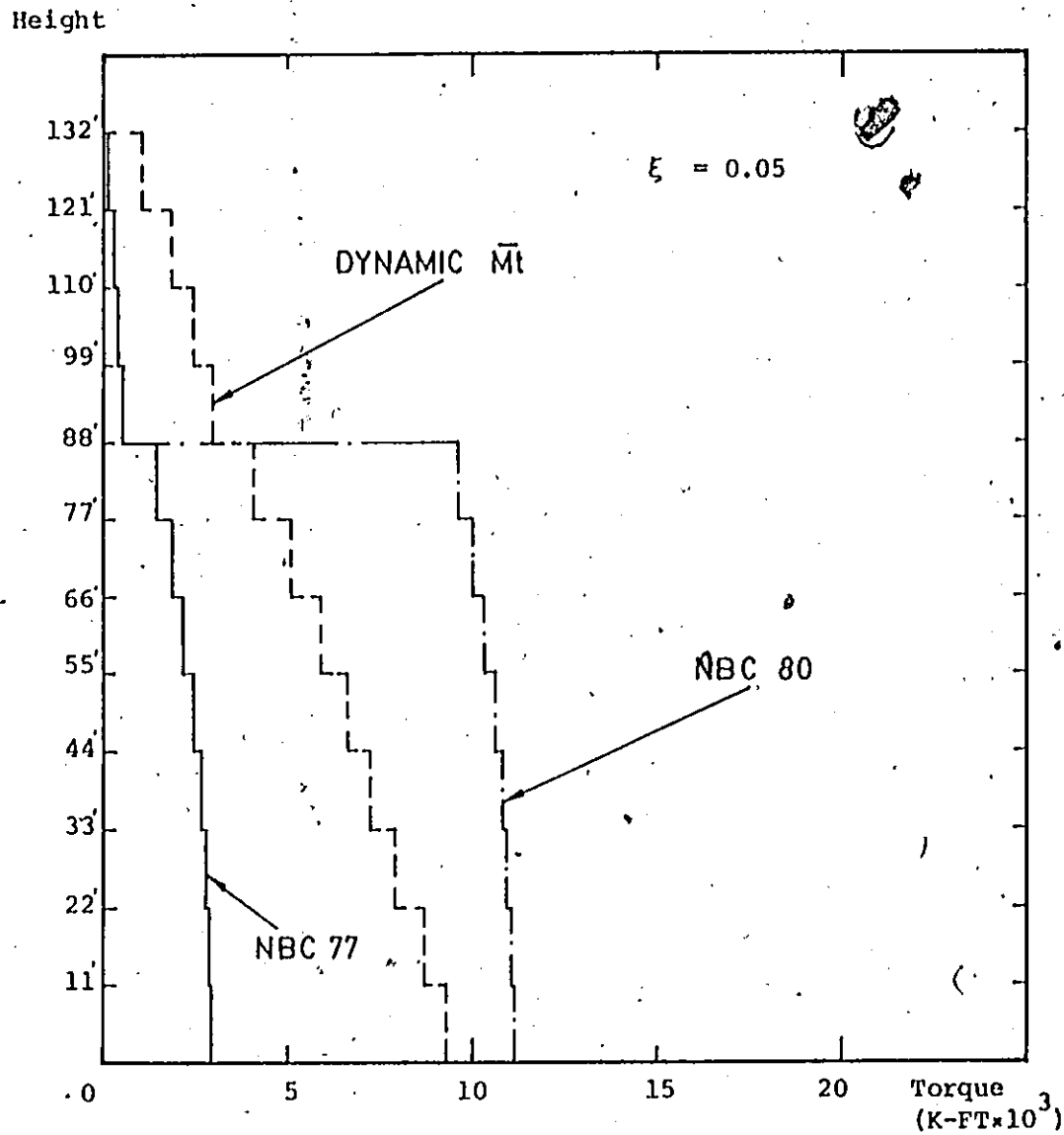
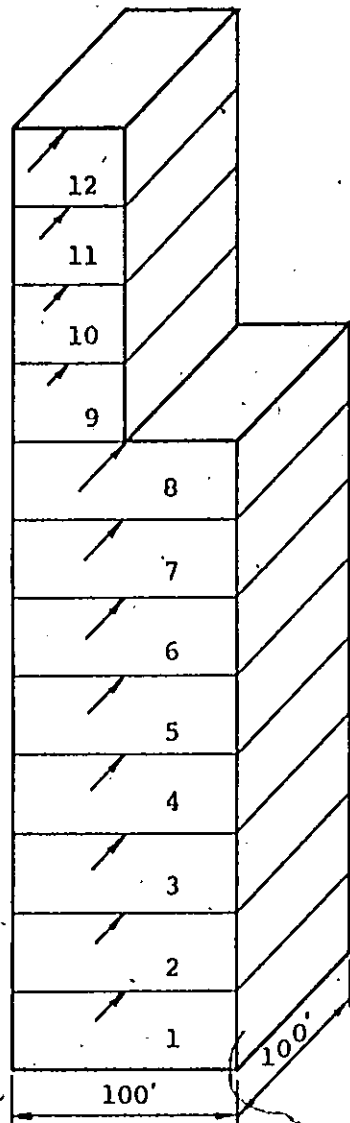


Fig. 4.8 Torque Envelope for Structure B

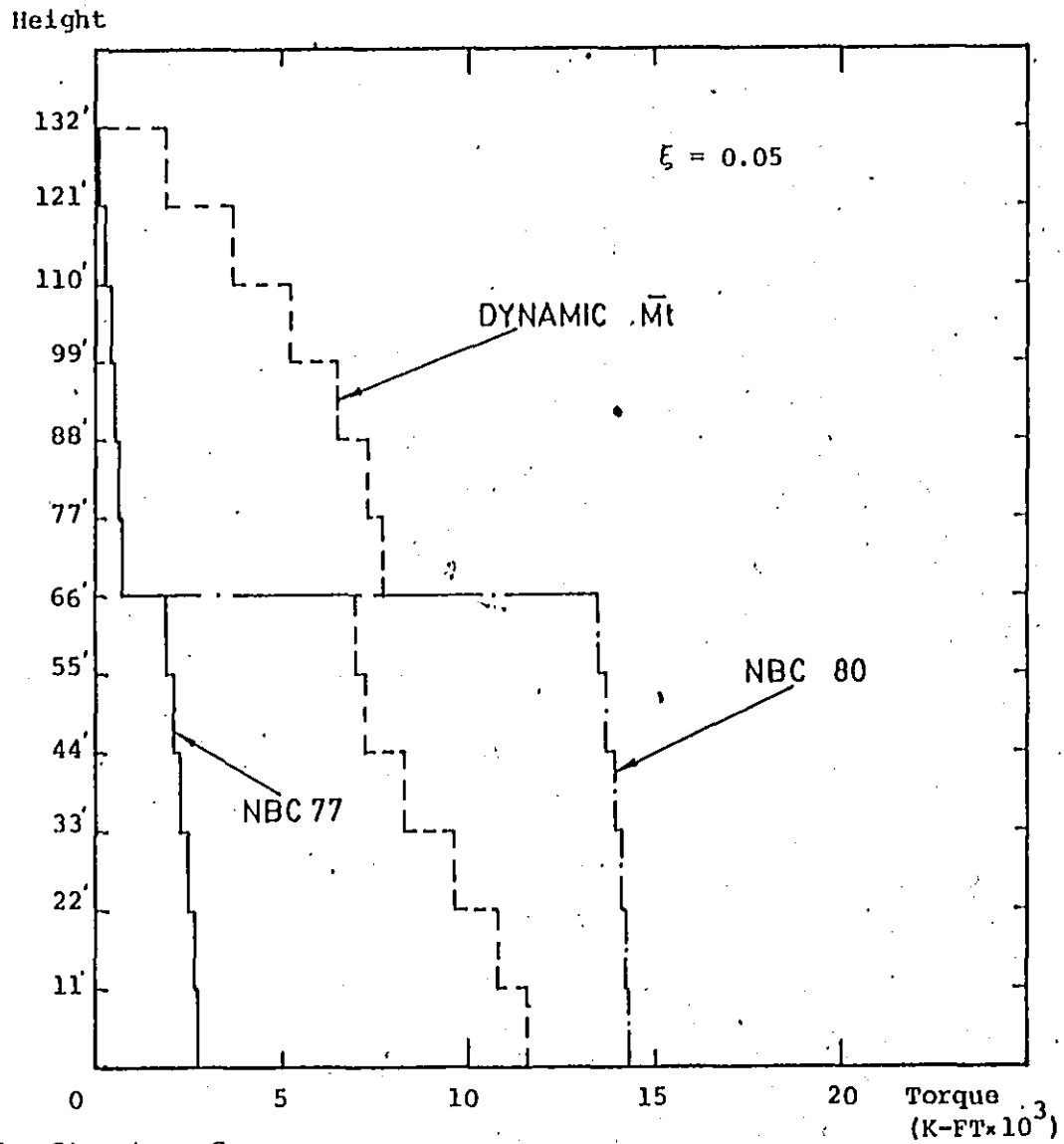
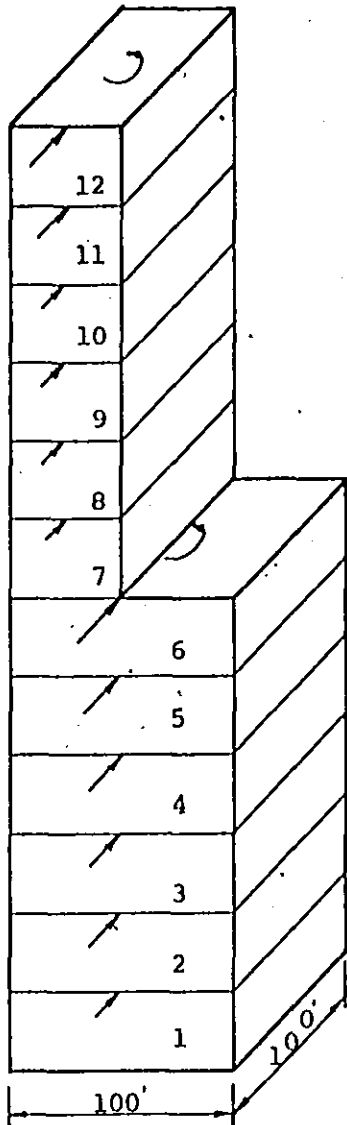


Fig. 4.9 Torque Envelope for Structure C

Mode	ω_1	ω_2	ω_3	ω_4	ω_5	ω_6	ω_7	ω_8	ω_9	ω_{10}	ω_{11}	ω_{12}
Structure A	4.834	6.909	14.304	20.109	22.076	27.484	32.105	36.880	42.216	46.099	52.179	54.448
Structure B	5.134	7.693	12.932	17.381	22.057	30.050	31.922	37.069	43.400	45.208	51.892	54.628
Structure C	5.324	7.900	11.692	17.682	23.298	28.121	33.224	38.792	41.374	44.639	52.489	54.934

Table 4.2 The Frequencies of Eccentric Offset Structures A, B and C

It can be seen that the proposed structural eccentricity (e) by NBC 80 improves the storey torque at the lower portion of the structure due to the top offset. However, it overestimates the dynamic analysis even if the doubling torque requirement is ignored when the design eccentricity (e_x) exceeds 25% of the length of the structure.

At the top offset part, the storey torques retain the same formats for both NBC 77 and NBC 80, but the dynamic torque diagrams show that there are substantial torsional moments. For example, in the building with six-storey offset, the dynamic torque at the bottom of the offset is more than seven times the static value predicted by the code formulae.

The replotting of three dynamic torque curves are shown in Fig. 4.10. It is interesting to note that not only the magnitude of the storey torque increases as the number of offset floors increases, but also the shapes of the curves changing. For the building with six offset floors, the dynamic torque at the bottom of the offset stories is larger than the torque of the floor below it. No static code has been able to simulate such a distribution of torque and it can have considerable design implications since the torsional stiffness of the offset stories is normally smaller than the lower part of the building.

The study described above demonstrates that the modification of the structural eccentricity e in NBC 80 is applicable to buildings with eccentric offsets, but its application to such buildings should be carried out with caution. The new formula leads to conservative estimates on the main portion of the building, but it has the same drawback at the offset portion as NBC 77. So, the improvement is only partial. Buildings with eccentric offsets are irregular buildings, only a dynamic approach can lead to a realistic estimate of the torque distribution. Building codes

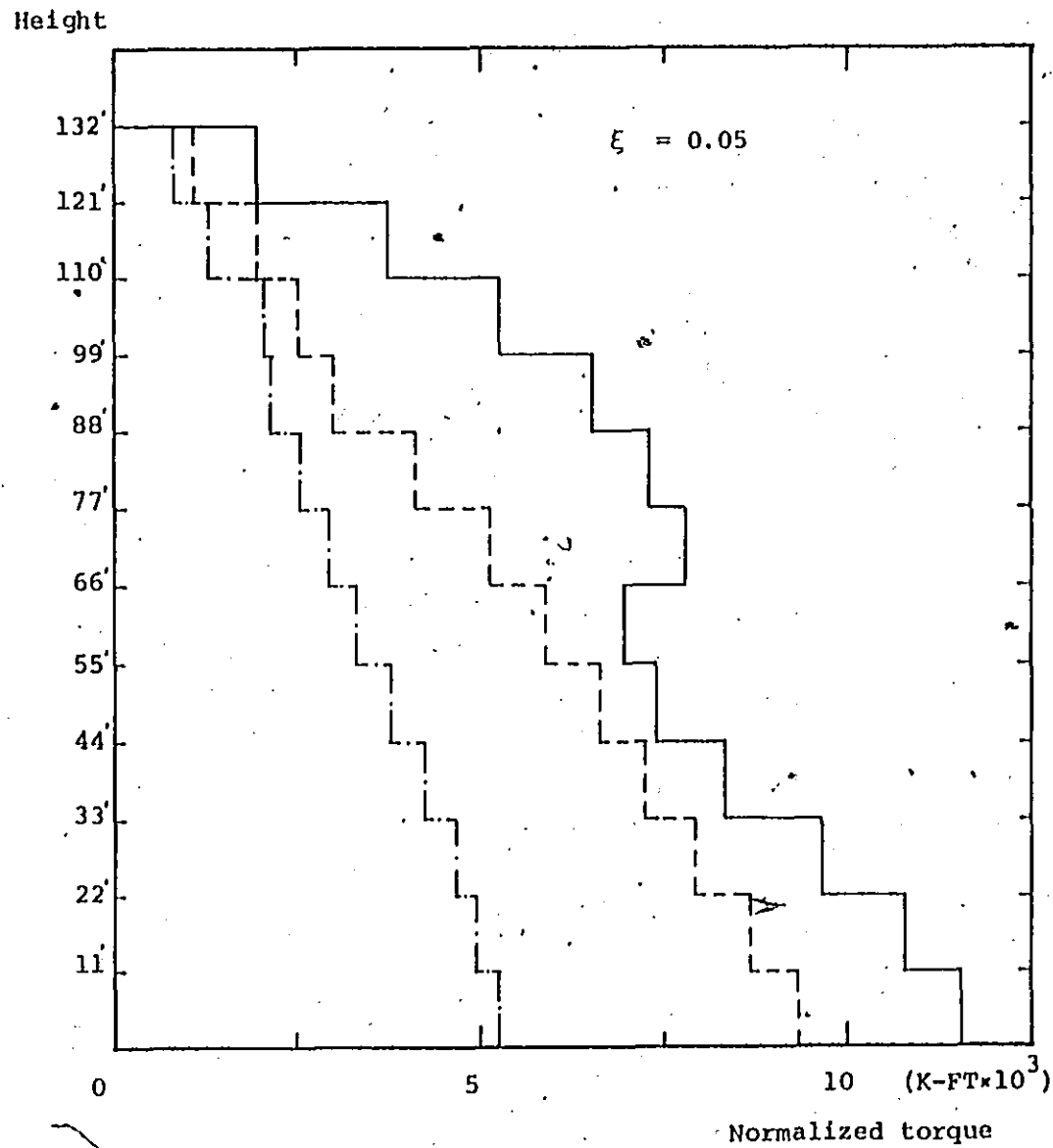
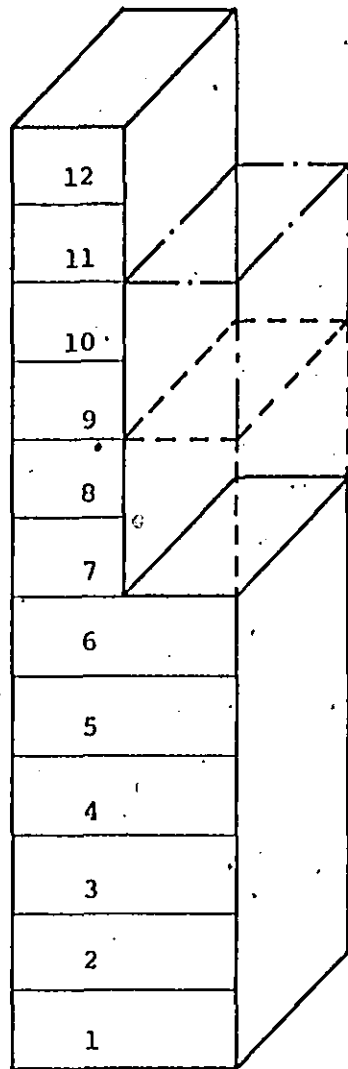


Fig. 4.10 Comparison of Torque Calculation of Different Offset Structures

should state explicitly that the static method is only applicable to buildings whose centers of mass and centers of resistances lie on two vertical lines. A dynamic analysis is necessary if the structures does not satisfy such stated conditions.

CHAPTER 5

CONCLUSIONS

The use of the mathematical models has enabled the dynamic analysis to be applied to symmetrical, monosymmetrical and asymmetrical uniform buildings and irregular buildings. The research indicated in the previous chapters concentrates on the effects of coupled translational and torsional motions of the frame buildings due to earthquake excitation. Based on NBC77, both static and dynamic analyses on shear force and torsional provisions are performed and studied. The results of the investigation can be stated as follows:

1. NBC77 static torque formula provides adequate description of storey torques along the height of the building when the mass centers and centers of resistance of the floors lie on two vertical axes and the effect of sympathetic coupled resonance is not significant.
2. Sympathetic coupled resonance of torsional and lateral vibrations occurs in the buildings with small eccentricities when uncoupled torsional and lateral periods are close to each other. In this kind of building, the closeness of pair-wise lower natural periods creates severe modal coupling. However, when the uncoupled torsional period is not within 20% of the uncoupled lateral period, the effect of sympathetic resonance can be neglected.

- 3.- Sympathetic coupled resonance occurring in a building reduces shear force response and stimulates torque.
4. Buildings with large eccentricities do not possess the closeness of pair-wise lower periods. Sympathetic coupled resonance is unlikely to occur in buildings of this kind even when the uncoupled torsional period is almost equal to the uncoupled lateral period. For such buildings, the Building Code (NBC77) static torque formulae adequately estimates the storey torque. Doubling of the static torque when the design eccentricity exceeds $0.25 D_n$ is a very conservative requirement.
5. Compared with static code provisions, dynamic analysis permits a more realistic description of the behaviour of a building which is subjected to earthquake loadings. To reflect the dynamic and static properties of a complex building, (for example, uncoupled translational and torsional periods, various structural eccentricities and an irregular layout in plan and/or elevation) only dynamic analysis can take these into account. Therefore, the necessity of dynamic analysis is apparent.
6. The use of the RSS rule in the response spectrum technique should be carried out with caution. It is believed that the expression given in Eq. 3.6 provides the 'best' maximum combined solution for each mode. The RSS rule will overestimate the torque values and underestimate the shear forces when the pair-wise lower periods of the structure are close.
7. A comparison of the building codes from five different countries with respect to torsional provisions shows that the current German Code provides a good estimate of torsion. An additional factor in the calculation of design eccentricities should be

considered in the Canadian Building Code when the effect of sympathetic coupled resonance is significant.


8. The modification of structural eccentricity in NBC80 is applicable to buildings with eccentric offsets. However, the investigation shows that the improvement is only partial. The new formula indicates a conservative estimate on the main portion of the building and keeps the same torque value as NBC77 at the eccentric offset portion. Dynamic study demonstrates that the torques at the offset portion are grossly underestimated. Buildings with eccentric offsets are irregular buildings. Only the dynamic approach, such as the response spectrum technique, can lead to a realistic estimate of the torque distribution.

The study of the eccentric offset building also shows that the doubling of the torque requirement is not applicable to the torsional calculation for irregular buildings when the design eccentricity exceeds $0.25 D_n$.

REFERENCES

1. National Building Code of Canada, 1977, Subsection 4.1.9.1 (16) & (17).
2. Supplement No. 4 to the National Building Code of Canada, 1977, Commentary J, "Effects of Earthquakes".
3. Supplement No. 4 to the National Building Code of Canada, 1977, Commentary K, "Dynamic Analysis for the Seismic Response of Buildings".
4. Kan, C.L. & Chopra, A.K., "Effects of Torsional Coupling on Earthquake Forces in Buildings", Journal of Structural Division, ASCE, Vol. 103, No. ST4, 1977, P. 805-819.
5. Tso, W.K. & Asmis, K.G., "Torsional Vibration of Symmetric Structure". Proceedings of the First Canadian Conference on Earthquake Engineering, U.B.C., P. 178-186, 1965.
6. Keintzel, E., "On the Seismic Analysis of Unsymmetrical Storied Buildings". Proceedings Fifth World Conference on Earthquake Engineering, Rome, 1973. Paper No. 10 Session 1B.
7. Newmark, N.M., "Torsion in Symmetrical Buildings". Proceedings of the Fourth World Conference on Earthquake Engineering Vol. II 1960, P. 19-32.
8. Hart, G.C., DiJulio, R.M. & Lew, M., "Torsional Response of High Rise Buildings", Journal of Structural Division, ASCE 1975, P. 397-416.
9. Tso, W.K. & Hsu, T.I., "Torsional Spectrum for Earthquake Motions", Earthquake Engineering and Structural Dynamics Vol. 6, P. 375-382, 1978.
10. Tso, W.K. & Biswas, J.K., "Seismic Analysis of Asymmetrical Structures Subjected to Orthogonal Components of Ground Acceleration". The sixth world conference on Earthquake Engineering. Proceedings Vol. II, India 1977, P. 1217.

11. Fajfar, P. & Zelez, B., "Spatial Seismic Effects in Multistorey Structures", Earthquake Resistant Design 2. Sixth European Conference on Earthquake Engineering, Sept. 18-22, 1978 Dubrovnik, Yugoslavia.
12. Kan, C.L. & Chopra, A.K., "Elastic Earthquake Analysis of a Class of Torsionally Coupled Buildings", Journal of Structural Division, ASCE, Vol. 103 No. ST4, 1977, P. 821-838.
13. Kan, C.L. & Chopra, A.K., "Earthquake Response of a Class of Torsionally Coupled Buildings", the sixth world conference on Earthquake Engineering. Proceedings Vol. II, India 1977, P. 1211.
14. Rutenberg, A., Hsu, T.I. & Tso, W.K., "Response Spectrum Techniques for Asymmetric Buildings", Earthquake Engineering and Structural Dynamics, Vol. 6, 1978, P. 427-435.
15. Müller, F.P. and Keintzel, E., "Approximate Analysis of Torsional Effects in the New German Seismic Code DIN 4149". Proceedings of Sixth European Conference on Earthquake Engineering, Vol. 2, P. 101-108, Dubrovnik, 1978.
16. National Building Code of Canada, 1980, 4.1.9.1 (17).
17. Heidebrecht, A.C. & Smith, B.S., "Approximate Analysis of Tall Wall-Frame Structures", Journal of Structural Division, ASCE, 1973, P. 199-221.
18. Schueller, W., "High-Rise Building Structures", Wiley-Interscience, 1977, P. 153.
19. Clough, R.W. & Penzien, J., "Dynamics of Structures", McGraw Hill, 1975.
20. Newmark, N.M. & Rosenblueth, E., "Fundamentals of Earthquake Engineering", Prentice Hall, 1971.
21. DIN 4149, Bauten in Deutschen Erdbebengebieten Entwurf, Dezember 1976.
22. Proposed Building Code for Mexico's Federal District, 1975.

23. New Zealand Standard NZS 4203, 1976, Part 3 (Earthquake Provisions).
 24. Ministry of Reconstruction and Resettlement, Turkish Government, Earthquake Research Institute, Ankara, 1975.
 25. Recommended Lateral Force Requirements and Commentary, SEOAC, 1975.
 26. Tentative Provisions for the Development of Seismic Regulations for Buildings, ATC3-06, Applied Technology Council, 1978.
- 

APPENDIX

LIST OF SYMBOLS

A	- cross sectional area of column of the frame building
a_i, b_i	- floor plan dimensions of the building in x, y axes respectively for unit (i)
C.M.	- center of mass
C.R.	- center of rigidity
D_n, D	- plan dimension of the building in the direction of the computed eccentricity
D_y	- plan dimension of the building in y axis direction
e	- computed structural eccentricity between the center of mass and center of rigidity at the level being considered
e_x, e_y	- computed structural eccentricity in x and y axes direction
e_{ix}	- distance between centre of mass at floor i to center of rigidity at floor x
e_i	- supplementary fictitious eccentricity in German code DIN 4149
E	- Young's modulus
EM_{xi}, EM_{yi}	- mass eccentricity related to reference point in x,y directions of unit (i)
ER_{xi}, ER_{yi}	- eccentricity of center of rigidity related to reference point in x,y directions of unit (i)
F	- developed spring force of the mathematical model
G	- shear modulus

$\ddot{g}_x, \ddot{g}_\phi$	- ground lateral acceleration in x direction and ground torsional acceleration
h_i	- unit (i) height of the building
I	- moment of inertia
$I_{\phi i}$	- mass polar moment of inertia of unit (i)
$I_{\theta i}$	- mass moment of inertia in rocking motion
$I_{m i}$	- mass polar moment of inertia refer to mass center of unit (i)
$I_{p i}$	- mass polar moment of inertia refer to arbitrary point P of unit (i)
$K_{R i}$	- torsional stiffness refer to center of rigidity of unit (i)
$K_{p i}^\phi$	- torsional stiffness refer to arbitrary point P of unit (i)
$K_{xx}, K_{\theta\theta}, K_{\phi\phi}, K_{x\theta}, K_{x\phi}$ and $K_{\theta\phi}$	- symbols of stiffness matrices of the model
K_{sxi}, K_{syi}	- shear spring stiffness in x and y directions respectively of the mathematical model for unit (i)
K_{xi}, K_{yi}	- flexural spring stiffness in x and y directions respectively of the mathematical model for unit (i)
$K_{\phi i}$	- torsional spring stiffness of the mathematical model for unit (i)
$[K]$	- stiffness matrix of model
$[\bar{K}]$	- condensed stiffness matrix of model
M_{tx}	- static torsional moment at level x
M_{t0}	- dynamic base torque
M_t	- dynamic torque
\bar{M}_t	- normalized dynamic torque

M_i	- mass of unit (i) of the model
$M_{\theta i}$	- overturning moment at unit (i)
P_i	- lateral force at unit (i)
γ_i	- model participation factor of mode i
γ_i^r	- polar radius of gyration of mass (i) of the model
T_x	- uncoupled period of lateral vibration of the building in seconds in the x axis direction
T_ϕ	- uncoupled torsional period of vibration of the building in seconds
$U_p, V_p, U_m, V_m, U_r, V_r$	- displacements of points P, C.M. and C.R.
V or V_s	- minimum lateral seismic static force at the base of the structure
V_d	- dynamic base shear
ω_i	- natural frequencies of mode i
ω_i^d	- damped frequency
$X_p, Y_p, X_m, Y_m, X_r, Y_r$	- positions of points P, C.M. and C.R. in x-y cartesian coordinate axes
X_i	- absolute lateral displacements of unit (i)
θ_i	- absolute overturning rotation of unit (i)
Δ_i	- relative lateral displacement between unit (i-1) and unit (i)
ϕ_i	- absolute torsional rotation of unit (i)
τ	- ratio of uncoupled torsional period (T_ϕ) to uncoupled lateral period (T_x) of vibration of the building
$S a_i^k$	- spectral acceleration in mode i

$\{\phi\}_i$ ξ ρ

$$I = \begin{Bmatrix} 1 \\ 1 \\ 1 \\ \vdots \\ \vdots \end{Bmatrix}$$

- mode shapes of mode i

- damping ratio

- mass density of unit

- unit column vector